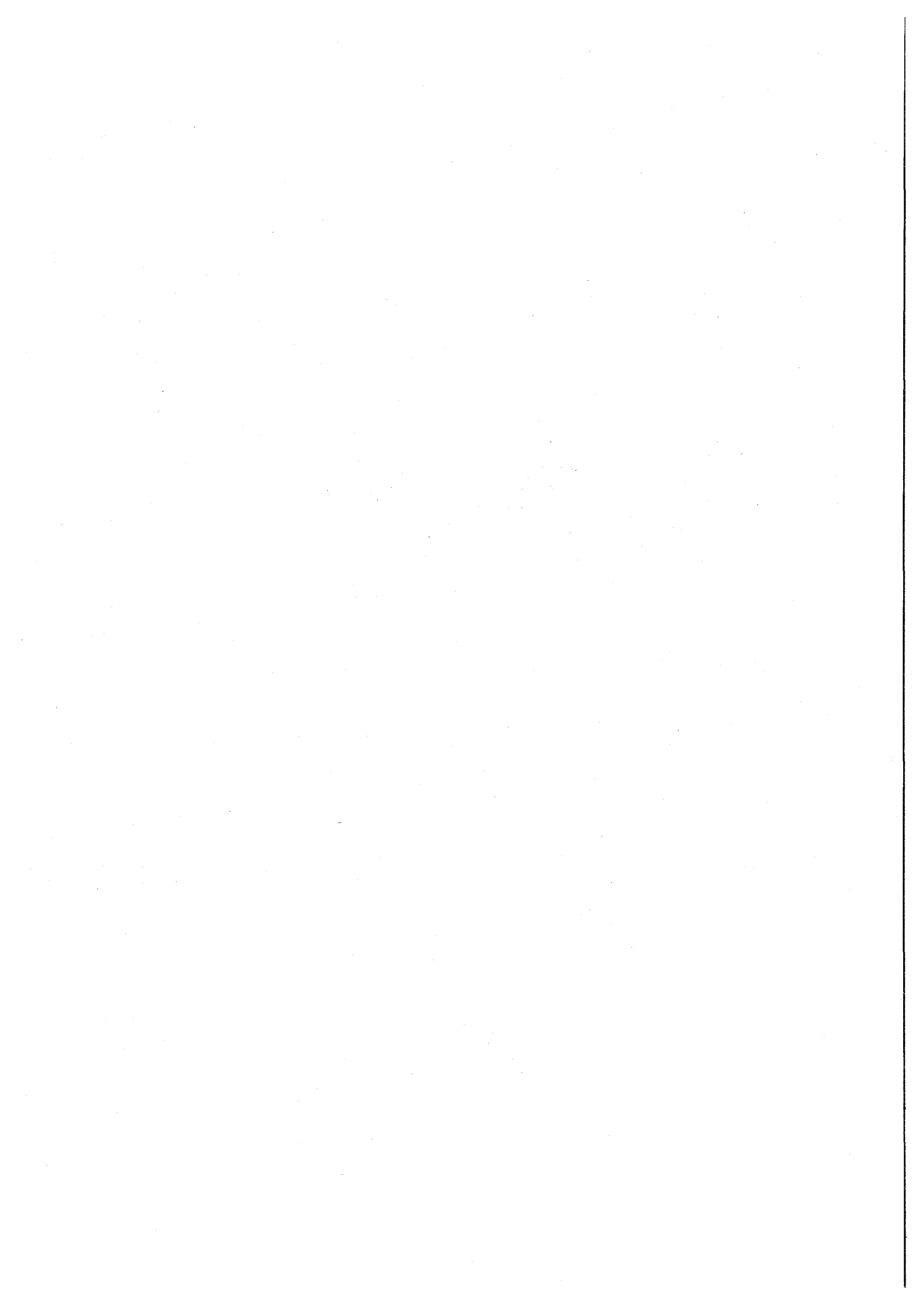


**CONTRIBUTOR'S ABSTRACTS**

**2<sup>nd</sup> day**



2A1

## SIMULATION OF THE TEMPERATURE DISTRIBUTIONS IN THE SPIRAL-II TARGET FOR THE PRODUCTION OF RADIOACTIVE ION BEAM

Dalia NAYAK<sup>1</sup>, M. G. SAINT LAURENT, F. PELLEMOINE and V. DUBOIS

Grand Accelérateur National d'Ions Lourds, B. P. 55027-14076 CAEN CEDEX5,  
FRANCE

<sup>1</sup>Chemical Sciences Division, Saha Institute of Nuclear Physics, 1/AF Bidhannagar,  
Kolkata-700 064, INDIA

There is currently in the nuclear physics community a strong interest in the use of beams of accelerated radioactive ions. Radioactive beam of neutron rich isotopes may determine the location of neutron -drip line and give information about the properties of the exotic nuclei near this line. Moreover, it can be noted that the astrophysics community is very interested in nuclear data for calculations of nucleosynthesis.

The SPIRAL-II RTD program aims at studying the techniques for delivering beams of neutron-rich radioactive nuclides at energies of a few MeV per nucleon. The technique proposed for SPIRAL-II is the use of energetic neutrons to induce fission of natural uranium. The neutrons are generated by the break-up of deuterons in a thick target, the so called converter (carbon), or by the direct interaction of deuteron with the uranium target. The highest primary beam intensity is desirable as it proportionally increases nuclide production. So it is necessary to determine the intensity and energy of the primary deuteron giving the best yields of radioactive nuclides of interest for radioactive beams while taking into account beam power evacuation and safe operation of the facility. The maximum beam power that can be stood by the target determines the achievable radioactive beam intensity.

Keeping these facts in mind effort has been made to study the optimisation of energy and intensity of the deuteron beam, designing of the converter and fissionable target (UCx), temperature distribution inside the converter and/or UCx target for different geometries and cooling of the target. Thermal simulations have been performed using the SYSTUS and SPIRAL codes at different energies, intensities and three different geometries. The beam intensity and target size were chosen according to the temperature simulations in order to get about  $10^{13}$  fissions/s. The three configurations are as follows:

- i. A carbon converter followed by a UCx target (converter method)
- ii. A UCx target not thick enough to stop the beam, followed by a beam catcher (direct method)
- iii. A UCx target in which the beam is stopped (direct method)

SYSTUS simulation revealed that (i) a carbon converter followed by a UCx target (56 slices) allow a maximum beam intensity  $350 \mu\text{Ae}$  for 100 MeV deuteron beam energy (beam power = 35 kW) which gives  $6 \times 10^{12}$  fission/s. Amongst these three methods the converter method is the most reliable because the location where the deuteron beam deposited (C) can be separated from the diffusion target (UCx) where the radioactive elements are produced. Thus cooling of the converter target and heating of the diffusion target for a good diffusion, with an oven independently of the beam power becomes easier. Even if a somewhat lower number than  $10^{13}$  fissions/s is obtained with  $350 \mu\text{Ae}$  in case (i), the nuclei are more neutron-rich than in case (ii). This is a consequence of neutron capture instead of a deuteron before fission and of the lower projectile energy.

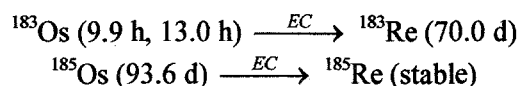
## PRODUCTION AND SEPARATION OF $^{183}\text{Os}$ AND $^{183}\text{Re}$ FROM $^7\text{Li}$ IRRADIATED TANTALUM TARGET

Susanta LAHIRI<sup>1</sup>, Kakoli BANERJEE<sup>1</sup>, A. RAMASWAMI<sup>2</sup> and S. B. MANOHAR<sup>2</sup>

<sup>1</sup>Chemical Sciences Division, Saha Institute of Nuclear Physics, 1/AF Bidhannagar, Kolkata-700 064, INDIA

<sup>2</sup>Radiochemistry Division, Bhabha Atomic Research Centre, Trombay, Mumbai 400 085, INDIA

Simulation studies through PACE 2 code indicates that at > 45 MeV projectile energy there is an appreciable cross sections for the production of  $^{183}\text{Os}$  through  $^{181}\text{Ta}(^7\text{Li}, 5n)^{183}\text{Os}$  reaction. PACE 2 results also predicted that some amount of  $^{185}\text{Os}$  will be formed via  $^{181}\text{Ta}(^7\text{Li}, 3n)^{185}\text{Os}$  at an energy below 40 MeV. The carrier free radionuclides of osmium,  $^{183,185}\text{Os}$ , thus produced, decay by electron capture to generate corresponding rhenium radionuclides following the scheme:-



An attempt has been made for the separation of carrier free osmium and rhenium radionuclides from bulk tantalum target using trioctylamine (TOA) as an extractant.

The radionuclides of osmium and rhenium were produced by irradiation of natural tantalum metal foil by  $^7\text{Li}^{3+}$  beam at an energy of  $\sim 48$  MeV at BARC-TIFR Pelletron, Mumbai, India. The thickness of tantalum foil was  $7.3 \text{ mg/cm}^2$  and irradiation was carried out for about nine hours. The energy loss due to  $2.06 \text{ mg/cm}^2$  aluminum foil, used for covering the target, for 48 MeV lithium beam was calculated by the software TRIM and it was found to be  $\sim 0.84$  MeV. Thus, the energy of the lithium beam on the tantalum target was  $\sim 47$  MeV. Also, the energy loss due to the tantalum metal foil target was found to be 1.60 MeV and in this degraded energy no other radionuclides would be formed in the target matrix. The irradiated tantalum metal foil was dissolved in minimum quantity of concentrated hydrofluoric acid in presence of few drops of concentrated nitric acid.

Studies on the LLX separation of bulk tantalum and the carrier free activation products were made by equilibrating a few drops of the active solution in a definite volume of HCl of a particular strength with an equal volume of the organic extractant, TOA diluted in cyclohexane.

The non-destructive  $\gamma$ -spectrum of the  $^7\text{Li}$  irradiated tantalum target revealed the formation of the radioisotope,  $^{183}\text{Os}$ , which is in good agreement with PACE 2 results. The tantalum fraction was separated from the carrier free product by extracting with 0.01 M TOA at 0.1 M HCl. It was found that at this condition, tantalum was quantitatively extracted by the liquid anion exchanger from the aqueous acid medium and under the experimental condition the osmium radioisotopes remained in the aqueous phase. For tantalum, the formation of the anionic complexes of the type  $[\text{TaX}_6]^{2-}$  is well established and these species might be responsible for the extraction of the element easily by TOA. The osmium radioisotope, left in the aqueous phase was allowed to decay for 15 days after which the  $\gamma$ -ray lines of pure rhenium radioisotope,  $^{183}\text{Re}$ , was observed.

Takayuki ICHIHARA<sup>1</sup>, Koichi TAKAMIYA<sup>2</sup>, Takayuki SASAKI<sup>2</sup> and Seiichi SHIBATA<sup>2</sup>

<sup>1</sup>Graduate School of Engineering, Kyoto University, Sakyo-ku, Kyoto 606-8501, JAPAN,

<sup>2</sup>Research Reactor Institute, Kyoto University, Noda, Kumatori-cho, Sennan-gun, Osaka, 590-0494, JAPAN

Radioactive isotopes are employed to trace the chemical behavior of various elements in a wide range of research fields, for example, medical, pharmaceutical, biological, chemical, and environmental sciences. We have developed preparation method of a multitracer using thermal neutron induced fission of <sup>235</sup>U at Kyoto University Reactor (KUR)<sup>1</sup>. In this method, fission products are used as tracer elements. The multitracer solutions prepared are being provided for the purpose of medical research at Kanazawa University, chemical research at Osaka University and Niigata University. However, it is often requested by users to separate alkali earth or rare earth elements from the fission products. Therefore, in the present work we have tried to develop the separation method of those elements contained in the multitracer solution by solvent extraction using TTA, TBP and so on.

The multitracer solution was prepared as follows. At first, <sup>nat</sup>.U and NaCl (1:1) were mixed and the mixture was shaped as a pellet. The pellet was irradiated using the pneumatic transferring system (Pn-2) at KUR. The typical irradiation time was 20min. After cooling for a week, the irradiated sample including fission products captured by the catcher material of NaCl was dissolved in 0.01N HCl. The solution containing fission products (multitracer) was filtered with suction to remove the UO<sub>2</sub> undissolved. From this solution, Zr, Sb, I and Np were extracted by using TBP, Y, Ru, La, Ce and Nd by TTA and TBP, and Sb by TBP. The scheme of the solvent extraction is shown in Fig.1. The separation efficiencies were estimated by the ratios of  $\gamma$ -ray intensities in organic phase to aqueous phase, and were obtained to be more than 95% except for Ru, Sb and I. The experiment for establishing the separation method is still under way.

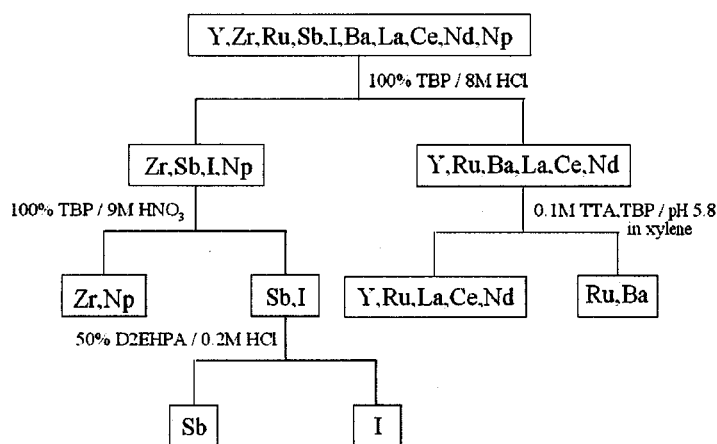


Fig. 1. Scheme of Solvent Extraction.

#### Reference

1. K. Takamiya, M. Akamine, S. Shibata, A. Toyoshima, Y. Kasamatsu, A. Shinohara, *J. Nucl. Radiochem. Sci.*, 1(2), 81-82 (2000).

## 2A4 *In vivo* assessment of dynamics of various elements in living rat using multitracer

Ken-ichiro Matsumoto,<sup>1</sup> Iori Ui,<sup>1</sup> Rieko Hirunuma,<sup>2</sup> Shuichi Enomoto,<sup>2</sup> and Kazutoyo Endo<sup>1</sup>

<sup>1</sup> Department Physical Chemistry, Showa Pharmaceutical University, 3-3165 Higashi-Tamagawagakuen, Machida, Tokyo 149-8543, Japan,

<sup>2</sup> Division of Radioisotope Technology, Cyclotron Center, RIKEN (The Institute of Physical and Chemical Research), 2-1 Hirosawa, Wako, Saitama 351-0198, Japan

*In vivo* time courses of distributions of bio-trace elements in the upper abdomen or the head of a living Wistar male rat were examined using multitracer analysis technique. Advantage and possibility of this technique as a non-invasive diagnostic tool for distribution of bio-trace elements in living experimental animals were discussed. The distribution of an element in a section of the living rat was estimated as the relative distribution (% in measured section).

A hydrochloric acid solution containing multitracer was prepared from a silver foil irradiated with a <sup>14</sup>N beam of 135 MeV/nucleon at the RIKEN Ring Cyclotron. The solution was evaporated into dryness and then the multitracer was dissolved in 2 mL of isotonic citrate buffer (pH 6.2) for administration to rats.

A six week old Male Wistar rat was anesthetized with 0.05 mg/g b.w. intraperitoneal injection of pentobarbital. The rat was fixed to a plastic rat holder with adhesive tape and placed in the desired position. Then, 200  $\mu$ L of multitracer solution was administered (i.v.) to the rat. Immediately after administration, the  $\gamma$ -ray spectra of the upper abdomen ( $n = 4$ ) or head ( $n = 3$ ) of the rat were measured successively with the high-purity Ge semiconducting detector.

Uptakes of an element to organs and/or tissues in the measured section were estimated by comparing the relative distribution with that of As. Since As distributes mainly to the red blood cells, the relative distribution of As indicates the distribution of blood itself. In the head, most elements were distributed mainly into the bones and muscles, except that Co and Se might be in blood circulation. In the upper abdomen, Mn, Co, Zn, Se, Rb, V, and Y were distributed into the liver, which is a main organ for accumulating metals. It is the first report that the dynamics of bio-trace elements within an hour was non-invasively obtained in a living whole animal.

2A5

## WATER MOVEMENT IN A PLANT SAMPLE BY NEUTRON BEAM ANALYSIS AS WELL AS POSITRON EMISSION TRACER IMAGING SYSTEM

T. M. Nakanishi, Y. Okuni, J. Furukawa, K. Tanoi, H. Yokota, N. Ikeue, <sup>1</sup>\*M. Matsubayashi, <sup>2</sup>\*N. S. Ishioka, <sup>2</sup>\*S. Watanabe, <sup>2</sup>\*A. Osa, <sup>2</sup>\*T. Sekine, <sup>2</sup>\*S. Matsushashi, <sup>2</sup>\*T. Ito, <sup>2</sup>\*T. Kume, <sup>3</sup>\*H. Uchida, <sup>3</sup>\*A. Tsiji

*Graduate School of Agricultural & Life Sciences, The University of Tokyo, Tokyo, Japan, 113-8657*

<sup>1</sup>*Japan Atomic Energy Research Institute, Tokai Establishment, Japan, 319-1195*

<sup>2</sup>*Japan Atomic Energy Research Institute, Takasaki Establishment, Japan, 370-1292*

<sup>3</sup>*Hamamatsu Photonics, Co., Hamamatsu, Japan, 434-8601*

**Summary:** This is a summarized report for imaging water in a plant for the first time, using both neutron beam analysis and positron emission tracer imaging system (PETIS). Neutron image showed dynamic change of special water profile around the soybean root and <sup>15</sup>O-labeled water enabled to analyze real time water movement within a plant by PETIS.

**Key words:** water movement, spatial water image, soybean, soil water around a root, neutron beam analysis, X-ray film method, CT construction, positron emission tracer imaging system, <sup>18</sup>F-labeled water, <sup>15</sup>O-labeled water

This is a summarized report on water imaging of a plant sample both by neutron beam analysis and positron emission tracer imaging system (PETIS). The former method provided static water profile in a plant sample as well as that in the vicinity of a root imbedded in soil. Not only X-ray film method but also CT method using a cooled CCD camera will be presented. Through non-destructive water image in an X-ray film, root development as well as 2-dimensional water movement toward the root was analyzed. Spatial water image was constructed from 180 CT projection images, taken at an interval of one degree while rotating the sample, through a CCD camera. In the case of a soybean root, there was a water gradient toward a root in soil and gave minimum value at about 1mm far from the surface of a root. The water absorbing part in a root was gradually shifted downward with the root development. We also present real time water movement by PETIS, where water was labeled with a positron emitting nuclide, <sup>18</sup>F or <sup>15</sup>O. The water labeled with <sup>18</sup>F moved much faster than that with <sup>15</sup>O. There was a circadian rhythm observed in <sup>15</sup>O labeled water uptake.

FAX: +81-3-5841-8193, Email: atomoko@mail.ecc.u-tokyo.ac.jp

PRODUCTION AND CHARACTERIZATION  
OF ACTINIDE METALLOFULLERENES

K. AKIYAMA<sup>1, 2</sup>, K. SUEKI<sup>1</sup>, H. HABA<sup>2</sup>, K. TSUKADA<sup>2</sup>, M. ASAI<sup>2</sup>, T. YAITA<sup>3</sup>, Y. NAGAME<sup>2</sup>, K. KIKUCHI<sup>1</sup>, M. KATADA<sup>1</sup>, and H. NAKAHARA<sup>1</sup>

<sup>1</sup>Graduate School of Science, Tokyo Metropolitan University,  
Hachioji, Tokyo 192-0397, Japan

<sup>2</sup>Advanced Science Research Center, Japan Atomic Energy Research Institute,  
Tokai, Ibaraki 319-1195, Japan

<sup>3</sup>Department of Materials Science, Japan Atomic Energy Research Institute,  
Tokai, Ibaraki 319-1195, Japan

A metallofullerene is a clathrate compound with one or more metal atoms encapsulated in the fullerene cage, and its unique structure has attracted many scientists to the study of its physical and chemical properties. It has been reported, for example, that the encapsulated metal atoms often take unique chemical states due to the  $\pi$  electrons of the surrounding carbon atoms which can rarely be observed in the atmosphere of air [1]. For this reason, it is significant to investigate the chemical states of the actinide atoms in the fullerene cages for probing a new field of the actinide science. Previously, we reported the HPLC elution behaviors of the Th, Pa, U, Np, and Am metallofullerenes and the UV/vis/NIR absorption spectra of the Th@C<sub>84</sub> and U@C<sub>82</sub> species [2, 3]. In this symposium, the following will be reported: (1) the HPLC elution behavior of the Pu metallofullerene investigated in the radio-tracer technique and (2) the properties of the Th@C<sub>84</sub> and U@C<sub>82</sub> in macroscopic quantity determined by XANES (X-ray Absorption Near Edge Structure) measurements and by the <sup>13</sup>C-NMR observation for Th.

The fullerenes encapsulating actinide atoms were synthesized by the arc discharge method using the porous carbon rods absorbing La(NO<sub>3</sub>)<sub>3</sub> and the radiotracers of actinide elements. The HPLC elution behaviors of the actinide fullerenes were examined by the detection of the  $\gamma$ -rays from the tracers. For the investigation of the properties of the actinide fullerenes, the macroscopic quantity of the thorium and uranium fullerenes were also synthesized by the method mentioned above using the carbon rods containing a few grams of thorium and uranium, respectively.

The HPLC elution behavior of the Pu metallofullerene was almost the same as those of the Np and Am metallofullerenes. The valence state of U atom was estimated to be 3+ from the XANES spectroscopy. Therefore, the electronic state of U@C<sub>82</sub> was suggested to be U<sup>3+</sup>@C<sub>82</sub><sup>3-</sup>. This result strongly supports the previous result. More details of these results will be discussed in the symposium.

1. T. Okazaki *et al.*, *Chem. Phys. Lett.*, **320**, 435 (2000)
2. K. Akiyama *et al.*, *J. Nucl. Radiochem. Sci.*, **1**, Suppl. 2, 76 (2000).
3. K. Akiyama *et al.*, *J. Am. Chem. Soc.*, **123** (1), 181 (2001).



SYSTEMATIC STUDY OF LANTHANOID  
ENDOEDRAL METALLOFULLERENES

Keisuke SUEKI<sup>1</sup>, Kazuhiko AKIYAMA<sup>1</sup>, Yuliang ZHAO<sup>1</sup>, Idumi ITO<sup>1</sup>, Yoshitaka OHKUBO<sup>2</sup>, Koichi KIKUCHI<sup>1</sup>, Motomi KATADA<sup>1</sup>, and Hiromichi NAKAHARA<sup>1</sup>

1 Graduate School of Science, Tokyo Metropolitan University, Hachioji, Tokyo 192-0397, JAPAN

2 Research Reactor Institute, Kyoto University, Kumatori, Osaka 590-0494, JAPAN

We investigated relative production yields and HPLC retention times of lanthanoid metallofullerenes by using the radiochemical method which was most suited for quantitative determinations and detections of small amounts of fullerene species containing specific metal atoms in the presence of many other metallofullerenes. We also investigated the overall effects of the reactor irradiation (the effects due to neutron capture reactions and the gamma irradiations. The experimental data inevitable include recovery yields from the sample container.) on the survivability (or retention yield) of metallofullerenes.

Two types of carbon rods of 6 mm diameter, the first type containing lanthanoid oxides of La, (Ce), Pr, Gd, Tb, Ho, Er, Lu, and the second one, La, Ce, Pr, Nd, Gd, (Tb), with the ratios of numbers of atoms of Ln/C = 1/50, 1/120, 1/200 were fabricated. The arc discharge was carried out with the electric current of 50 A in the 400 Torr He atmosphere.

Neutron irradiations were carried out for both the "crude" samples without HPLC separations and the "composite metallofullerenes" eluted at the retention time expected for the mono-metallofullerene of M@C<sub>82</sub>, and for di-atomic metallofullerenes of M<sub>1</sub>M<sub>2</sub>@C<sub>82</sub> and M<sub>1</sub>M<sub>2</sub>@C<sub>80</sub> ( The presence of the metallic atoms of M<sub>1</sub> and M<sub>2</sub> was ascertained by the gamma-ray measurements in the HPLC fractions expected for the above di-atomic metallofullerenes, but no information could be obtained in the present experiment on the combination of two atoms, namely, di-metallofullerene of M<sub>1</sub>=M<sub>2</sub> (homo type) or M<sub>1</sub>≠M<sub>2</sub> (hetero type) or a mixture of both.). For the study of the survivability of M@C<sub>82</sub>, the irradiated samples were treated as described in the previous report[1].

The production yields of M@C<sub>82</sub> relative to La@C<sub>82</sub> were found to decrease as the atomic number of M became larger and as the number of atoms ratio, C/M, in the carbon rod became smaller. On the other hand, the production yields of M<sub>1</sub>M<sub>2</sub>@C<sub>82</sub>, relative to that of LuM@C<sub>82</sub> were found to increase as the atomic number became larger. Production of M<sub>1</sub>M<sub>2</sub>@C<sub>80</sub> was observed only for La, Ce and Pr with the maximum yield for Ce.

In the Buckyprep elution, some small difference of the retention time was observed for M@C<sub>82</sub> species even among lanthanoid elements that had been reported to take the +3 oxidation state. The retention time was found to become slightly longer for the larger atomic number and, also, those for Gd and Tb were found to be longer by 3-5 % compared with other neighboring elements.

The overall survivability of 19.7±2.1 % in the reactor irradiation was deduced by the experiments on La@C<sub>82</sub> that were aimed to cancel out the corrections required for chemical yields during the chemical treatment.

I. K. Sueki, K. Kikuchi, K. Tomura, H. Nakahara, *J. Radioanal. Nucl. Chem.*, 234, 95 (1998).

## A POSSIBILITY TO STUDY SUBSTANCE PROPERTIES USING POSITRONIUM AS THE SIMPLEST "LABELED" ATOM

Victor P. SHANTAROVICH<sup>1,2</sup>, Takenori SUZUKI<sup>2</sup>, Chunqing HE<sup>2</sup>

<sup>1</sup>Semenov Institute of Chemical Physics Russian Academy of Sciences, 4 Kosygin str., Moscow, 117334, Russia.

<sup>2</sup>High Energy Acceleration Research Organization (KEK), Tsukuba, Ibaraki 305-0801, Japan.

Due to a special structure and properties, a bound state of positron ( $e^+$ ) and electron, which is called positronium (Ps), can be considered as a kind of hydrogen-like atom and a simplest free radical, which has a positron instead of a heavy nucleus. Annihilation  $\gamma$ -rays are coming out in the moment of positronium annihilation. They are used as a label of this short-lived atom. Therefore, positronium chemistry can be considered as radiochemistry of the lightest short-lived "labeled" atom [1]. At present, the most of positronium chemical reactions and mechanisms of Ps formation are studied. Some of the reactions are very similar to those of atomic hydrogen or of usual free radicals (oxidation, spin exchange, formation of intermediate complex or of the bound state with acceptor (PsAc), etc). Investigations of these reactions elucidate the role of steric hindrances in spin-exchange interactions of stable radicals with coordinated paramagnetic ions, provide some information on distribution of electron density in organic molecules with conjugated bonds.

On the other hand, Ps atom is a "quantum" particle, and therefore some peculiarities, typical for light particles, such as tunneling, "bubble" formation around Ps in liquids occur. They can be interesting for the quantum theory of light particles.

While some aspects of positronium radiochemistry can be compared with chemistry of heavy particles, positronium formation and inhibition are strongly related to radiation chemistry. For instance, Ps atoms in liquids and solids are formed in positron spur (track), consisting of electrons, which are produced by moderating positron [2]. Therefore, Ps formation is mostly controlled by the same fast processes in the spur, as formation and inhibition of radiolytic hydrogen (RH). Therefore, activity of different inhibitors of Ps formation can be used for estimation of their activity as scavengers of RH (scavengers of RH precursors). Sometimes, however, accuracy of this approach can be destroyed, when inhibition of Ps is produced not by trapping of spur electrons, but by scavenging of  $e^+$  by some atomic groups or ions which have dipole moment or negative charge. Fortunately, they can be distinguished by using Ge-Ge coincidence measurements of annihilation radiation, which are able to distinguish mechanisms of  $e^+$  annihilation, and also thermostimulated luminescence glow (TSLG) experiments, which are sensitive to electron trapping.

Finally, annihilation of Ps in polymers supplies valuable information on elementary free volumes in these systems [3,4].

1. V. I. Goldanskii; V. P. Shantarovich, *Radiat. Phys. Chem.*, **28**, 25 (1986).
2. O. E. Mogensen, *Positron Annihilation in Chemistry*. Springer-Verlag, Berlin, 1995.
3. K. Tanaka; T. Kawai; H. Kita; K. Okamoto; Y. Ito, *Macromolecules* **33**, 5513 (2000).
4. V. P. Shantarovich; I. B. Kevdina; Yu.P.Yampolskii, *Macromolecules* **33**, 7453 (2000).

Yutaka ITO

Radiation Science Center , High Energy Accelerator Research Organization (KEK)

It has been considered that positrons in C60 are distributed in the interstitial sites between the C60 molecules. It is demonstrated by the measurement of the temperature dependence of Doppler-broadening of positron annihilation radiation.

On the other hand, in K6C60, the maximum positron density distribution move to the cavity space inside the C60 molecule because the positrons are repelled by Coulomb interaction from K atoms. In this report, positron annihilation characteristics in C60 and K6C60 are reported.

Michael K. Kubo<sup>1</sup> and Kusuo Nishiyama<sup>2</sup>

<sup>1</sup>Department of Chemistry, School of Science, the University of Tokyo, 7-3-1 Hongo, Bunkyo-ku, Tokyo 113-0033, Japan

<sup>2</sup>Institute of Materials Structure Science, High Energy Accelerator Research Organization, 1-1 Oho, Tsukuba 305-0801, Japan

Positive muons form muonium by combining with electrons during and after thermalization in implanted media. Muonium yield varies with physical and chemical state of the stopping materials. Water exhibits a sharp muonium yield drop on melting, which is attributed to the breakage of long-range hydrogen-bond network. Ammonia (mp 195K, bp 240K), a simple binary compound and a common polar solvent like water, has a unique property that it dissolves alkali and alkaline-earth metal to form stable solvated electron solution. Since a positive muon picks up an electron from media to form a muonium, solvated electron may assist the formation of muonium in ammonia. In this study we have investigated the physical and chemical behaviors of positive muons method in condensed phase ammonia and ammonia solution of sodium by using the  $\mu$ SR method.

High-purity ammonia (99.999%) was purified with a KOH dehydration column and reacted with metallic sodium. After repeating freeze-pump-and-thaw cycles, pure ammonia was sealed in a 35mm $\phi$  glass bulb. In order to prepare ammonia solutions of sodium appropriate amount of sodium chips were placed in the bulbs before introduction of ammonia. A sample bulb was set in a cryostat at the  $\mu$  port of KEK-MSL where residual magnetic field around the sample was compensated to less than 2 $\mu$ T with correction coils for muonium spin rotation measurement.

Transverse field  $\mu$ SR measurement of pure ammonia revealed that in liquid and in solid above 125K the diamagnetic muon yield ( $P_D$ ) was constantly 0.66 $\pm$ 0.01. Below 100K a new diamagnetic muon component with a large muon spin relaxation rate appeared in solid and  $P_D$  monotonously decreased to 0.31 $\pm$ 0.01 at 10K. No spin relaxation was observed for diamagnetic muon in liquid. The zero-field muon spin relaxation function in solid changed from Kubo-Toyabe type at higher temperatures to exponential around 100K. The Kubo-Toyabe type relaxation evidences the diamagnetic environment of the muon where the muon spin relaxes due to the randomly oriented magnetic field mainly originated from the protons in ammonia. The exponential type relaxation function at low temperatures suggests that the muon resides in paramagnetic environment prepared by the unpaired electrons radiolytically produced by the muon passage. Diamagnetic muon yields in Na solutions depended on the Na concentration. In 1.5% mol/mol solution  $P_D$  was 0.98 $\pm$ 0.01. The large  $P_D$  value could be explained by the result of (1) prevention by the dense paramagnetic environment from coherent interaction of muon and electron in muonium to give apparent diamagnetic muon signal, or (2) local insulator-to-metal change due to the increase of free electron density by the addition of radiolytically liberated electrons to original ones. Muonium was observed in pure solid above 125K and in liquid.

Muonium signal decayed with a larger rate at higher temperatures in liquid. The decay could be caused by the reaction of muonium with solvated electrons, which induces muonium spin state change from triplet to singlet and leads to apparent spin relaxation.

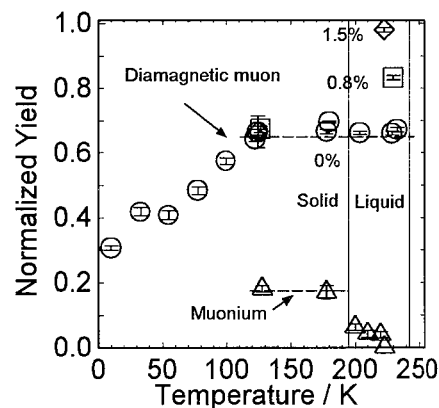


Fig. 1. Temperature dependence of diamagnetic muon yields (open circles for pure  $\text{NH}_3$ , open squares for Na solutions of  $\text{NH}_3$ ) and muonium yield (triangles). Numbers refer to Na concentration.

**DETERMINATION OF ANTIPROTON MASS FROM THE  
CALCULATION OF ENERGY LEVELS OF  
ANTIPROTONIC HELIUM ATOMS**

Yasushi KINO,<sup>1</sup> Masayasu KAMIMURA<sup>2</sup> and Hiroshi KUDO<sup>1</sup>

<sup>1</sup>Department of Chemistry, Graduate School of Science, Tohoku University, Sendai 980-8578, Japan

<sup>2</sup>Department of Physics, Graduate School of Science, Kyushu University, Fukuoka 812-8581, Japan

A few percent of antiprotons stopped in the helium target form antiprotonic helium atoms ( $\bar{p}\text{He}^+$ ) consisting of an antiproton ( $\bar{p}$ ), an electron ( $e^-$ ) and a helium nucleus ( $\text{He}^{2+}$ ) in metastable states with an extremely long lifetime of the order of a microsecond. Such a long-lived antiprotonic atom has stimulated spectroscopic studies from a viewpoint of antimatter science: CPT invariance and weak equivalence principle, interaction between matter and antimatter, etc. We precisely calculated the energy levels of the metastable states to predict the transition frequencies for the laser spectroscopy of the antiprotonic helium atoms. The accuracy of more than nine significant figures has been achieved. In Table 1, transition frequencies and uncertainty of antiproton mass are listed. The calculated values are in good agreement with the latest experimental values<sup>1</sup>. According to the Ref. [2], uncertainty of antiproton mass  $\Delta m_{\bar{p}}/m_{\bar{p}}$  is estimated by changing the antiproton mass. We calculated the frequency as a function of a shift parameter  $x$ :  $x \equiv (m_{\bar{p}} - m_p)/m_p$ . The uncertainty is given by

$$\Delta m_{\bar{p}}/m_{\bar{p}} = (v_{\text{theory}} - v_{\text{experiment}}) \left( dv_{\text{theory}}/dx \right)^{-1}.$$

The result reduced the uncertainty of the antiproton mass by two orders of magnitude as compared to the literature value obtained by X-ray measurements of antiprotonic atoms<sup>3</sup>.

TABLE 1. Transition frequencies  $\nu$  and uncertainty of antiproton mass  $\Delta m_{\bar{p}}/m_{\bar{p}}$

$(J_i, \nu_i) \rightarrow (J_f, \nu_f)$	$\nu_{\text{theory}}/\text{GHz}$	$\nu_{\text{experiment}}/\text{GHz}$	$\Delta m_{\bar{p}}/m_{\bar{p}}$
(32,0) $\rightarrow$ (31,0)	1012445.559	1012445.52(17)	9.44[-8]
(33,1) $\rightarrow$ (32,1)	804633.127	804633.11(11)	5.41[-8]

1. M. Hori *et al.*, *Phys. Rev. Lett.*, **87**, 093401 (2001).

2. Y. Kino, M. Kamimura and H. Kudo, *Hyperfine Interactions*, **119**, 201 (1999).

3. P. Roberson *et al.*, *Phys. Rev. C*, **16**, 1945 (1977).

Wataru SATO,<sup>1</sup> Hideki UENO,<sup>1</sup> Hiroshi WATANABE,<sup>1</sup> Hiroshi OGAWA,<sup>2</sup> Hisanori MIYOSHI,<sup>3</sup> Nobuaki IMAI,<sup>4</sup> Akihiro YOSHIMI,<sup>1</sup> Ken-ichiro YONEDA,<sup>1</sup> Daisuke KAMEDA,<sup>3</sup> Yoshio KOBAYASHI,<sup>1</sup> and Koichiro ASAHI<sup>1,3</sup>

<sup>1</sup>Applied Nuclear Physics Laboratory, RIKEN, Hirosawa, Wako, Saitama 351-0198, Japan

<sup>2</sup>Photonics Research Institute, AIST, Tsukuba, Ibaraki 305-8568, Japan

<sup>3</sup>Department of Physics, Tokyo Institute of Technology, Meguro, Tokyo 152-8551, Japan

<sup>4</sup>Department of Physics, University of Tokyo, Bunkyo, Tokyo 113-0033, Japan

On-line time-differential perturbed angular correlation (TDPAC) measurements were, for the first time, performed with  $^{19}\text{F}$  probes at the RIKEN accelerator research facility. The RIKEN projectile-fragmentation separator (RIPS)<sup>1</sup> was used for the separation of the  $^{19}\text{O}$  beam, the precursor of  $^{19}\text{F}$ , out of various kinds of fragments produced by a projectile-fragmentation reaction of the primary  $^{22}\text{Ne}$  beam. The  $^{19}\text{O}$  beam was first introduced in distilled water for the purpose of observing the directional anisotropy of the (1357-197)-keV cascade  $\gamma$  rays emitted from the probes. A preliminary TDPAC spectrum of  $^{19}\text{F}$  in the water is shown in Figure. Precise analysis allows us to evaluate the experimental value of the angular correlation coefficient. For an application of this on-line TDPAC method to solid state physics, fullerene  $\text{C}_{60}$  was adopted as a host matrix of the  $^{19}\text{F}$  probes. The data analysis is now in progress, and the details will be discussed in the presentation.

Because the precursor beam is oxygen, this implantation method is expected to be applicable to studies of a wide variety of substances with oxygen atoms.

1. T. Kubo, M. Ishihara, N. Inabe, H. Kumagai, I. Tanihata, K. Yoshida, T. Nakamura, H. Okuno, S. Shimoura, and K. Asahi; *Nucl. Instr. and Meth.* **B70**, 309 (1992).

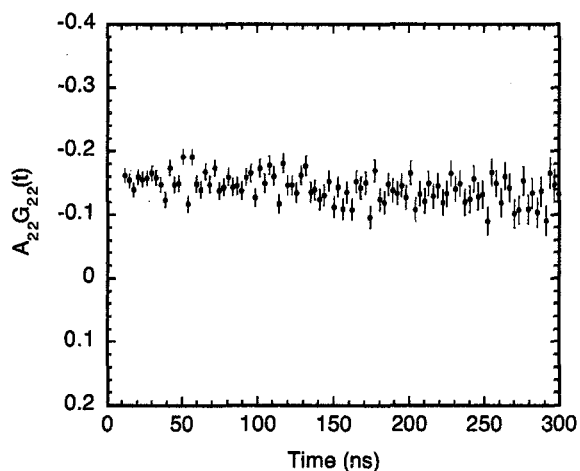


Fig. A preliminary TDPAC spectrum of  $^{19}\text{F}$  in distilled water.

## 2B8 Characterization of Perovskite Related Oxides by Nuclear Resonance Inelastic Scattering of Synchrotron Radiation.

K. Nomura, T. Misui\*, A. Rykov, Y. Yoda\*\*, Y. Kobayashi\*\*\*, M. Seto\*\*\*,  
School of Engineering, The University of Tokyo, 113-8656

\*Japan Atomic Energy Research Institute,

\*\* Japan Synchrotron Radiation Research Institute,

\*\*\* Institute of Atomic Reactor, Kyoto University,

Nuclear Resonance Inelastic Scattering (NIS) spectra of  $(\text{Sr,Ca})(\text{Fe,Co})\text{O}_{3-\delta}$  and  $(\text{Ba,Ca})(\text{Fe,Co})\text{O}_{3-\delta}$  for rapid  $\text{CO}_2$  absorption at high temperatures were observed by detecting 6.3 keV with avalanche photodiode detectors after Mössbauer effect of the monochromatized beam of 14.41 keV (energy resolution: 3.5 meV) in SPring8 facility. The measuring time was about 2 hours for a sample including natural abundance of  $^{57}\text{Fe}$ .

The phonon peaks around 8 meV, 16 and 24 meV were observed in NIS spectra of the  $(\text{Sr}_{0.5}\text{Ca}_{0.5})(\text{Fe}_{0.5}\text{Co}_{0.5})\text{O}_{3-\delta}$ . These peaks are similar to those of  $\text{SrFeO}_{2.5}$  [1]. The phonons in  $\text{CaFeO}_{2.5}$  showed the peaks at 7, 14 and 21 meV. The specific phonon peaks were not so clearly observed in NIS spectra of  $(\text{Sr}_{0.95}\text{Ca}_{0.05})(\text{Fe}_{0.5}\text{Co}_{0.5})\text{O}_{3-\delta}$  and  $(\text{Sr}_{0.7}\text{Ca}_{0.3})(\text{Fe}_{0.5}\text{Co}_{0.5})\text{O}_{3-\delta}$ . These are the cubic structures with oxygen vacancies, and the multi phonons created may be caused by random oxygen vacancies.

On the other hand, Ba substituted oxides,  $(\text{Ba,Ca})(\text{Fe,Co})\text{O}_{3-\delta}$ , were also characterized by the NIS. In the Ba substituted oxides, the phonon modes were a little harder than those in the Sr substituted oxides.

After  $\text{CO}_2$  absorption, the peak intensity around 8 meV phonon decreased relatively and some other specific peaks appeared in the NIS spectra. The difference is considered to depend on the amount and arrangement of the trapped  $\text{CO}_2$  and the oxygen vacancies. Ba, Sr and Ca ions are in turn of strong affinity to  $\text{CO}_3^{2-}$ . It is found that the vibration modes around Fe atoms are affected by the trapped  $\text{CO}_2$  although it was hard to distinguish between the related oxides with the trapped  $\text{CO}_2$  and with the oxygen vacancies by a conventional Mössbauer spectrometry.

[1] W. Sturhahn et al, Phys. Rev. Lett., 74(1955)3822.

Zoltán KLENCSÁR<sup>1</sup>, Ernő KUZMANN<sup>1</sup>, Attila VÉRTES<sup>1</sup>, Athanassios SIMOPOULOS<sup>2</sup>,  
Eamon DEVLIN<sup>2</sup>, George KALLIAS<sup>2</sup>, Amar NATH<sup>3</sup>

<sup>1</sup>Research Group for Nuclear Methods in Structural Chemistry at the Eötvös Loránd  
University, Hungarian Academy of Sciences, H-1518, P.O.Box 32, Budapest 112, Hungary

<sup>2</sup>Institute of Materials Science, NCSR Demokritos, 153 10 Aghia Paraskevi, Athens-Greece

<sup>3</sup>Department of Chemistry, Drexel University, Philadelphia 19104, USA

It is widely accepted that the negative magnetoresistance observed in Mn based perovskite structures can be explained by the so called double-exchange (DE) phenomenon. According to the DE model – originating from Zener<sup>1</sup> and adapted later on to the case of Mn based CMR systems – in La<sub>1-x</sub>M<sub>x</sub>MnO<sub>3</sub> (M=Ca, Sr, Ba) the electrical conductivity is determined by the hopping of the electrons between Mn<sup>3+</sup> and Mn<sup>4+</sup> cations. As the hopping is promoted only by the parallel alignment of the Mn<sup>3+</sup> and Mn<sup>4+</sup> spins, applying an external magnetic field on a magnetically disordered or only partly ordered system will enhance electrical conductivity by aligning the spins of manganese cations in the same direction. As described, the DE model can be effective only in heterovalent systems.

Recently, however, colossal magnetoresistance has been observed in the ferrimagnetic FeCr<sub>2</sub>S<sub>4</sub> with the cubic spinel structure<sup>2</sup>. It was suggested that the DE model couldn't account for the negative magnetoresistance in this material, because there is not any valence variation in a stoichiometric FeCr<sub>2</sub>S<sub>4</sub> spinel. Moreover, it was claimed<sup>3</sup> that, in contrast with Mn based perovskite systems, in FeCr<sub>2</sub>S<sub>4</sub> there is not any appreciable structural discontinuity around the Curie temperature. At the same time ESR spectra indicated that in FeCr<sub>2</sub>S<sub>4</sub> the paramagnetic phase might coexist with the ferrimagnetic one below the Curie temperature ( $\approx 175$  K)<sup>3</sup>.

In order to gain insight into the magnetic and electronic state of iron in FeCr<sub>2</sub>S<sub>4</sub>, we acquired the original sample of A.P. Ramirez et al.<sup>2</sup>\*, and performed detailed <sup>57</sup>Fe Mössbauer spectroscopy measurements in the temperature range of 75 K – 290 K. Additionally, <sup>57</sup>Fe Mössbauer measurements in H = 6 T magnetic field were carried out at T = 90 K and at T = 186.5 K the latter temperature being in the neighborhood of the Curie temperature.

Our results provide evidence that by lowering the temperature in FeCr<sub>2</sub>S<sub>4</sub> a seemingly paramagnetic phase can coexist with the ferrimagnetic one due to superparamagnetic-like relaxation behavior below the Curie temperature. Around T = 160 K the ferrimagnetic to paramagnetic transition is accompanied by a sudden change in the Mössbauer parameters including the <sup>57</sup>Fe isomer shift, the Mössbauer-Lamb factor and the width of the absorption lines. Further anomalous changes of the Mössbauer parameters were obtained around T = 120 K and T = 80 K. Below the Curie temperature Fe<sup>3+</sup> ( $\approx 5-8$  %) and Fe<sup>2+</sup> was found to coexist.

The origin of the anomalous changes of the <sup>57</sup>Fe Mössbauer parameters, the superparamagnetic-like relaxation and their possible relation to the CMR effect in FeCr<sub>2</sub>S<sub>4</sub> will be discussed.

#### Acknowledgement

\* We thank Dr. A.P. Ramirez for providing us with the original FeCr<sub>2</sub>S<sub>4</sub> sample.

1. C. Zener, *Phys. Rev.*, **82**, 403(1951).

2. A.P. Ramirez, R.J. Cava, J. Krajewski, *Nature*, **386**, 156(1997).

3. Z. Yang, S. Tan, Y. Zang, *Solid State Communications*, **115**, 679(2000).



Crystal Structures and  $^{155}\text{Gd}$  Mössbauer Spectra of Some Gd(III)- $\beta$ -diketonato Complexes

Junhu Wang\*, Masashi Takahashi, Takafumi Kitazawa, and Masuo Takeda  
Department of Chemistry, Faculty of Science, Toho University, 2-2-1  
Miyama, Funabashi, Chiba 274-8510, Japan

We have prepared a  $^{155}\text{Eu}/^{154}\text{SmPd}_3$  (about 231 MBq) source and started the  $^{155}\text{Gd}$  Mössbauer spectroscopic studies on the structural chemistry of a number of gadolinium compounds. In the course of the investigation of the Gd(III)-EDTA complexes, some difference was observed in quadrupole coupling constant ( $e^2qQ$ ), but not in isomer shift ( $\delta$ ). In order to examine the applicability of  $\delta$  for Gd(III) complexes, we have carried out a systematic study using the Gd(III)- $\beta$ -diketonato complexes. We have also made several X-ray structural determinations to obtain crystal and molecular structures of the complexes.

The distorted square antiprism structures for  $\text{Gd}(\text{bfa})_3 \cdot 2\text{H}_2\text{O}$  and  $\text{Gd}(\text{pta})_3 \cdot 2\text{H}_2\text{O}$  have been determined by the X-ray crystallography. The  $^{155}\text{Gd}$  Mössbauer spectra are typical patterns of electric quadrupole interactions for  $^{155}\text{Gd}$  nucleus. The spectra are computer-fitted to quadrupole-split five-lines ( $\eta = 0$ ) using a sum of the Lorentz approximation. The difference in  $\delta$  for these complexes ( $0.55 \sim 0.65 \text{ mms}^{-1}$  relative to the source) are smaller than that for the reported intermetallic compounds ( $-0.2 \sim 0.9 \text{ mms}^{-1}$ )<sup>1)</sup>. Comparing the  $\delta$  values for  $\beta$ -diketone, EDTA and the cyano-bridged Gd(III) complexes, a tendency that the  $\delta$  value decreases with the increase in the number of the coordinating nitrogen atoms is found: i.e. the  $\delta$  values are decreased in the order of  $\beta$ -diketonato complexes (Coordination sphere:  $\text{GdO}_7$  or  $\text{GdO}_8$ ) > EDTA complexes ( $\text{GdN}_2\text{O}_6$  or  $\text{GdN}_2\text{O}_7$ ) > cyano-bridged complexes ( $\text{GdN}_6\text{O}_2$ ). On the other hand the  $e^2qQ$  values from 1.67 to  $7.56 \text{ mms}^{-1}$  are observed. It reflects the difference in the coordination number and the symmetry of the coordination polyhedron around gadolinium ion.

1. Gordon Czjzek, in: *Mössbauer Spectroscopy Applied to Magnetism and Materials Science*, Gary J. Long and Fernande Grandjean(Eds), Plenum Press, New York, 1993, Vol. 1, p373.

fax: +81-474-75-1855 e-mail: wangjh@alchemist.chem.sci.toho-u.ac.jp

2C1

## Natural Po-organic compounds in the black shales as a consequence of nuclear recoils effects

R. V. Bogdanov, S. A. Ozernaya, and S. A. Timofeev

Chemical department, Saint-Petersburg State University, Russia;

The alpha -activity of fractions of humic and fulvic acids, as well as the mineral fractions of metal hydroxides isolated by using alkaline extraction from oil shale (dictionema) was studied. All three fractions contain the uranium-ionium spectrum component. The activity of fractions in the energetic range of about 5.3 MeV corresponding to  $^{210}\text{Po}$  is as follows: humates 7-10%, fulvates 20%, hydroxides less than 1% of the total activity of sources.  $^{226}\text{Ra}$  and its short-lived decay products ( $^{222}\text{Rn}$ ,  $^{218}\text{Po}$ ,  $^{214}\text{Po}$ ) were not detected in any fraction, which results from decalcination of humus acids during chemical procedures. The results made it possible for the authors to conclude that recoil-effects after the alpha-decay of  $^{214}\text{Po}$  and the two subsequent alpha-decays do not prevent the reconstruction of initially destroyed molecules of humus acids and the formation of polonium humates and fulvates. The authors believe that 'hot' synthesis of natural organic derivatives labelled with polonium take place.

Toshiaki MITSUGASHIRA<sup>1</sup>, Mitsuo HARA<sup>1</sup>,  
Poong KIM<sup>2</sup>, Kouichi NAKASHIMA<sup>3</sup>, Kouji NAKAYAMA<sup>3</sup>,

<sup>1</sup>The Oarai-branch, IMR, Tohoku University, 311-1313 Oarai-machi, Ibaraki, Japan

<sup>2</sup>Vacum Metallurgical Co., Ltd(ULVAC), 289-1297 Sanbu-machi, Tiba, Japan

<sup>3</sup>ULVAC Materials Technology Co., Ltd, 899-6301 Yokogawa-machi, Kagoshima, Japan

### 1. Introduction

Since software-errors by natural  $\alpha$ -emitters in memory materials was pointed out to be one of major issues influencing the VLSI and ULSI qualities, the techniques for the removal of uranium and thorium and for the trace analysis of these chemical elements have become the main research target for modern semiconductor industry. Today, ICP-Mass spectrometry (ICP-MS) and radiochemical neutron activation analysis (RNAA) are used as the most sensitive method for analyzing sub ppb-level of uranium and thorium. Though these two methods are equally effective in analyzing  $^{238}\text{U}$  and  $^{232}\text{Th}$ , these method are not useful for analyzing their daughter  $\alpha$ -emitters. This report describes the results of  $\alpha$ -spectrometry that were obtained by applying the Sm-method<sup>1)</sup> to the analysis of  $\alpha$ -emitters in high purity semiconductor materials.

### 2. Experimental

The samples used for this research were high purity commercial aluminum (5N-up Al) and the tail end of the zone refined aluminum rod (Tail Al). The samples were dissolved in HCl solution for uranium analysis and in  $\text{HNO}_3$  solution for thorium analysis, respectively. The solution was passed through an anion exchange resin column to trap uranium and thorium. After the removal of aluminum, uranium and thorium were recovered in diluted HCl solution and co-precipitated with  $\text{SmF}_3$ . The precipitates were mounted as a counting source for  $\alpha$ -spectrometry.

### 3. Results and discussion

The analytical results are summarized in Table 1. As is shown in the table, the results of  $\alpha$ -spectrometry are in quite good agreement with those of ICP-MS. Radioactivity ratios in Tail Al are calculated to be  $^{234}\text{U}/^{238}\text{U}=1.1$ ,  $^{230}\text{Th}/^{238}\text{U}=1.4$ , and  $^{228}\text{Th}/^{232}\text{Th}=2.2$ , respectively, and those in 5N-up Al are  $^{234}\text{U}/^{238}\text{U}=1.1$ ,  $^{230}\text{Th}/^{238}\text{U}=1.5$ , and  $^{228}\text{Th}/^{232}\text{Th}=1.7$ , respectively. This finding suggests that the radioactivity of daughter nuclide is larger than that of each precursor nuclide.

Table-1 Analysis of aluminum

Sample	Nuclides	$\alpha$ -spectrometry	ICP-MS
5N-up Al	$^{238}\text{U}$	$0.072 \pm 0.008$ mBq/g (5.8ppb)	$5.4 \pm 1.0$ ppb
	$^{234}\text{U}$		
	$^{230}\text{Th}$		
	$^{232}\text{Th}$		
	$^{228}\text{Th}$		
Tail Al	$^{238}\text{U}$	$0.70 \pm 0.08$ mBq/g (57ppb)	$36 \pm 10$ ppb
	$^{234}\text{U}$		
	$^{230}\text{Th}$		
	$^{232}\text{Th}$		
	$^{228}\text{Th}$		

1) T. Mitsugashira, et al., J. Radioanal. Nucl. Chem., 239(2), 345-349(1999).

## Development for a High Efficiency Radon-222 Collection System Utilizing Silicone Oil as a Cold Trap Agent

Naoyuki.Hirose,<sup>1</sup> Noriyoshi.Tsuyuzaki,<sup>1</sup> Hiroyasu.Yamamoto,<sup>1</sup> Toshiaki.Mitsugashira<sup>2</sup>  
and Mitsuo.Hara<sup>2</sup>

<sup>1</sup>IWAKI Electronics Co.,Ltd. Iwaki, Fukushima 972-8322, Japan

<sup>2</sup>The Oarai-branch, IMR, Tohoku Univ., Oarai, Ibaraki 311-1313, Japan

We are developing a random number generator and a probability generator that utilizes detection of alpha-decay as a natural random phenomenon.<sup>1)</sup> In considering on environmental impact, a natural radioactive isotope  $^{210}\text{Pb}$  that is a precursor of  $^{210}\text{Po}$  is the best choice for such industrial application.

In order to get highly pure and carrier free  $^{210}\text{Pb}$  actively, we have examined silicone oil as a cold trap agent for approximately  $30\text{ kBq/m}^3$  of  $^{222}\text{Rn}$  that is emanated from natural uranium ores (6.4 g of  $^{238}\text{U}$  per 260 g of the powder). The collection system was operated at 196K by using solid  $\text{CO}_2$  and methanol as the freezing mixture. Nitrogen gas (40 ml/min) was used to carry the radon into the silicone oil (370 ml, approximately 40 mm in diameter by 300 mm long, see Fig.1). By this simple arrangement,  $^{222}\text{Rn}$  was trapped at the collection efficiency of approximately 22% for one week continuous operation. So as to trap  $^{222}\text{Rn}$  with higher efficiency, we tried to lead  $^{222}\text{Rn}$  with nitrogen gas into a glass tube set in liquid nitrogen. The result will be opened at the symposium.

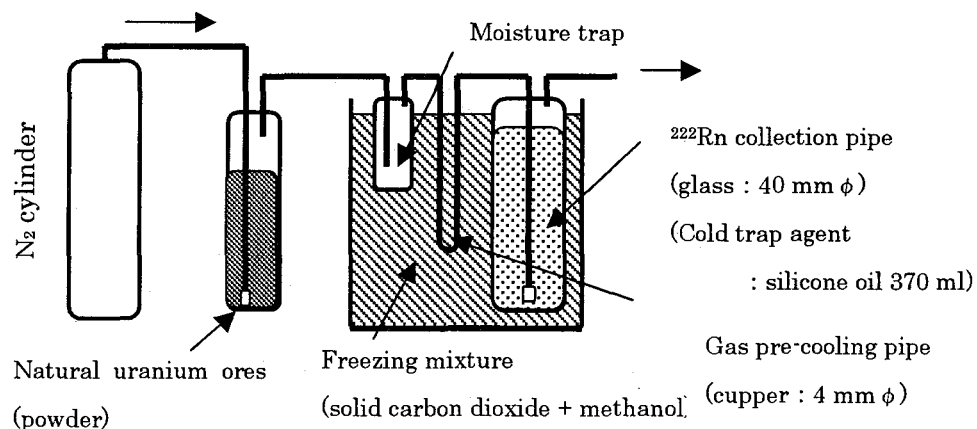


**Fig.1 Diagram of  $^{222}\text{Rn}$  collection system utilizing silicone oil as a cold trap agent.**

1. N.Tsuyuzaki et.al.: Development of the Random Pulse System using of the alpha-particle, Proceedings of the Electronics, Information and Systems Conference, *Electronics, Information and Systems Society I.E.E. of Japan.*, p367-368, Aug. (1995).

## APPLICATION OF LOW BACKGROUND $\gamma$ -RAY SPECTROMETRY TO ENVIRONMENTAL MONITORING SAMPLES

### --- WATER LEACHING TREATMENT FOR $^{40}\text{K}$ -REMOVAL ---

Mutsuo INOUE, Hisaki KOFUJI, Masayoshi YAMAMOTO, Hideki SASAGAWA and  
Kazuhisa KOMURA

Low Level Radioactivity Laboratory, Faculty of science, Kanazawa University,  
Tatsunokuchi, Ishikawa 923-1224, Japan

Gamma-ray measurement has been carried out for monitoring of natural and artificial radionuclides in marine and agricultural products. Especially, for careful examination, low background (low S/N) measurement is inevitable to evaluate extremely low-level radionuclides. In the conventional gamma-ray spectrometry, however, Compton scattering of the 1461 keV gamma-ray from  $^{40}\text{K}$  severely interferes the detection of artificial radionuclides because potassium is one of main constituents of marine and agricultural products. In order to eliminate the interference of  $^{40}\text{K}$ , we have developed a *simple* and *convenient* "water leaching treatment" method applicable to seaweed samples. By this treatment, most of  $^{40}\text{K}$  (>~98%) could be removed without notable loss of artificial nuclides (e.g., radioactive corrosion products) as well as cosmogenic  $^7\text{Be}$  and U- and Th-series nuclides. In combination with the low-level counting in Ogoya underground Laboratory (270 mwe), the detection limit could be improved >2 orders of magnitude than before (Fig. 1).

Seaweeds have been used for monitoring samples in coastal areas. By applying water leaching method, a number of measurements have been made for seaweed samples (sargasso; Dec. '98 ~) collected in the vicinity of the Shika Atomic Power Station, Ishikawa Prefecture. From these results, we can discuss environmental behaviors of natural and artificial radionuclides in the coastal marine environment (e. g., disequilibrium of U- and Th series).

This method, however, does not give satisfactory merit for other marine and agricultural products. We will also discuss the applicability of present method to other of samples and propose more refined method based on recent experiments.

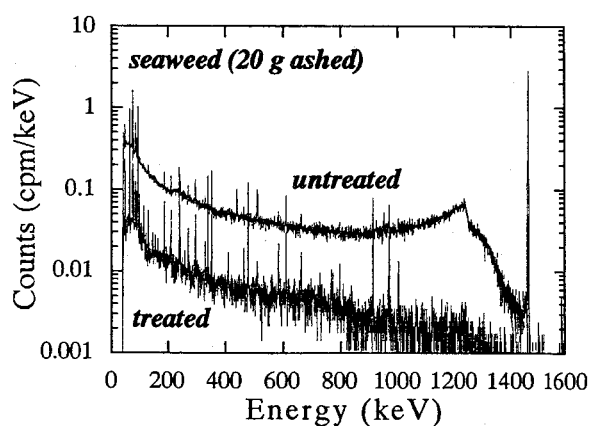


Fig. 1 Improvement of S/N ratio in extremely low background gamma-ray spectrum.

## ACTIVITY LEVELS OF RADIOACTIVE Co AND Eu ISOTOPES INDUCED BY ENVIRONMENTAL NEUTRONS, AND THEIR CONTRIBUTION TO A-BOMB EXPOSED SAMPLES IN HIROSHIMA AND NAGASAKI

Kazuhisa KOMURA<sup>1</sup> and Ahmed. M. YOUSEF<sup>2</sup>

<sup>1</sup>Low Level Radioactivity Laboratory, Kanazawa University, Tatsunokuchi, Ishikawa 923-1224, Japan,

<sup>2</sup>Department of Physics, Faculty of Science, South Valley University, Kena, Egypt

More than 20 radionuclides induced by environmental neutrons have been detected by using ultra low background Ge installed in Ogoya underground laboratory<sup>1</sup>. Among these, natural production of <sup>60</sup>Co and <sup>152</sup>Eu are very important because activities of both <sup>60</sup>Co and <sup>152</sup>Eu in Hiroshima and Nagasaki A-bomb exposed samples are found to be much higher than calculated values (particularly the samples at > 1000 m from the hypo-center). One of the sources of this discrepancy is considered to be the contribution of natural production of these nuclides.

Concentration of natural <sup>60</sup>Co and <sup>152</sup>Eu (<sup>154</sup>Eu and <sup>155</sup>Eu) have been measured for various cobalt and europium reagents purchased recently and also for old ones purchased many years ago up to half-century. Following results have been obtained ; <sup>60</sup>Co = 0.08 - 1.39 mBq g<sup>-1</sup>, <sup>152</sup>Eu = 1.62 - 8.65 mBq g<sup>-1</sup>, <sup>154</sup>Eu = 0.11 - 1.12 mBq g<sup>-1</sup>. These values are 5 to 85 % and only 2 - 11% and 2 - 21 % of saturation activities of 1.63 mBq g<sup>-1</sup> for <sup>60</sup>Co, 80.3 mBq g<sup>-1</sup> for <sup>152</sup>Eu and 5.30 mBq g<sup>-1</sup> for <sup>154</sup>Eu, respectively, which are calculated by assuming environmental neutron flux being 0.008 n cm<sup>-2</sup> s<sup>-1</sup> (at sea level) and no self-shielding of neutron within the target. Existence of <sup>155</sup>Eu (0.09 - 2.63 mBq g<sup>-1</sup>) can be explained as beta-decay product of <sup>154</sup>Sm induced by <sup>154</sup>Sm(n,γ)<sup>155</sup>Sm reaction. Lower values of <sup>60</sup>Co and <sup>152,154</sup>Eu than calculated ones, particularly of <sup>152,154</sup>Eu, may be explained by neutron self-shielding within target and partly by insufficient exposure time compared with their half-lives.

Contribution of natural production of <sup>60</sup>Co and <sup>152</sup>Eu are found to be at most < 10 % and < 1 % on 2001, respectively, at around 1.5 km from the explosion center. Therefore, other unknown sources must be searched to explain large discrepancy between observed and calculated activities.

1. K. Komura and Ahmed M. Yousef, Natural radionuclides induced by environmental neutrons, *Proc. Int. Workshop on Distribution and Speciation of Radionuclides in the Environment*, Rokkasho, Asomori, Japan, October 11-13, 2000. pp 210 – 217 (2000).

W.R. Alexander, W. Kickmaier, I.G. McKinley, M. Hugi

Nagra (National Cooperative for the Disposal of Radioactive Waste)

Hardstrasse 73, 5430 Wettingen, Switzerland

kickmaier@nagra.ch

#### Abstract

Two underground rock laboratories (URLs) in Switzerland allow access to strongly contrasting deep geological environments - a fractured crystalline rock at Grimsel and a very tight sediment (Opalinus Clay) at Mont Terri. A wide range of international collaborative projects run at both of these sites, including studies using radionuclides in-situ. A wide range of safety relevant radionuclides have already been used at Grimsel, where it currently is planned to expand past work with isotopes of U and Np to include other actinides (isotopes of Th, Pu and Am in addition to U and Np). The use of such radionuclides obviously implies strict radioprotection measures and so an IAEA Level B radionuclide controlled zone was built 5 years ago in one of the URL's tunnels.

In the Mont Terri URL, working with radionuclides is at an early stage but the first study of radionuclide migration in the rock matrix has recently been completed and further work is currently being planned.

To date, processes studied at the two URLs include radionuclide retardation in water-conducting features (eg sorption, dispersion, filtration), diffusion in the rock matrix, radionuclide speciation and solubility, the role of colloids and potential influence of hyperalkaline fluids on host rocks radionuclide retardation capacity. At both facilities, new programmes of long-term projects are presently being planned and there are opportunities for interested groups to join as partners or to use the unique infrastructure available for their own experiments.

Finally, in the view of the current international status of repository development, the benefits of generic rock laboratory programmes will be discussed in depth.

## 2C9     **Depth profiles of long lived radionuclides in Chernobyl soils after 10 years from the accident**

Hikaru AMANO<sup>1</sup> and Yoshikazu ONUMA<sup>2</sup>

1 Department of Environmental Sciences, Japan Atomic Energy Research Institute,  
Tokai-mura, Naka-gun, Ibaraki 319-1195, Japan

2 Institute of Radiation Measurement, Tokai-mura, Naka-gun, Ibaraki 319-1106, Japan

Chernobyl 30km zone is unique environment where most deposited radionuclides are in the form of hot particles (HPs) which are fine particles of exploded reactor core. Depth profiles of <sup>137</sup>Cs, <sup>90</sup>Sr, Pu isotopes and <sup>241</sup>Am in uncultivated soils sampled at Chernobyl 30km zone after 10 years from the accident have been analyzed. The examined are sandy, peaty and podzol core soils. Sequential selective extraction was carried out on the soil samples to validate the chemical forms of the radionuclides. In short, the used chemical speciation separates in water soluble, exchangeable under pH 7, exchangeable under pH 4.5, fulvic acid, humic acid, and humin plus insoluble fractions. In general, most radionuclides in the uncultivated soils still exist in the surface, though there are minor penetrating fractions into deeper parts of the soils. Depth profiles of radionuclides in examined soils were different, reflecting the soil component and the chemical speciation of each radionuclide. In common, actinide elements have strong affinity for humic substances. Strontium-90 migrates downward in soils mainly by ion exchange processes after dissolved from HPs. Cesium-137 mainly exists in insoluble fractions in the surface soils, but ion exchangeable fractions of <sup>137</sup>Cs increase in subsurface soils. Among 3 kinds of soils examined, the downward movement of <sup>137</sup>Cs was largest in the peaty soil.



## Variation of $^{14}\text{C}$ , $^{137}\text{Cs}$ and Stable Carbon Composition in Forest Soil and its Implications

Jiangfeng GUO<sup>1,2</sup> Mariko ATARASHI-ANDOH<sup>1</sup> Hikaru AMANO<sup>1</sup>

<sup>1</sup> Dept. of Environmental Science, Tokai Research Establishment, Japan Atomic Energy Research Institute, Tokai-mura, Naka-gun, Ibaraki-ken 319-1195, JAPAN

<sup>2</sup> Institute of Nuclear Agricultural Science, Zhejiang University (Huajiachi campus), Hangzhou, Zhejiang 310029, P.R. CHINA

In Japan, more than half of land area is covered by forest. Therefore, forest ecosystem plays a vital role in ultimate fate of radionuclides in terrestrial environment. In this study, we determined soil organic matter content,  $\delta^{13}\text{C}$ ,  $^{14}\text{C}$  and  $^{137}\text{Cs}$  radioactivity in 3 undisturbed forest soil profiles in Ibaraki prefecture, Japan to estimate  $^{14}\text{C}$  migration in surface environment.

The  $^{137}\text{Cs}$  activities were determined with a germanium gamma detector coupled to a multichannel analyzer. The  $^{137}\text{Cs}$  data illustrate that no disturbance has occurred during past years in 3 soil profiles. The peak values are observed in the top 10 cm of the soil profiles. Considering the local historical record of atmospheric concentration of  $^{137}\text{Cs}$ <sup>[1]</sup>, the maximum fallout deposition of  $^{137}\text{Cs}$  took place around 1964.  $^{14}\text{C}$  activities were determined with fast bomb combustion-liquid scintillation counting method.  $^{14}\text{C}$  determination shows that  $^{14}\text{C}$  also has peak values in the top 10 cm of the soil profiles ascribed to the highest bomb  $^{14}\text{C}$  level in 1960's.

$\delta^{13}\text{C}$  values were measured with isotope ratio mass spectrometer and the data are expressed (in  $\delta$  notation) as per mil and relative to the PDB standard.  $\delta^{13}\text{C}$  values vary from  $-26.6\text{‰}$  to  $-20.3\text{‰}$ ,  $-24.7\text{‰}$  to  $-19.9\text{‰}$  and  $-26.2\text{‰}$  to  $-17.8\text{‰}$  respectively in 3 soil profiles with increasing soil depth. Enrichment of deeper soils in isotope ratio probably results from discrimination against  $^{13}\text{C}$  during mineralization and loss of isotopically lighter carbon from soils due to root uptake, leaching etc. Meanwhile soil organic matter content decreases continuously with increasing soil depth. It shows that  $\delta^{13}\text{C}$  is an excellent indicator of soil carbon turnover and belowground process.

### Reference:

1. A. Kasai, K. Sekine, T. Imai, H. Amano, N. Yanase, T. Matsunaga: Survey data of radionuclides in environmental materials (I), Japan Atomic Energy Research Institute, 1986, JAERI-M reports 86-047, pp40-56;

Norikazu KINOSHITA<sup>1</sup> and Takashi NAKANISHI<sup>2</sup>

<sup>1</sup>Department of Chemical Science, Graduate School of Natural Science and Technology, Kanazawa University, Kakuma-machi, Kanazawa 920-1192, Japan

<sup>2</sup>Department of Chemistry, Faculty of Science, Kanazawa University, Kakuma-machi, Kanazawa 920-1192, Japan.

Samarium-147 is a naturally occurring long-lived alpha emitter. The nuclide has recently been proved to be useful as an internal reference in the determination of alpha emitting nuclides of mBq level by alpha spectrometry. The half-life value currently adopted for the nuclide was determined in 1970 to be  $(1.06 \pm 0.02) \times 10^{11}$  y (Fig. 1).

In the present work, the half-life of  $^{147}\text{Sm}$  has been reevaluated as a part of our research project searching for supernova-produced  $^{146}\text{Sm}$  (alpha emitter, half-life  $1.03 \times 10^8$  y), now extinct in the solar system, accumulated in open ocean deep-sea sediment through cosmic dust deposition. In the project the half-life value of  $^{146}\text{Sm}$  is an important parameter to set a limit for accretion flux of supernova-produced matter onto Earth, and it was planned to reevaluate the half-life of  $^{146}\text{Sm}$  by reference to the half-life of  $^{147}\text{Sm}$  and by measuring  $^{146}\text{Sm}/^{147}\text{Sm}$  alpha-activity ratio and  $^{146}\text{Sm}/^{147}\text{Sm}$  atomic ratio for a mixture of  $^{146}\text{Sm}$  and  $^{147}\text{Sm}$  prepared by irradiating enriched  $^{147}\text{Sm}$  with photons to produce  $^{146}\text{Sm}$  through  $^{147}\text{Sm}(\gamma, n)$  reaction; hence, it is necessary to confirm the half-life of  $^{147}\text{Sm}$  for the reevaluation of the half-life of  $^{146}\text{Sm}$ .

In this work, the half-life of  $^{147}\text{Sm}$  was measured as follows: known amount of standard solution of natural Sm was mixed with known amount of  $^{210}\text{Po}$  or  $^{238}\text{U}$  or  $^{241}\text{Am}$  standard solution, and alpha spectrometry using Si surface barrier detector was carried out for thin deposit of the mixture to determine the disintegration rate of the known amount of  $^{147}\text{Sm}$  by referring to the alpha activity of  $^{210}\text{Po}$  or  $^{238}\text{U}$  or  $^{241}\text{Am}$ . The half-life values obtained in this work are shown in Fig. 1. It is obvious that the mean of the values obtained in this work— $(1.23 \pm 0.05) \times 10^{11}$  y—is longer than currently adopted value.

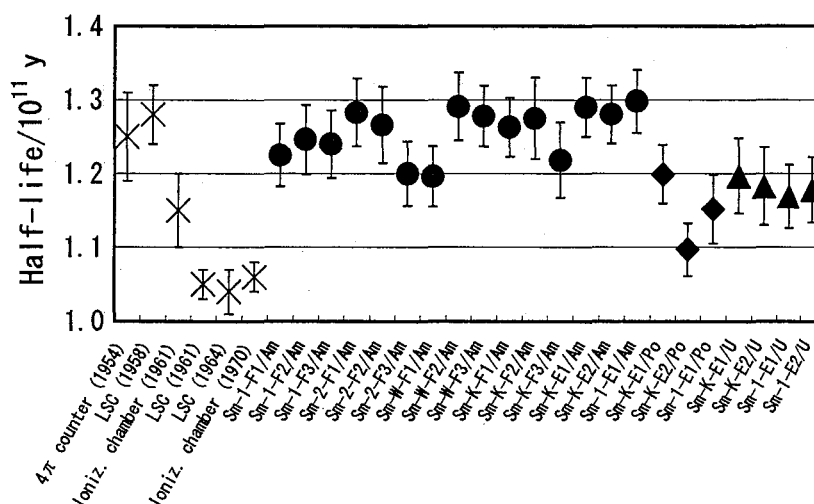


Fig. 1 The half-life of  $^{147}\text{Sm}$ .

×: literature value

●◆▲: this work

## RADIOCHEMICAL STUDY OF PHOTON-INDUCED SPALLATION AT INTERMEDIATE ENERGIES

Hiroshi MATSUMURA<sup>1</sup>, Masumi YAMASHITA<sup>2</sup>, Hidetoshi KIKUNAGA<sup>2</sup>, Hiromitsu HABA<sup>3</sup>, Koshin WASHIYAMA<sup>4</sup>, Yutaka MIYAMOTO<sup>3</sup>, Yasuji OURA<sup>5</sup>, Koh SAKAMOTO<sup>6</sup>, Seiichi SHIBATA<sup>7</sup>, Michiaki FURUKAWA<sup>8</sup> and Ichiro FUJIWARA<sup>9</sup>

<sup>1</sup>College of Humanities and Science, Nihon University, Setagaya-ku, Tokyo 156-8550, Japan, <sup>2</sup>Graduate School of Natural Science and Technology, Kanazawa University, Ishikawa 920-1192, Japan, <sup>3</sup>Japan Atomic Energy Research Institute, Tokai, Ibaraki 319-1195, Japan, <sup>4</sup>Faculty of Medicine, Kanazawa University, Kanazawa, Ishikawa 920-0942, Japan, <sup>5</sup>Graduate School of Science, Tokyo Metropolitan University, Hachioji, Tokyo 192-0397, Japan, <sup>6</sup>Faculty of Science, Kanazawa University, Kanazawa, Ishikawa 920-1192, Japan, <sup>7</sup>Research Reactor Institute, Kyoto University, Sennan-gun, Osaka 590-0494, Japan, <sup>8</sup>Faculty of Environmental and Information Science, Yokkaichi University, Yokkaichi, Mie 512-8512, Japan, <sup>9</sup>Faculty of Economics, Otomon-Gakuin University, Ibaragi, Osaka 567-8502, Japan

Photons of intermediate energies interact electromagnetically with nuclei through giant dipole resonance, quasi-deuteron disintegration (QDD), or (3,3) resonance. The QDD and the (3,3) resonance indicate the interactions with nuclei through a resonance absorption by a proton-neutron pair or a nucleon inside the target nucleus. After the photon absorptions, the nuclear reactions would develop collision cascades. Therefore, photons are expected to be unique probes to look inside nuclei. Our group has measured many yields of photospallation reaction.<sup>1,2</sup> In this study the measured yields of photospallation from a heavy target nucleus, <sup>nat</sup>Ta, in irradiation with bremsstrahlung with maximum end-point energy up to 1100 MeV were added to many ones from other targets accumulated in our group. The experimental data were compared with the results from a calculation code for high-energy photonuclear reactions. As the calculation code, a combination of the PICA3 code by T. Sato<sup>3</sup> updated the PICA95 by C. Y. Fu<sup>4</sup> and the GEM code developed by S. Furihata<sup>5</sup> was used. It was found that the many modification processes of the PICA3/GEM tend to reproduce the experimental values well. We will discuss about the view of photonuclear reactions derived from the comparison between the experimental data and the PICA3/GEM results.

1. S. R. Sarkar, M. Soto, Y. Kubota, M. Yoshida, T. Fukasawa, K. Matsumoto, K. Kawaguchi, K. Sakamoto, S. Shibata, M. Furukawa, I. Fujiwara, *Radiochim. Acta* **55**, 113 (1991).
2. M. Yamashita *et al.*, private communication (2001).
3. T. Sato, private communication. (2001).
4. C. Y. Fu, 'PICA95, An Intra-nuclear Cascade Code for 25-MeV to 3.5-GeV Photon-Induced Nuclear Reactions', presented to T. Sato at SATIF-3, Sendai, 12-13 May, 1997.
5. S. Furihata, *Nucl. Inst. Meth. in Phys. Res. B* **171**, 251 (2000).

Hiroki SHIBATA, Yasushi KINO and Hiroshi KUDO

Department of Chemistry, Graduate School of Science, Tohoku University, Sendai 980-8578, Japan

Low energy nuclear scattering experiments, such as  $T(d,n)^4\text{He}$ , have been done to investigate the nuclear fusion reaction in stars. These experiments, however, contain ambiguity due to the electron screening effects. On the other hand, nuclear fusion processes in muonic molecules provide a direct information on the low energy nuclear reactions, because the electron screening effects are negligible in muonic molecules.

In the present paper, the nuclear fusion rates in the muonic molecules ( $dd\mu$ ), ( $dt\mu$ ), ( $tt\mu$ ) and ( $d^3\text{He}\mu$ ) were calculated with three-body wave functions obtained by the non-adiabatic coupled rearrangement channel method<sup>1</sup>. The optical model was applied to the interaction between two constituent nuclei of the muonic molecules. The shape of optical potential was assumed to be a Woods-Saxon shape with soft repulsive core. The parameters of optical potentials were determined to reproduce the nuclear fusion cross sections, differential cross sections and fusion rates. The optical potential for ( $tt\mu$ ) is shown in Fig. 1. We found that the soft core in the optical potential plays an important role in the nuclear fusion reaction.

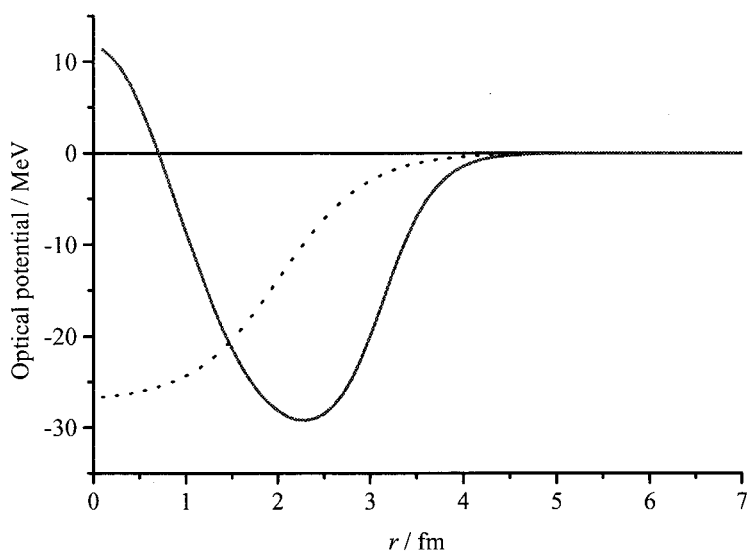


Fig.1: The optical potential for ( $tt\mu$ ). Solid line stands for the real part of optical potential and dotted line stands for the imaginary part of optical potential.

1. M. Kamimura, *Phys. Rev.* **A38**, 621(1988).

2P 04

TRACE ELEMENT DETERMINATION IN SOFT TISSUES  
OF MARINE BIVALVES BY ACTIVATION ANALYSIS

Michiko FUKUSHIMA<sup>1</sup>, Hidetoshi TAMATE<sup>1</sup>, Yoshiyuki NAKANO<sup>2</sup>

<sup>1</sup>Faculty of Science and Engineering, Ishinomaki Senshu University, Minamisakai,  
Ishinomaki, Miyagi 986-8580 Japan

<sup>2</sup>Research Reactor Institute, Kyoto University, Noda, Kumatori, Sennan, Osaka 590-0451  
Japan

Trace elements in soft tissues of marine bivalves were determined by neutron activation analysis(NAA) and photon activation analysis(PAA). Samples were; mantles, muscles, and gills of Giant ezoscallops, mantles, muscles, gills, kidney, byssuses, posteriors, and pedal retractors of Giant clams, mantles muscles gills, and hepatopancreas of Rock oysters. Each organ was separated, freeze-dried, pulverized, and irradiated. After gamma counting, levels of Ag, Co, Fe, Se, and Zn were obtained by NAA, As, Br, Cu, I, Mn, Ni, and Rb by PAA. We could find several characteristics on the elemental levels of three species of marine bivalves. The most remarkable thing was high concentrations of silver in Rock oysters. The role of silver in the organisms is not known well. To investigate the chemical form of elements, we extracted proteins from the mantles of Giant ezoscallops and several organs of rock oysters. Then the extracted roteins were separated by gel chromatography. We could get the profiles of filtration by measuring the absorbance of proteins at 220 and 280nm and irradiation of each fraction, and we found that Ag and Se are bound to the proteins. We will further investigate the chemical form of silver in marine bivalves.

2P 05

**Instrumental Neutron Activation Analysis  
of Extractable Organohalogens (EOX)  
in Antarctic Marine Organisms**

**Masahide Kawano<sup>1</sup>, Jerzy Falandysz<sup>2</sup> and Tadaaki Wakimoto<sup>1</sup>**

1: Department of Environment Conservation, Ehime University  
Tarumi 3-5-7, Matsuyama, 790-8566 Ehime, Japan

2: Department of Environmental Chemistry and Ecotoxicology, University of Gdansk  
ul. Sobieskiego 18, PL 80-952, Gdansk, Poland

Man-made organohalogens, PCBs, DDTs and dioxins, are persistent and toxic to organisms including humans. Many papers are available on the determination of the compounds residued in the environment. However, it is known that a large amount of unknown compounds are still present in the global environment and accumulated in wildlife. Neutron activation analysis is a useful technique to measure the halogen elements (chlorine, bromine and iodine) of such compounds. The present study is to determine the organically-bound halogens and to compare them with the levels of known man-made organohalogen compounds.

Extractable organohalogens (EOX) in organisms collected in the Antarctic marine ecosystem were measured. Instrumental neutron activation analysis was conducted using the JRR-4 reactor of the Japan Atomic Energy Research Institute, Ibaragi, Japan. The results show that the highest and lowest concentrations of EOX were found in ascidian and Adelie penguin samples, respectively. The concentration of extractable organochlorine (EOCl) is the highest among the halogens. The concentration order of chlorine, bromine and iodine was same as the order of element abundance in the earth's crust. The EOCl/EOBr ratio was the highest in the Weddell seal samples, suggesting persistency properties of EOCl in the marine Antarctic ecosystem. The contribution of known man-made organochlorines in EOCl was less than 10%. It means that a large amount of unknown organochlorine compounds are present in Antarctic marine organisms. It may be that some constituents are produced intentionally or unintentionally by human activities and distributed in the Antarctic marine environment. Others might originate from natural sources.

## A STUDY OF ENVIRONMENTAL ANALYSIS OF URBAN RIVER SEDIMENTS USING ACTIVATION ANALYSIS

Yuto TANAKA, Akihito KUNO, and Motoyuki MATSUO  
Graduate School of Arts and Sciences, The University of Tokyo  
3-8-1 Komaba, Meguro-ku, Tokyo 153-8902, Japan

The behaviors of metal and other elements in urban river sediments are of great interest from the aspect of environmental chemistry. A deeper layer of river sediment is often very anoxic due to organic materials from municipal effluent, and sulfate ion from seawater is reduced to hydrogen sulfide. But metal elements may react with hydrogen sulfide to become metal sulfide, which means a decrease of malodor in the atmosphere. And when sediments are dredged and used for other purposes, the concentrations and behaviors of poisonous metal elements should be understood accurately. From these points of view, we clarified the vertical profiles of 30 and several elements using activation analyses and discussed the characteristics of behaviors of elements in urban river sediments.

Sediment samplings were carried out in the Kitajukkengawa River and the Tatekawa River (Sumida-ku, Tokyo). The vertical sediment cores of ca. 50 cm in length were collected and cut at every 3 cm interval. Concentrations of 30 and several elements for each sample were determined by instrumental neutron activation analysis (INAA) and prompt gamma-ray analysis (PGA), both of which are non-destructive methods and advantageous for simultaneous multi-element determination.

Figure 1 shows depth profiles of Ca and Cr of a Kitajukkengawa River sediment core collected in Oct. 2000. The Ca concentration took minimum value at the middle layer (20-30 cm from the sediment surface), while the Cr concentration took maximum value at the middle layer. Correlation coefficient of depth profiles between two elements was calculated for each couple of elements to form a correlation table. Table 1 shows a correlation table for some elements of the core. Ca strongly correlated with Na, while Cr did with Cd. These results were consistent with the results of a Kitajukkengawa River sediment core of May 1999. It is known that alkaline and alkaline earth metals easily dissolve during a weathering process, and the results therefore suggest that a weathering process and adsorption of trace elements in interstitial water are occurring simultaneously in sediments.

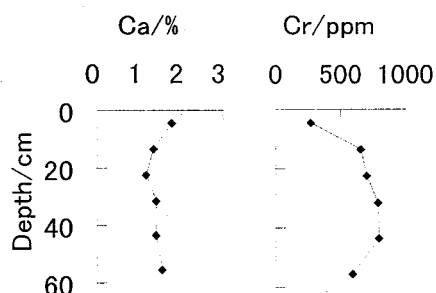


Fig. 1 Depth profiles of Ca and Cr of the Kitajukkengawa River sediment

Table 1 A correlation table of elements of the Kitajukkengawa River sediment

	Ca	Na	H	Al	Cr	Cd
Ca	1.00	0.84	-0.51	-0.95	-0.78	-0.74
Na	0.84	1.00	-0.19	-0.83	-0.64	-0.63
H	-0.51	-0.19	1.00	0.54	0.83	0.77
Al	-0.95	-0.83	0.54	1.00	0.86	0.73
Cr	-0.78	-0.64	0.83	0.86	1.00	0.92
Cd	-0.74	-0.63	0.77	0.73	0.92	1.00

## 2P 07 Determination of $^{36}\text{Cl}$ in Environmental Samples by AMS

R. SEKI<sup>1,2</sup>, D. ARAI<sup>2</sup>, Y. NAGASHIMA<sup>2</sup>, T. TAKAHASHI<sup>2</sup>, T. MATSUHIRO<sup>2</sup>

<sup>1</sup>Department of Chemistry, University of Tsukuba, Tsukuba, Ibaraki 305-8577, Japan

<sup>2</sup>AMS Group, Tandem Accelerator Center, University of Tsukuba, Tsukuba, Ibaraki 305-8577, Japan

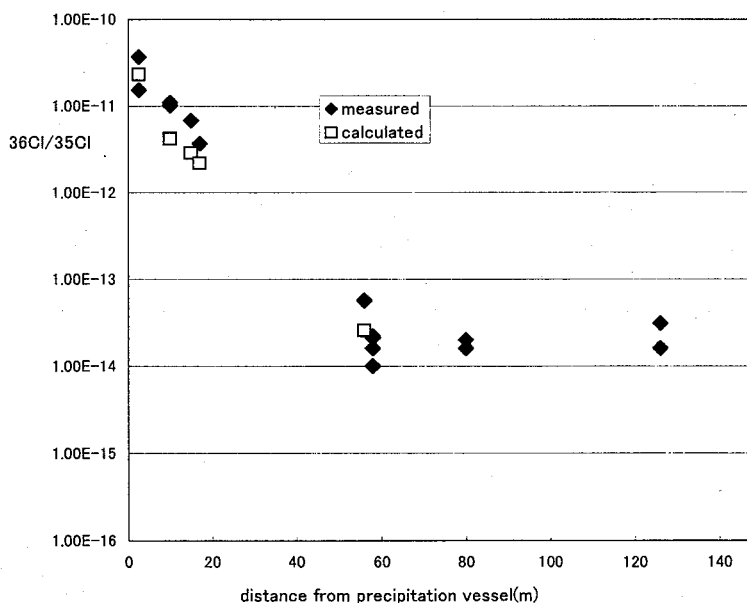
Long-lived chlorine,  $^{36}\text{Cl}$  ( $T_{1/2} = 301,000$  y) is a good tracer for hydrology. Naturally it is produced in the atmosphere by cosmic-ray-induced nuclear reactions mainly on atmospheric argon and in situ in lithosphere by cosmic-ray neutrons. Artificially it was produced by atomic bomb test in the atmosphere and is also produced by the nuclear operation.

The Accelerator Mass Spectrometry (AMS) system is strong tool for the determination of  $^{36}\text{Cl}$ . The AMS system for  $^{36}\text{Cl}$  has been developed on the 12UD tandem accelerator in the Tandem Accelerator Center of the University of Tsukuba<sup>1</sup>. A tri-molecular  $^{12}\text{C}_3^-$  pilot beam method is used to stabilize the terminal voltage of the tandem. A small amount of pure carbon graphite is well mixed into a AgCl target material for creating  $\text{Cl}^-$  and  $^{12}\text{C}_3^-$  in the ion source. A  $^{36}\text{S}$  isobaric interference in the system is a critical problem because the  $^{36}\text{S}$  passes same trajectory as  $^{36}\text{Cl}$ . We

need to remove  $^{36}\text{S}$  contaminants from the sample by chemical separation. Through the careful treatment of chemical separation and production of AgCl we designed the system for determination of environmental  $^{36}\text{Cl}$ . Remained problem is to remove sulfur from the carbon that is added to make a pilot beam.  $^{36}\text{Cl}$  may be produced in a criticality accident occurred at JCO, Tokai-mura, Japan in

1999 due to the released neutrons<sup>2</sup>. The atomic ratios  $^{36}\text{Cl}/\text{Cl}$  in some soil and reagent samples collected in the JCO vicinity have been determined (shown in Figure).

1. Y. Nagashima, R. Seki, T. Takahashi, D. Arai, *Nucl. Instr. Meth.* **B172**, 129-133(2000)
2. K. Komura, et al., *J. Environ. Radioactivity*, **50**, 3-14, (2000)





## 2P 08 Relativistic density functional study on the nitrate complexes of tetravalent rutherfordium and its homologues

Masaru Hirata<sup>1</sup>, Hiromitsu Haba<sup>1</sup> and Yuichiro Nagame<sup>1</sup>

<sup>1</sup>Research Group for Nuclear Chemistry of Heavy Elements,  
Advanced Science Research Center, Japan Atomic Energy Research Institute,  
Tokai-mura, Naka-gun, Ibaraki 319-1195, Japan

Theoretical predictions of chemical behavior of element 104 rutherfordium (Rf) are very important for sophisticated "one-atom-at-a time" experiments. Recently, distribution coefficient ( $K_d$ ) of Rf on ion exchange resins at various HCl and HNO<sub>3</sub> concentrations have been measured by Haba and co-workers[1]. In order to discuss the sorption behavior of Rf and its homologues, we have carried out the relativistic density functional calculations[2] on hexanitate complexes of tetravalent cations [  $M^{4+}(\text{NO}_3)_6^{2-}$  : M=Zr, Hf, Th and Rf]. First, we optimized interatomic distances between cation and nitrate ions by the total energy calculations. Cation - coordinated oxygen distances decrease in the order of Th > Rf > Zr=Hf and the calculated Coulomb part of binding energy shows that the Th complex is more stable than the other cations. The significant difference in the electronic structure of this system is the contribution of 5f orbital in unoccupied state of the Th complex. The 5f electrons of Rf are localized in the core part, so that the Rf is considered to be a d-like element.

[1] H. Haba et al.: a separate paper of this abstract

[2] S. Varga et al.: J. Phys. Chem. 104, 6495 (2000).

$\text{Cm}^{3+}\text{-F}^-$  INTERACTION IN A MIXED SYSTEM  
OF METHANOL AND WATER

Isamu SATOH,<sup>1</sup> Toshihiko WATANABE,<sup>2</sup> Yasuo ISHII,<sup>2</sup> Mikio KAWASAKI<sup>2</sup> and  
Hideo SUGANUMA<sup>2</sup>

<sup>1</sup>Institute for Materials Research, Tohoku University, Katahira 2-1-1, Aoba-ku, Sendai-shi  
980-8577, Japan

<sup>2</sup>Radiochemistry Research Laboratory, Faculty of Science, Shizuoka University, 836 Ooya,  
Shizuoka-shi, 422-8529, Japan

The stability constants ( $\beta_1$ ) of the monofluoro complex of Cm(III) have been determined in mixed solvents of methanol and water at a 0.10 mole·dm<sup>-3</sup> ionic strength using solvent extraction technique. The values of  $\ln \beta_1$  increase as the mole fraction of methanol ( $X_s$ ) in the mixed solvent system increases. The variation in the stability constants mainly depends on the solvation of F<sup>-</sup> and slightly depends on both (1) the solvation of cations in connection with the complexation of CmF<sup>2+</sup> and (2) electrostatic attraction of Cm<sup>3+</sup>-F<sup>-</sup>. The variation in  $\ln \beta_1$  for Cm(III) due to the effect of the both (1) and (2) is similar to that for Sm(III),<sup>1</sup> but dissimilar to that for Am(III).<sup>2</sup> It was determined by analyzing the former values that the coordination number (CN) of Cm(III) varied from a mixture of CN=9 and CN=8 to CN=8 at about a 0.02 mole fraction of methanol ( $X_s$ ) in the mixed solvent. The  $X_s$  value of the inflection point of the CN for Cm is slightly lower than  $X_s = 0.06$  for Sm(III)<sup>1</sup> and  $X_s = 0.03$  for Eu(III)<sup>3</sup> previously obtained.

1. M. Arisaka, H. Suganuma, *J. Radiochem. Nucl. Chem.*, **242**, 349(1999).
2. H. Suganuma, I. Satoh, T. Omori, M. Yagi, *Radiochim. Acta*, **77**, 207(1997).
3. H. Suganuma, M. Arisaka, I. Satoh, T. Omori, G. R. Choppin, *Radiochim. Acta*, **83**, 153(1998).

Toshihumi Maruyama<sup>1</sup>, Daiya Kaji<sup>1</sup>, Tetsuya Kaneko<sup>1</sup>, Shin'ichi Goto<sup>1,2</sup>, Kazuaki Tsukada<sup>2</sup>, Hiromitsu Haba<sup>2</sup>, Masato Asai<sup>2</sup>, Shin'ichi Ichikawa<sup>2</sup>, Yuichiro Nagame<sup>2</sup>, and Hisaaki Kudo<sup>1</sup>

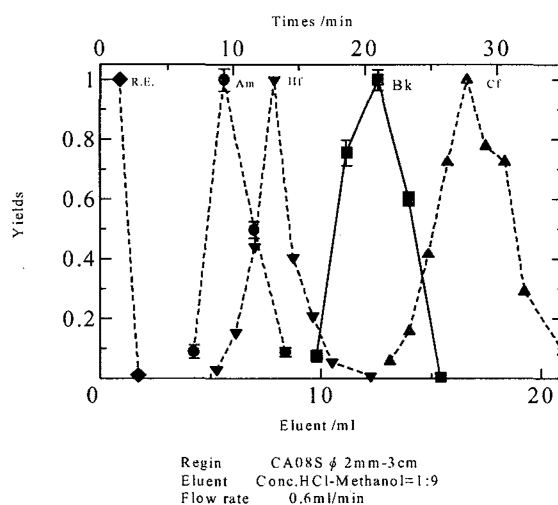
<sup>1</sup>Department of Chemistry, Niigata University, Niigata 950-2181, Japan

<sup>2</sup>Advanced Science Research Center, Japan Atomic Energy Research Institute, Tokai, Ibaraki 319-1195, Japan

It is difficult to produce neutron rich nuclei of heavy actinides. Therefore, many nuclides have not been discovered so far even though they are expected to have long half-lives. It is expected that  $^{252}\text{Bk}$  decays by  $\beta^-$  emission with half-lives of about 10 minutes and also has a probability of  $\beta^-$ -delayed fission. The  $\beta^-$ -delayed fission is important to clarify fission process.  $^{252}\text{Bk}$  could be produced by the reaction  $^{248}\text{Cm}(^{18}\text{O}, \text{X})^{252}\text{Bk}$ . In this reaction, however many kinds of nuclides will be produced at the same time and may disturb the detection.

Rapid chemical separation of  $^{252}\text{Bk}$  from other nuclides is essential in order to measure  $^{252}\text{Bk}$  activity. For  $\alpha$  and fission measurement, no residue is desirable after chemical separation so that we chose an anion exchange of  $\text{HCl}-\text{CH}_3\text{OH}$  system. We searched the optimum conditions for the separation of Bk from other actinoides and lanthanoides. The degree of contamination of fission products in Bk fraction was also evaluated.

Preliminary experiments were performed at the JAERI tandem accelerator. Reaction products were transported to a chemistry room by a gas-jet system. An elution curve of Bk was obtained (Fig.1). All procedures of the separation could be completed within 30 min after the end of bombardment. Rear earths elements (Lu, Yb) and Hf seen in Fig.1 are produced from Gd which was added in Cm target.  $^{241}\text{Am}$  is added as a tracer for the estimation of chemical yields.  $^{250}\text{Bk}$  ( $T_{1/2}=3.2\text{h}$ ) and  $^{251}\text{Bk}$  ( $T_{1/2}=56\text{m}$ ) were measured in this experiment.



## Hot Atom Chemical Behavior of Tritium Produced by ${}^6\text{Li} (n, \alpha) {}^3\text{H}$ in $\text{Li}_4\text{SiO}_4$

S. Akahori<sup>1</sup>, E. Tega<sup>1</sup>, Y. Morimoto<sup>1</sup>, K. Okuno<sup>1</sup>, M. Nishikawa<sup>2</sup>, K. Munakata<sup>2</sup>,  
H. Moriyama<sup>3</sup>, K. Kawamoto<sup>3</sup>, and M. Okada<sup>3</sup>

<sup>1</sup>Radiochemistry Research Laboratory, Faculty of Science, Shizuoka University, Oya, Shizuoka-shi, Shizuoka 422-8529, Japan

<sup>2</sup>Kyushu University, Department of Advanced Energy Engineering Science, Interdisciplinary Graduate School of Engineering Science, Kasuga 816-8580, Japan

<sup>3</sup>Research Reactor Institute, Kyoto University, Kumatori-cho, Sennan-gun, Osaka 590-0494, Japan

Studies on chemical behavior of hot tritium produced by the  ${}^6\text{Li} (n, \alpha) {}^3\text{H}$  reaction in lithium ceramics are very interesting research subjects from not only a viewpoint of hot atom chemistry, but also application to developing D-T fusion reactor blanket system. In D-T fusion reactors, establishing effective tritium recovery techniques from lithium ceramics (tritium solid breeder materials) is a significant. Therefore, it is very important to elucidate chemical existing states and detrapping processes of tritium produced in lithium ceramics. Effects of the damages induced by the neutron irradiation on tritium release processes have been also studied.<sup>1,2</sup> Okuno *et al.* have reported that the tritium release processes correlated with the thermal annealing processes of damages,  $\text{F}^+$ -centers (oxygen-ion vacancy occupied by one electron) induced by the  ${}^6\text{Li} (n, \alpha) {}^3\text{H}$  reaction in  $\text{Li}_2\text{O}$ . Lithium orthosilicate ( $\text{Li}_4\text{SiO}_4$ ) is one of the most attractive candidates for tritium breeding materials. We used  $\text{Li}_4\text{SiO}_4$  as a sample in the present work and investigated the correlation between the tritium release processes and the thermal annealing processes of damages in neutron-irradiated  $\text{Li}_4\text{SiO}_4$ .

Tritium release processes are consisted of the bulk diffusion and the surface reaction. To clarify damage effects in the bulk, the surface reaction effect should be excluded from the whole tritium release processes because irradiation damages were induced in the bulk. It has been known that the surface reaction effect on the "Catalytic Breeders"<sup>3</sup>, of which surface is deposited Pd or Pt, was less than that of non-deposited breeders. We used  $\text{Li}_4\text{SiO}_4$  deposited Pd as a catalytic breeder, Pd/ $\text{Li}_4\text{SiO}_4$ . Sintered pebbles of Pd/ $\text{Li}_4\text{SiO}_4$  and  $\text{Li}_4\text{SiO}_4$  (more than 98% TD, approximately 0.2 g) were irradiated in Kyoto University Research Reactor (KUR) with the thermal neutron flux of  $2.8 \times 10^{13} \text{ cm}^{-2} \text{ s}^{-1}$  for 60 s. Tritium release experiments were carried out using the Pd/ $\text{Li}_4\text{SiO}_4$  samples. The samples were heated from room temperature to 673 K, and then heated up to 1073 K to release completely the residual tritium at a heating rate of  $3.1 \text{ K min}^{-1}$ . In the ESR measurements for the isochronal annealing experiments of the damages,  $\text{Li}_4\text{SiO}_4$  samples were annealed stepwise up to 698 K at intervals of 25 K for 10 min in an electric furnace. They were also annealed at 398, 498, and 598 K in the isothermal manner.

From the tritium release experiment, the amount of tritium released until 673 K was about 78% of all released tritium. It was also found that there could be some tritium release processes. From the isothermal annealing experiments of the damages using ESR, the thermal annealing processes were found to be consisted of the "fast" and "slow" process.

1. K. Okuno and H. Kudo, *J. Nucl. Mater.*, **138**, 31 (1986).
2. Y. Morimoto *et al.*, *Fusion Technol.*, **39**, 634 (2001).
3. K. Munakata *et al.*, *J. Nucl. Sci. Technol.*, **36**, 962 (1999).

## 2P 12 Installation of Neutron Irradiation Apparatus for Low Temperature Experiments at JRR-3M

Yasuyuki Aratono

Advanced Science Research Center, Japan Atomic Energy Research Institute, Tokai-mura,  
Ibaraki-ken 319-1195, Japan

At very low temperature, the thermal motions of atoms and molecules are suppressed. Therefore, the quantum mechanical effects such as tunneling reaction and quantum diffusion play a predominant role in their physico-chemical behaviors. From such a point of view, there has been increasing interest in physico-chemical behaviors of atoms and molecules in the quantum media such as hydrogen and helium in condensed states. These phenomena are more enhanced in a lighter particle. Hydrogen (H) is the lightest atom and has two isotopes, deuterium(D) and tritium(T). Therefore, the most remarkable phenomena including isotope effect are expected in reaction system associated with hydrogen isotopes. Table 1 shows comparison of the isotope effect at various temperatures in abstraction reaction of T with H<sub>2</sub> and D<sub>2</sub> including our previous results from low temperature experiments at JRR-2 (1.3K) and JRR-4 (77 K). It is obvious from Table 1 that the isotope effect markedly increase below 77 K. These results were explained by tunneling reaction mechanism.

The first problem confronted with experiment is how to introduce reactive species into reaction medium in condensed state at very low temperature. In order to solve the problem, several methods such as  $\gamma$ - or x-ray radiolysis, laser ablation have been proposed. The author and his collaborators proposed radiochemical method, nuclear transformation, and successfully applied it to study of the tunneling abstraction of T, which is produced by <sup>3</sup>He(n, p)T reaction, with H<sub>2</sub>, HD and D<sub>2</sub> in liquid <sup>3</sup>He - <sup>4</sup>He mixture at 1.3 K.[4].

In order to promote low temperature experiments from radiochemical view point, the author designed and installed an equipment for low temperature chemistry at neutron beam guide of the JRR-3M. It is consisted of low temperature irradiation apparatus made up of radiation shielding and cryostat, temperature controlling system and gas manipulating system. The equipment has two main features, pure-neutron beam port(free from reactor  $\gamma$ -rays) and very low irradiation temperature of 1.3 K. Thermal and cold neutron fluxes at the irradiation port are 3 - 4 x 10<sup>6</sup> cm<sup>-2</sup> sec<sup>-1</sup> with a peak neutron energy of 23 nm(15 meV) and 5 - 6 x 10<sup>7</sup> cm<sup>-2</sup> sec<sup>-1</sup> with a peak neutron energy of 52 nm(3.0 meV), respectively. Though the apparatus is designed mainly for neutron irradiation at low temperature, it can be also used for high temperature irradiation up to about 1300 K. Cryostat designed for low temperature optical spectroscopy was modified for neutron irradiation. Operating time at 1.3 K is more than 40 hours. The whole set of the apparatus can be moved to thermal (T1-4-1A) and cold(C2-3-2A) neutron beam ports.

The experiments on hydrogen and tritium atom recombination, H + T  $\rightarrow$  HT and T + T  $\rightarrow$  T<sub>2</sub>, in normal- and super-fluid liquid helium are in progress at 1.4 - 2.5 K using the apparatus. The results will be shown in the following poster presentation.

Table 1 Isotope effects for T + H<sub>2</sub>(D<sub>2</sub>)  $\rightarrow$  HT(DT) + H(D)

Phase	Temp.	Isotope Effect	I.K.E.*	Ref.
gas	room	2.7	192 keV	(1)
gas	room	1.55±0.06	192 keV	(1)
gas	room	0.98±0.03	2.8 eV	(2)
solid	77 K	7	2.7 MeV	(3)
liquid	1.3 K	146, 158	192 keV	(4)

\*) I.K.E.: Initial Kinetic Energy.

1. J. K. Lee;, et al., *J. Chem. Phys.* **32**, 1266(1960).
2. C. C. Chu;, et al., *J. Chem. Phys.* **46**, 812(1967).
3. T. Miyazaki;, et al., *Bull. Chem. Soc. Jpn.* **65**, 735(1992).
4. Y. Aratono;, et al., *J. Phys. Chem., A* **102** 1501(1998).

**2P 13** Radiochemical study on recombination reactions of  $H + T \rightarrow HT$  and  $T + T \rightarrow T_2$  in superfluid and normalfluid  ${}^3\text{He}$ - ${}^4\text{He}$  media at 1.4 - 2.5 K

Kazunari IGUCHI<sup>a</sup>, Takayuki KUMADA<sup>b</sup>, Kenji OKUNO<sup>a</sup>, Yasuyuki ARATONO<sup>b</sup>

<sup>a</sup>Radiochemistry Research Laboratory, Faculty of Science, Sizuoka University, Ohya, Sizuoka 422-8529, Japan

<sup>b</sup>Advanced Science Research Center, Japan Atomic Energy Research Institute, Tokai-mura, Naka-gun, Ibaraki 319-1195, Japan

Many peculiar phenomena of liquid helium arising from its quantum properties, such as superfluid, formation of electron and atom bubbles and snowball, have been attracting many scientists. However, the studies have been focused on physical aspects and chemical reaction in liquid helium has not been reported except two of the authors' (T. Kumada and Y. Aratono) previous work on hydrogen abstraction reaction at 1.3K. The reaction in liquid helium represents unique behavior because the reaction is affected by unusual properties of liquid helium and occurs at very low temperature.

In the present study, the simple recombination reactions of completely thermalized hydrogen isotopes,  $H + T \rightarrow HT$  and  $T + T \rightarrow T_2$ , have been investigated using radiochemical methods at 1.4 - 2.5 K. H and T atoms were produced via  ${}^3\text{He}(n, p)\text{T}$  by cold neutron irradiation at upgraded Japan Research Reactor No. 3 (JRR-3M). The atomic fraction of  ${}^3\text{He}$  in  ${}^3\text{He}$ - ${}^4\text{He}$  mixture solution was determined to be 0.3-0.4 by quadrupole mass spectroscopy. As shown in Fig. 1, the phase transition from normalfluid to superfluid occurs in the atomic fraction of 0.3-0.4 at about 1.6K. From the result of radio gas chromatogram in Fig. 2, HT, para- $T_2$ , and ortho- $T_2$  were identified as reaction products. More than 90% of  $T_2$  was ortho- form, being different from statistical ratio at experimental temperature (ortho- $T_2 = \sim 10^{-4}\%$ ) and at room temperature (ortho- $T_2 = \sim 75\%$ ). The yield of  $T_2$  was 1.5-3.5%. The yield tended to increase with the decrease in temperature below 1.6 K, while the monotonous increase was observed above 1.6 K. Since the point where the  $T_2$  yield become minimum value corresponds to transition temperature, the reaction mechanism may change between in superfluid and normalfluid states. It is suggested from these results that the peculiar phenomena of liquid helium influence the recombination reaction.

1. Y. Aratono, T. Matsumoto, T. Takayanagi, T. Kumada, K. Komaguchi, T. Miyazaki., *J. Phys. Chem. A*, **102**, 1501(1998).

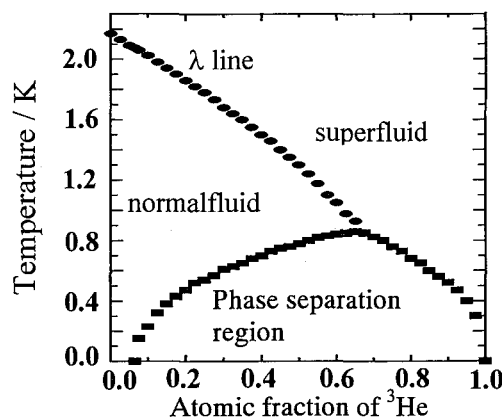


Fig. 1. Phase diagram of  ${}^3\text{He}$ - ${}^4\text{He}$  system under saturated vapor pressure.

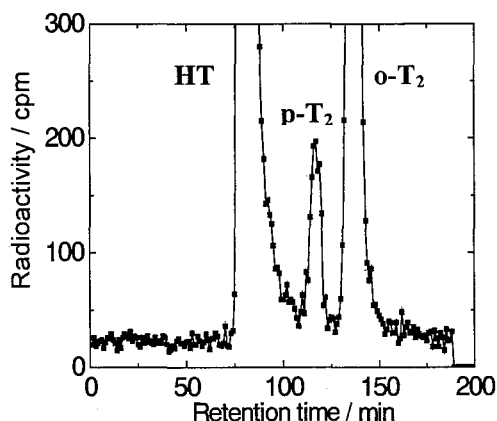


Fig. 2. Radio gas chromatogram of HT, para- $T_2$  and ortho  $T_2$ .

Tomoko Yoshida<sup>1</sup>, Tetsuo Tanabe<sup>1</sup>, Yoshinori Miyashita<sup>2</sup>, Hisao Yoshida<sup>2</sup> and Tadashi Hattori<sup>2</sup>

<sup>1</sup>Center for Integrated Research in Science and Engineering, Nagoya University, Nagoya 464-8603, Japan

<sup>2</sup>Department of Applied Chemistry, Graduated School of Engineering, Nagoya University, Nagoya 4646-8603, Japan

Endocrine disruptors are now one of the most serious concern because they may have a possibility to destroy even human future.<sup>1</sup> It is very important to know which chemicals are truly disruptors and where and how they have been spread over the environment. At the same time, in the view of technology, we must investigate the ways to remove or decompose those already distributed in the environment.

$\gamma$ -ray irradiation has been reported to effectively degrade some organic pollutants in water.<sup>2-4</sup> This technique seems to be promising for the degradation of the endocrine disruptors. On the other hand, as already pointed out, the degradation efficiency of the  $\gamma$ -ray irradiation is unfortunately much lower than that of UV or electron irradiations,<sup>5</sup> so that the improvement of the efficiency of the  $\gamma$ -ray irradiation process is still of interest.

In the present study, we first tried to use  $\gamma$ -ray to degrade dibutyl phthalate (DBP), one of the endocrine disruptors, diluted in water.

The concentration of DBP drastically decreased by  $\gamma$ -ray irradiation, whereas no change was observed without the irradiation. Even after a low dose irradiation of 750 Gy, 97 % of DBP disappeared, clearly indicating that the  $\gamma$ -ray irradiation is effective for the decomposition of DBP.

Moreover, we have carried out an effective energy conversion of  $\gamma$ -ray to lower energy electrons and phonons by the use of the interaction between  $\gamma$ -ray and metal materials (Compton effect), and found out that the degradation of DBP is enhanced especially by employing high mass materials. The present results are promising to develop a new method for the degradation of other organic pollutants in the environment.

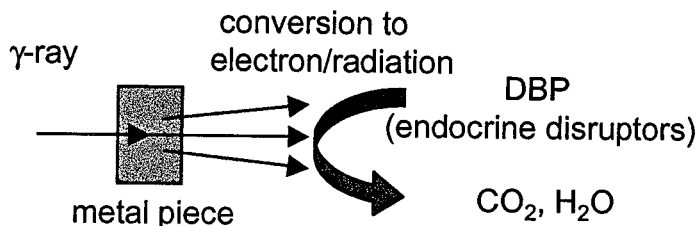


Fig. 1 Effective energy conversion of  $\gamma$ -ray to electrons and photons with low energy.

Tomoko Yoshida

Center for Integrated Research in Science and Engineering, Nagoya University, Nagoya 464-8603, Japan

1. L. H. Keith, *Environmental Endocrine Disruptors*, a handbook of property data., Newyork, Wiley 1997.
2. E. Proksch, P Gehringer, W. Szinovatz and H. Eschweiler, *Appl. Radiat. Isot.*, 38, 911 (1987).
3. M. G. Bettoli, M. Ravanelli, L. Tositti, O. Tubertini, L Guzzi, W. Martinotti, G. Queirazza and M. Tamba, *Radiat. Phys. Chem.*, 52, 327 (1998,)
4. P. Gehringer and H. Matshiner, *Wat. Sci. Tech.* 37, 195 (1998)
5. P. Gehringer, E. Proksch, W. Szinovatz and H. Eschweiler, *Appl. Radiat. Isot.*, 39, 1227 (1988).

Toshiro Sawasaki<sup>1</sup>, Tetsuo Tanabe<sup>2</sup>, Tomoko Yoshida<sup>2</sup> and Rikiya Ishida<sup>1</sup>

<sup>1</sup>Department of Nuclear Engineering, Graduate School of Engineering, Nagoya University, Nagoya 464-8603, Japan

<sup>2</sup>Center for Integrated Research in Science and Engineering, Nagoya University, Nagoya 464-8603, Japan

Gamma radiolysis has been extensively studied for its critical importance in water in nuclear environments. 1-3 Water is commonly used as a coolant and also a moderator for fast neutron in commercial nuclear power reactor, and its control is recognized to be very importance it preventing Stress Corrosion Cracking (SCC) and radioactive corrosion products accumulating on inner surfaces of the primary systems.<sup>4</sup> It has been well known that the gamma ray itself is not so effective to decompose water having G-value of only about 0.45. In order to apply gamma radiolysis of water for hydrogen production, there are two points to be overcome, i.e. (1) to increase the efficiency of decomposition and (2) to removal of H<sub>2</sub> product from the reaction system.

In the present work, we report our recent efforts to improve the efficiency by introducing heavy materials in a radiolysis system and to separate the H<sub>2</sub> product by absorption in exothermic hydrogen occluders such as Ta, Nb, and Pd.

As shown in Fig.1, gamma rays targeted to heavier materials are more efficiently converted to secondary electrons and photons than lighter materials do, so as hydrogen production rates are. It is also confirmed from thermal desorption that Pd and Ta put into the radiolysis system absorbed hydrogen.

Based on these results, we propose a new system for hydrogen production by using gamma radiolysis of water.

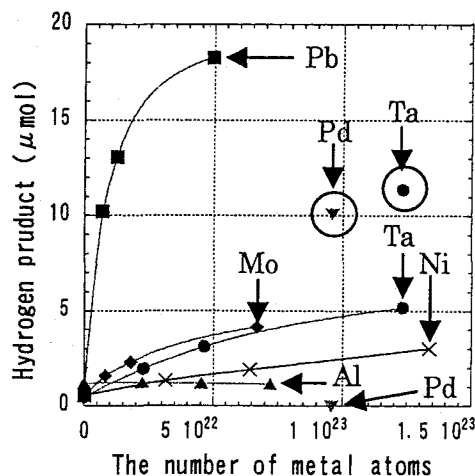


Fig1. The relation between the number of metal atoms coexisted with water and H<sub>2</sub> product (○ is the sum of the H<sub>2</sub> product estimated from gas-chromatography and thermal desorption.)

Toshiro Sawasaki

Department of Nuclear Engineering, Graduate School of Engineering, Nagoya University, Nagoya 464-8603, Japan

1. A. Appleby and H. A. Schwarz, *J. Phys. Chem.*, 75, 1937 (1969).
2. Y. Katsumura, Y. Takeuchi and K. Ishigure, *Radiat. Phys. Chem.* 32, 259 (1988).
3. G. R. Sunaryo, Y. Katsumura, I. Shirai, D. Hiroishi and K. Ishigure, *Radiat. Phys. Chem.* 44, 273 (1994).
4. K. Ishigure, N. Fujita, T. Tamura and K. Oshima, *Nucl. Technol.*, 50, 169 (1980).



**2P 16** Multitracer and neutron activation screening: Brain regional concentration and tracer uptake behavior in mice bred under controlled diets.

Yuko YABUSHITA,<sup>1</sup> Yousuke KANAYAMA,<sup>1</sup> Tohru TAROHDA,<sup>2</sup> Ryohei AMANO,<sup>1</sup> Shuichi ENOMOTO<sup>3</sup>

<sup>1</sup>School of Health Sciences, Faculty of Medicine, Kanazawa University, Kodatsuno, Kanazawa 920-0942, Japan <sup>2</sup>Graduate School of Natural Science and Technology, Kanazawa University, Kakuma, Kanazawa 920-1192, Japan <sup>3</sup>The Institute of Physical and Chemical Research (RIKEN), Wako 351-0198, Japan

Essential trace elements play important roles in the nutrition of humans and other animals, and their deficient and excess states cause various symptoms. It is thought that those symptoms are caused by various element-element interrelationships rather than by influence of a single element. In this study, we investigated the tracer behavior and elemental concentration in mouse brain under controlled (deficient and excessive) conditions of essential elements (Mn and Zn) to screen about element-element interrelationship in brain using a multitracer technique and INAA method.

Dam ICR mice were fed the Mn-deficient, -adequate or -excessive diets with pure water from the 16th day of pregnancy. Multitracer solution was intraperitoneally (i.p.) injected into 3-week-old weanling male mice (n=5). Forty-eight hour after i.p. injection, the brain was excised and dissected into 8 regions (cerebral cortex, striatum, hippocampus, thalamus and hypothalamus, midbrain, cerebellum, pons and medulla, olfactory bulb). These samples were measured using  $\gamma$ -ray spectra and evaluated in terms of uptake rate “% dose/g.” The identical samples were analyzed using INAA at the Kyoto University Research Reactor and evaluated in terms of “ppm  $\mu\text{g/g}$ .” Another series of experiments about mice fed Zn-controlled diets were performed in the same manner as mice fed the Mn-controlled diets. But it was difficult to survive under Zn-deficient state; only one mouse survived.

As a result, the multitracer enabled simultaneous tracing about <sup>46</sup>Sc, <sup>54</sup>Mn, <sup>58</sup>Co, <sup>65</sup>Zn, <sup>75</sup>Se and <sup>83</sup>Rb in mouse brain. Mn-deficient and -excessive states didn't influence the brain regional uptake of other trace elements except for <sup>54</sup>Mn. On the other hand, Zn-deficient and -excessive states significantly influences the brain regional uptake of other trace elements except for <sup>65</sup>Zn. The minor and trace elements, Na, K, Sc, Cr, Mn, Fe, Co, Zn and Se in all brain regions were determined using the INAA method. Mn concentrations in 8 brain regions were increased with Mn concentration of diets. However, in mice fed Zn-deficient, -adequate and -excessive diets, Zn concentrations in 8 brain regions were not significantly different among these three groups as shown in figure 1.

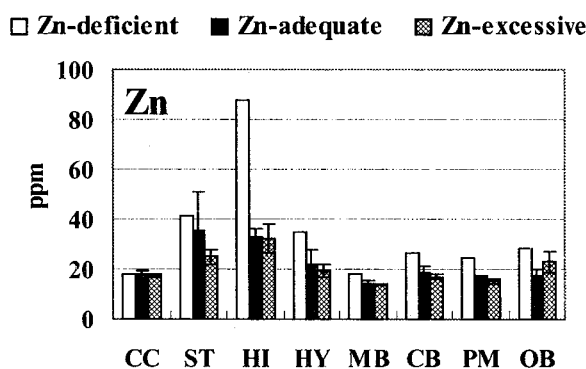


Fig. 1. Brain regional distribution of Zn in mice fed Zn-deficient, -adequate and -excessive diets. CC: cerebral cortex, ST: striatum, HI: hippocampus, HY: thalamus and hypothalamus, MB: midbrain, CB: cerebellum, PM: pons and medulla, OB: olfactory bulb.

## The Relation Between Sb – I Bond Lengths and Charges on Iodine Atoms Determined by $^{127}\text{I}$ Mössbauer Spectroscopy

Masuo Takeda and Masashi Takahashi

Department of Chemistry, Faculty of Science, Toho University  
Miyama 2-2-1, Funabashi, Chiba, 274-8510, Japan

Mössbauer spectroscopy of  $^{127}\text{I}$  is very useful in elucidating the orbital populations of the valence electrons of the iodine atoms, thus charges on them.

We have measured the  $^{127}\text{I}$  Mössbauer spectra of eleven organometallic antimony compounds with hypervalent bond (three center four electron bond),  $\text{E} - \text{Sb} - \text{I}$  ( $\text{E} = \text{O}, \text{I}, \text{N}, \text{C}$ ) and shown that  $\text{Sb} - \text{I}$  bond is composed of  $5s$  and  $5p_z$  orbitals of antimony and  $5p_z$  orbital of iodine [1–3].

The charges on iodine atoms fall between  $-0.54e$  for the compound with  $\text{Sb} - \text{I}$  bond length of  $2.83 \text{ \AA}$  and  $-0.82e$  for the one with  $3.31 \text{ \AA}$  (Fig. 1). In the former the bonding is more covalent and in the latter more ionic. The negative charges on iodine atoms have been found to increase with the increase in the  $\text{Sb} - \text{I}$  bond lengths. Since the bond lengths is related to bond order, the charges on the iodine atoms well correlates to  $\text{Sb} - \text{I}$  bond order (Fig. 2). Regarding to the dependence of the kind of  $\text{E}$  atoms, the negative charges on iodine atoms have been found to decrease with the increase in the electronegativities of  $\text{E}$  atoms ( $\text{O} : 3.5; \text{N} : 3.0; \text{C} : 2.5$ ).

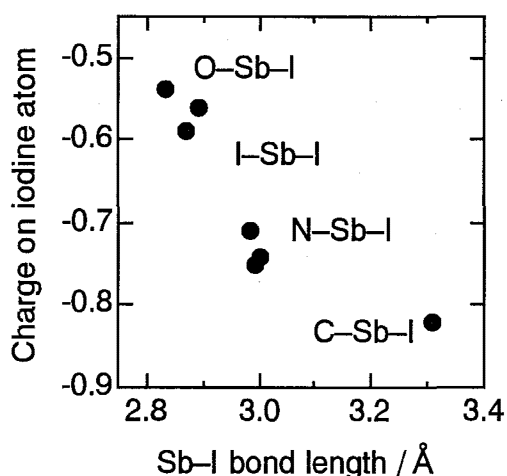


Fig. 1 Relation between charges on iodine atoms and  $\text{Sb} - \text{I}$  bond lengths.

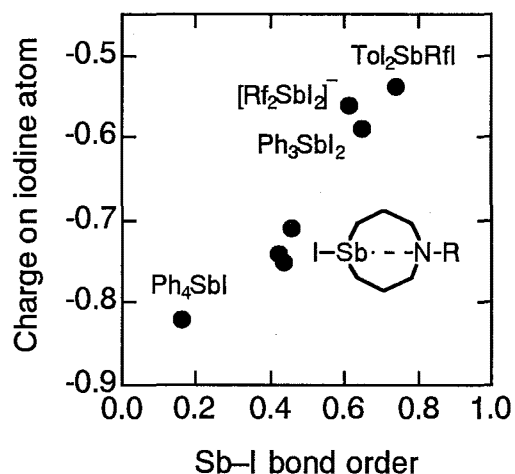


Fig. 2 Relation between charges on iodine atoms and Pauling's  $\text{Sb} - \text{I}$  bond orders estimated from  $\text{Sb} - \text{I}$  bond lengths.

### References

- [1] M. Takeda et al., *Hyperfine Interact.*, **84** (1994) 1439.
- [2] M. Takeda et al., *Chem. Lett.*, (1993) 2037.
- [3] E. Bräu et al., *Polyhedron*, **17** (1998) 2655.

## CHARACTERIZATION OF ULTRAMAFIC ROCKS FROM JINCHUAN NICKEL DEPOSIT IN CHINA BY $^{57}\text{Fe}$ MÖSSBAUER SPECTROSCOPY

Akihito KUNO,<sup>1</sup> Guodong ZHENG,<sup>1</sup> Motoyuki MATSUO,<sup>1</sup> Bokuichiro TAKANO,<sup>1</sup> Ji'an SHI<sup>2</sup> and Qi WANG<sup>2</sup>

<sup>1</sup>Graduate School of Arts and Sciences, The University of Tokyo, 3-8-1 Komaba, Meguro, Tokyo 153-8902, Japan

<sup>2</sup>Lanzhou Institute of Geology, Chinese Academy of Sciences, 324 West Donggang Road, Lanzhou 730000, China

The Jinchuan sulfide deposit in Gansu Province, northwest China, is the second largest Ni deposit in the world. Although several investigations have been carried out on the Jinchuan deposit, there have been few studies that focused on the iron speciation. These ores are considered to contain various iron species, of which distribution has an important bearing on the sulfide mineralization process. In this study,  $^{57}\text{Fe}$  Mössbauer spectroscopy has been applied to the ultramafic rocks collected from the Jinchuan nickel deposit to elucidate the genesis and mineralization process.

Samples were collected from locations that are different in distance from the orebody. The iron speciation in the samples was carried out using Mössbauer spectroscopy and X-ray absorption fine structure (XAFS). The Mössbauer spectra were measured using 1.11 GBq  $^{57}\text{Co}/\text{Rh}$  source. XAFS measurements were made using synchrotron radiation with a Si(111) double crystal monochromator at Photon Factory, Tsukuba, Japan.

Figure 1 shows the room temperature Mössbauer spectra of rock N-1 and N-5, which are the closest and farthest samples to the orebody, respectively. The Mössbauer spectra of the rock samples consisted of two sextets ascribable to magnetite ( $\text{Fe}_3\text{O}_4$ ) and three quadrupole doublets ascribable to paramagnetic high-spin  $\text{Fe}^{2+}$  and  $\text{Fe}^{3+}$  in chrome spinels.<sup>1</sup> The closest sample to the orebody (N-1) contained much amount of quadrupole doublet ascribable to diamagnetic low-spin  $\text{Fe}^{2+}$  that corresponds to pyrite ( $\text{FeS}_2$ ), which is consistent with the Fe- and Ni-XAFS spectra. The distribution of these species provided a better understanding of the environment for the formation of the Jinchuan deposit.

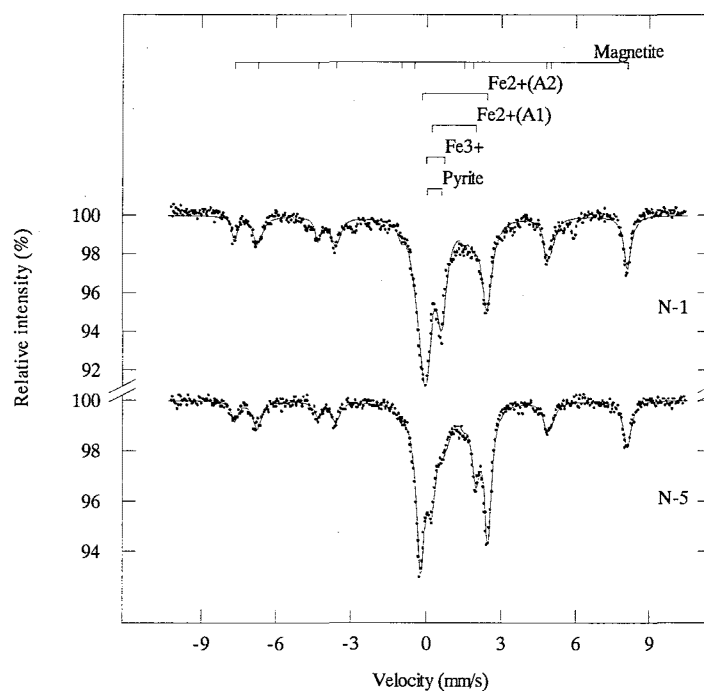


Fig. 1. Mössbauer spectra of rock samples from the Jinchuan deposit.

1. A. Kuno, R. A. Santos, M. Matsuo, B. Takano, *J. Radioanal. Nucl. Chem.*, **246**, 79 (2000).

## A STUDY ON VERTICAL DISTRIBUTION OF ELEMENTS AND THEIR CHEMICAL STATES IN YATSU TIDELAND SEDIMENTS

Masaki KATAOKA,<sup>1</sup> Akihito KUNO<sup>2</sup> and Motoyuki MATSUO<sup>2</sup>

<sup>1</sup>Graduate School of Science, The University of Tokyo, 3-8-1 Komaba, Meguro-ku, Tokyo 153-8902, Japan

<sup>2</sup>Graduate School of Arts and Sciences, The University of Tokyo, 3-8-1 Komaba, Meguro-ku, Tokyo 153-8902, Japan

Environmental monitoring of tideland areas, which have been decreased by reclamation for urbanization in Japan, receives much attention in these days. A tideland plays a significant role in environmental preservation, because it is the place where many creatures live and a tideland have an effect of water clarification. But a tideland is a very complicated system where fresh water and sea water are mixed. Accordingly, the migration of elements and their chemical reactions in a tideland sediments have not been understood. The above information is very important for environmental evaluation. We collected sediments vertically from the Yatsu Tideland, located in Tokyo Bay area, Japan. The length of vertical sediment cores are 40-60 cm. Using instrumental neutron activation analysis (INAA) and prompt  $\gamma$ -ray analysis (PGA), we obtained vertical distribution of thirty and more elements.

Chemical states of iron in the sediments were investigated by Mössbauer spectroscopy. Figure 1 shows the vertical distribution of iron species in the Yatsu Tideland sediments. The high distribution zone of pyrite was found in 20-40 cm, which was the middle layer of cores. The several cores showed similar distribution. This suggests that pyrite, one of iron sulfides, was formed under the reducing conditions with the aid of sulfate-reducing bacteria below the middle layer in the sediments. On the other hand, paramagnetic high-spin  $Fe^{2+}$  changed complementarily to pyrite. It seems that the  $Fe^{2+}$ , which was liberated from a solid phase to interstitial water, was used for pyrite formation. Chemical states of manganese in the sediments were investigated by X-ray absorption fine structure (XAFS). It indicated that much manganese sulfide distribution was found in the surface layer.

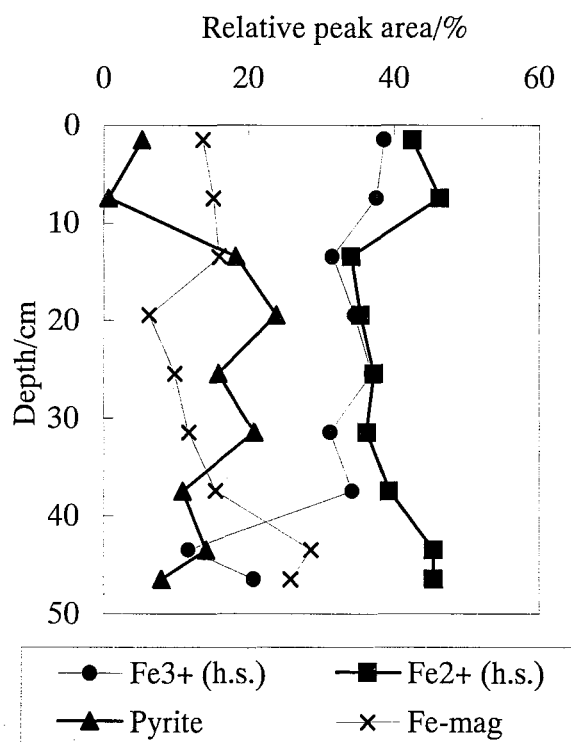


Fig. 1. The vertical distribution of iron species in the Yatsu Tideland sediments

## MÖSSBAUER STUDY OF REACTION OF LASER-EVAPORATED IRON ATOMS WITH OZONE

Keiichi KATSUMATA, Yasuhiro YAMADA

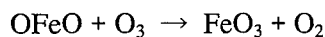
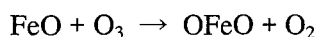
Department of Chemistry, Faculty of Science, Science University of Tokyo

1-3 Kagurazaka, Shinjuku-ku, Tokyo, 162-8601, Japan

Laser-evaporated iron atoms have high energy, and form novel compounds unavailable under normal conditions. We have reported the reaction mechanism of laser-evaporated iron atoms with oxygen molecules, and have shown that formation of ozone play an important role in the reaction of iron atoms with oxygen<sup>1</sup>. In this study, we investigate the reaction mechanism of iron atoms with ozone by introducing preformed ozone molecules.

Pulsed laser lights (532 nm, 150 mJ/pulse, 5 ns) from a Nd:YAG laser (Continuum, Surelite I-10) were focused onto a <sup>57</sup>Fe iron block. Laser-evaporated iron atoms were mixed with reactant gas introduced by a magnetic pulse valve and condensed on an aluminum plate which has been cooled down to 20 K by a closed cycle helium refrigerator (Iwatani, Cryomini). Ozone gas was produced by passing oxygen gas through a silent-discharge-ozonizer. The reactant gas was diluted in Ar gas before introduction. All the Mössbauer spectra were measured at 20 K in transmission geometry with <sup>57</sup>Co/Rh source. Infrared spectra of the species produced in the same way were also obtained. Molecular orbital calculations using Gaussian98 were performed in order to interpret the observed Mössbauer parameters and infrared frequencies.

Mössbauer spectra of the species produced by reactions of laser-evaporated iron atoms with ozone in Ar matrices are shown in Fig. 1. Three iron species A, B and C were observed, which were assigned to FeO, OFeO, and FeO<sub>3</sub>, respectively. On annealing the sample at 30 K for 24 h., OFeO and FeO<sub>3</sub> increased at the expense of FeO.



Infrared spectra and molecular orbital calculations of the products support these findings.

1 Y. Yamada, H. Sumino, Y. Okamura, H. Shimasaki, T. Tominaga, *Appl. Radiation and Isotopes*, **52**, 157 (2000)

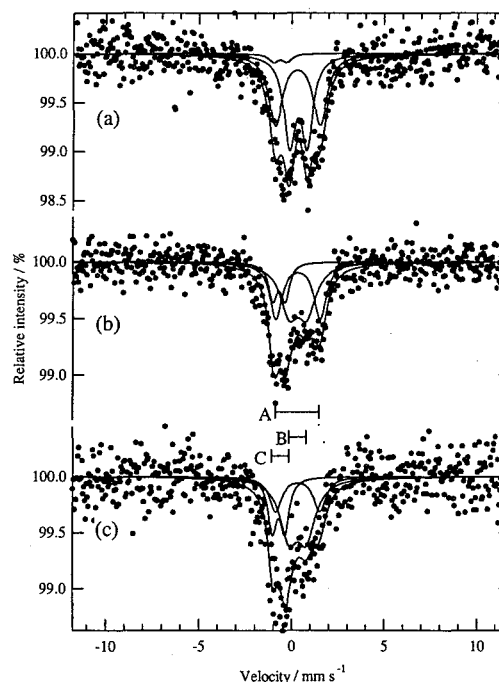


Fig. 1 Mössbauer spectra of reaction products of laser-evaporated iron atoms with ozone in Ar matrices

(a) <sup>57</sup>Fe / (O<sub>3</sub> + O<sub>2</sub>) / Ar = 1 : 7.6 : 800

(b) <sup>57</sup>Fe / (O<sub>3</sub> + O<sub>2</sub>) / Ar = 1 : 40 : 160

(c) after annealing (b) at 32 K for 24 h.

Species A:  $\delta = 0.32 \text{ mm s}^{-1}$ ,  $\Delta E_q = 2.42 \text{ mm s}^{-1}$

Species B:  $\delta = -0.03 \text{ mm s}^{-1}$ ,  $\Delta E_q = 1.65 \text{ mm s}^{-1}$

Species C:  $\delta = -0.62 \text{ mm s}^{-1}$ ,  $\Delta E_q = 0.75 \text{ mm s}^{-1}$

## 2P 21 Iron(III) LIESST Compounds – A Mössbauer Spectroscopic Study

JUHÁSZ Gergely<sup>1</sup>, HAYAMI Shinya<sup>1</sup>, SATO Osamu<sup>2</sup> and MAEDA Yonezo<sup>1</sup>.

<sup>1</sup>Department of Chemistry, Kyushu University, 6-10-1 Hakozaki, Higashi-ku, Fukuoka 812-8581, JAPAN, <sup>2</sup>Kanagawa Academy of Science and Technology, KSP Bldg. East 412, 3-2-1 Sakado, Takatsu-ku, Kawasaki-shi, Kanagawa 213-0012, JAPAN

In spite of the high interest on novel compounds that is switchable by illumination, most of the reported examples are iron(II) coordination compounds.<sup>1</sup> One of the first reported iron(III) compounds that exhibit LIESST effect is  $[\text{Fe}(\text{pap})_2]\text{ClO}_4 \cdot \text{H}_2\text{O}$  (**1**)<sup>2</sup>, where Hpap is a tridentate Schiff-base (Hpap: bis[2-hydroxyphenyl-(2-pyridyl)-methaneimine]). While due to the tunneling from photo-induced iron(III) high-spin states to low-spin states generally the iron(III) compounds rapidly relax to the ground spin state even at low temperature. In the case of iron(III)-pap compounds the strong  $\pi$ - $\pi$  interaction between the neighboring ligands results strong cooperativity between the iron(III) centers and makes the spin trapping possible. The size effect of the solvent molecules and the anions can influence the relative position of planar pap ligands, this is the reason that the present study focus on  $[\text{Fe}(\text{pap})_2]\text{PF}_6 \cdot \text{DMSO}$  (**2**). The temperature dependence of magnetic susceptibility of **2** has been recorded over the temperature range 5 - 350K. The transition of both compounds is complete, appears on cooling at  $T_{1/2\downarrow}=165$  K and on heating at  $T_{1/2\uparrow}=180$  K for **1** and  $T_{1/2}=290$ K for **2** (no hysteresis). LIESST of **2** was investigated by irradiating it at 5K. The critical temperature of the photoinduced high-spin state,  $T_c(\text{LIESST})$ , is lower than in the case of **1** ( $T_c(\text{LIESST})=105$ K for **1** and  $T_c(\text{LIESST})=55$ K for **2**). To study the local environment of iron(III), Mössbauer spectra of **2** were recorded at room temperature and 80K. Generally the iron(III) spin-crossover complexes has strongly broadened or averaged spectra due to the fast relaxation between the HS and the LS state. It means that these coordination compounds have an intense fluctuation between two spin states with  $10^{-6} - 10^{-7}\text{s}^{-1}$  or faster. In the case of **2** sharp Lorentzian peaks show the minor role of relaxation. It suggests, that not only the temperature independent tunneling, but also the temperature induced vibrational relaxation of HS and LS states is weak even at high temperatures. The Mössbauer parameter of **2** for HS:  $IS=0.42$  mm/s,  $QS=1.03$  mm/s at 80K, LS:  $IS=0.12$  mm/s,  $QS=3.08$  mm/s at 80K, HS:  $IS=0.31$  mm/s,  $QS=0.969$  mm/s at RT, LS:  $IS=0.02$  mm/s,  $QS=2.90$  mm/s at RT.

1 P. Gülich, A. Hauser, H. Spiering, *Angew. Chem. Int. Ed. Engl.* **33**, 2024-2054 (1994).

2 S. Hayami, Z.-Z. Gu, M. Shiro, Y. Einaga, A. Fujishima, and O. Sato, *J. Am. Chem. Soc.*, **122**, 7126-7127 (2000).

**METAL-METAL INTERACTION IN BINUCLEAR  
FERROCENE-ARENE COMPLEXES**

Satoru NAKASHIMA,<sup>1</sup> Hiroshi ISOBE,<sup>2</sup> Nozomi AKIYAMA,<sup>2</sup> Tsutomu OKUDA,<sup>2</sup> and Motomi KATADA<sup>3</sup>

<sup>1</sup>Radioisotope Center and <sup>2</sup>Graduate School of Science, Hiroshima University, Kagamiyama, Higashi-Hiroshima 739-8526, Japan; <sup>3</sup>Graduate School of Science, Tokyo Metropolitan University, Minami-Ohsawa, Hachioji 192-0397, Japan

The chemistry of binuclear ferrocene and binuclear arene complexes has been advanced. Especially, the mixed-valence binuclear ferrocene derivatives have been studied thoroughly. It is known that the cation symmetry and its packing affect the mixed-valence state. In the present study extremely unsymmetrical ferrocene-arene complexes ( $[\text{Fc}(\text{CH}_2)_n\text{PhFeCp}]^+\text{PF}_6^-$ ) were synthesized. The metal-metal interaction was studied by using <sup>57</sup>Fe Mössbauer spectroscopy and cyclic voltammetry (CV). The results were considered by using MO calculation.

<sup>57</sup>Fe Mössbauer spectra of  $[\text{Fc}(\text{CH}_2)_n\text{PhFeCp}]^+\text{PF}_6^-$  were the superposition of ferrocene and  $[\text{BenzeneFeCp}]^+\text{PF}_6^-$ . In the  $n=0$  complex, a slight decrease in QS of ferrocene moiety was observed. The decrease is explained by an increased back donation of  $e_{2g}$  electron to Cp ring because of electron-withdrawing character of arene moiety. Such decrease was not observed in  $n=1, 2, 3, 4,$  and  $6$  complexes. <sup>57</sup>Fe Mössbauer spectroscopy revealed that the ferrocene moiety is easily oxidized by iodine to become Fe(II)-Fe(III) mixed-valence complexes. A slight metal-metal interaction in the mixed-valence state was observed in  $n=0$  complex from the point of QS value, while no significant interaction was observed in  $n=1, 2, 3, 4,$  and  $6$  complexes. CV revealed the  $n$  dependence of redox potential in the oxidation process, while there was no significant  $n$  dependence in the reduction process. By comparing the CV data between  $\text{Fc}(\text{CH}_2)_n\text{Ph}$  and its arene complexes it was shown that the considerable metal-metal interaction exists in  $n=0$  complex, while no significant interaction exists in  $n=1, 2, 3, 4,$  and  $6$  complexes.

The HOMO and LUMO were calculated by using WinMOPAC. The HOMO mainly existed in ferrocene moiety, while the LUMO existed in arene moiety. The contribution from counterpart was observed in  $n=0$  complex, while no contribution was observed in  $n=1, 2, 3, 4,$  and  $6$  complexes. The energy of HOMO increased with increasing number of methylene carbon, while no significant change was observed in the LUMO. The results are in accord with CV data.

Z.Q. Chen<sup>1</sup>, A. Uedono<sup>1</sup>, T. Suzuki<sup>2</sup> and J.S. He<sup>3</sup><sup>1</sup>Institute of Applied Physics, University of Tsukuba, Tsukuba Ibaraki 305-8573, Japan<sup>2</sup>Radiation Science Center, High Energy Accelerator Research Organization (KEK), Tsukuba, Ibaraki 305-0801, Japan<sup>3</sup>State Key Laboratory of Engineering Plastics, Institute of Chemistry, Center for Molecular Science, The Chinese Academy of Sciences, Beijing 100080 P.R.China

Positron Annihilation Spectroscopy has been proved to be a very useful tool for the study of free volume holes in polymeric materials. The annihilation characteristics of ortho-positronium, one state of the positronium formed in polymers, can provide information about the number and size of free volume. This is very important to understand many polymer properties at a molecular level. In this paper, we used this technique to study the free volume properties in some polymers and polymer blends.

Positron lifetime spectra were measured as a function of elapsed time for PE, PA, PMMA and PC. Decrease of o-Ps intensity was observed in PE and PC, but not in PA and PMMA. Free radicals were supposed to be the most possible reason for the radiation effect. We also studied the effect of maleic-anhydride (maH) grafted copolymers and its ionomers as the compatibilizer in PE/PA blends. The o-Ps lifetime  $\tau_3$  showed decrease with increasing maH content from 0 to 0.5%, then kept constant. From the analysis of continuous lifetime distribution, we found that in the blend with no or smaller maH content, the o-Ps lifetime distribution was composed of two peaks, which indicated the evidence of phase separation in these blends. When the maH content was equal to or higher than 0.5%, there was only one o-Ps lifetime peak in the distribution, which suggested good compatibility of the sample. In the blends with Na<sup>+</sup> ionomer, the o-Ps lifetime showed further decrease, and the two o-Ps lifetime peaks merged into one at a lower content of maH. The result proved that maH grafted copolymer can be a very good compatibilizer for the PE/PA blends, and the ionomer has stronger effect.

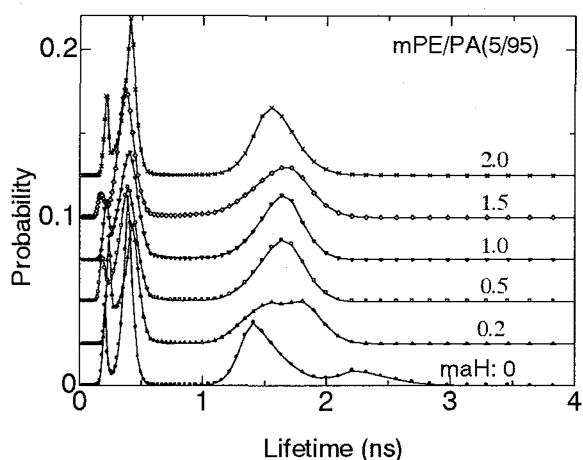


Fig.1 Positron lifetime distribution in the PE/PA(5/95) blend as a function of the maH content



## Clay wall of ancient iron smelting furnace studied by Mössbauer spectroscopy

Akio NAKANISHI<sup>1</sup>, Takayuki KOBAYASHI<sup>1</sup> and Naoki HAGIHARA<sup>2</sup>

<sup>1</sup>Department of Physics, Shiga University of Medical Science, Shiga 520-2192, Japan

<sup>2</sup>Department of Physics, Osaka City University, Osaka 558-5858, Japan

For the investigation of the ancient iron manufacturing technique, the Committee of Education in Katano City carried out a modern simulation experiment. The smelting furnace was made of clay and the top of the furnace was open to air. Charcoal and magnetite were installed from the top. After the charcoal was fired, air was blown into the furnace from its lower part. The oxygen in air reacts with the charcoal to form carbon monoxide that reduces the iron oxides to the metallic iron. The reduction reaction is mainly controlled by temperature and oxygen fugacity in the furnace. In order to estimate these two parameters, Mössbauer spectra of the furnace wall were taken at room temperature.

The section of the furnace wall can be divided into five or six layers with their color<sup>1</sup>. The innermost layer looks as black glass, which indicates almost all minerals in clay melted. The Mössbauer spectrum of this layer shows several sextets and doublets. From the hyperfine field and the isomer shift, these sextet are assigned to haematite and magnetite. Two doublets, which can be assigned to ferrous and ferric iron in silicate glass, are observed. Since the ferric / ferrous ratio in silicate glass reflects the oxygen fugacity in silicate melt<sup>2</sup>, the oxygen fugacity in the furnace can be derived from the ferric / ferrous ratio in the innermost layer. Mössbauer spectra of the other layers show ferric doublets. In the spectra the isomer shift and the quadrupole splitting of the doublet of one layer are different from those of other layers, which reflects the difference of the suffering temperature of clay<sup>3</sup>. The suffering temperature of clay can be estimated from the change of the isomer shift and the quadrupole splitting. The temperature of the innermost layer can be estimated from the temperature gradient of the furnace wall. Therefore, the temperature and the oxygen fugacity in the furnace can be estimated from the Mössbauer spectra of the furnace wall.

1. N.Hagihara, S.Miono, S.Manabe, A.Nakanishi, *Quat. Sci. Rev.*, **20**,987(2001).
2. Ö.Helgason, S.Steinthorsson, S.Mørup, *Hyp.Int.*, **45**,287(1989).
3. Ch.Janot, P.Delcroix, *J. Phys.(Paris)*, **35**,C6-557(1974).

## Iron(II) Compounds

Kazunori KAWAMURA, Shinya HAYAMI and Yonezo MAEDA

Department of Chemistry, Kyushu University, 6-10-1 Hakozaki, Higashi-ku, Fukuoka 812-8581, Japan

A number of spin-crossover iron(II), iron(III) and cobalt(II) compounds have been studied. Some of them exhibit spin transition from low-spin (LS,  $S = 0$ ) to metastable high-spin (HS,  $S = 2$ ) states by light illumination at low temperature. This light-induced spin transition effect is termed LIESST (Light-Induced Excited Spin-State Trapping). Supramolecular compounds are useful for catalyst and molecular sieve because of the porosity of their molecules. One of the most important subjects for supramolecular science is to control a size of the supramolecular porosity. The size of supramolecular porosities self-assembled by spin transition compounds can be controlled by temperature or illumination, because metal-ligand bond distances in the spin transition compounds change with spin transition depending on temperature or illumination. Here we have attempted to construct supramolecules with a several of porosity size by using self-assembly of photo functional molecular building blocks; LIESST Iron compounds.

Along the strategies, some supramolecules with polypyridine ligand were synthesized. The compound  $[\text{Fe}(\text{4tpt})_2(\text{NCS})_2(\text{CH}_3\text{OH})_2] \cdot \text{CH}_3\text{OH}$  (1) (4tpt = 2,4,6-tri(4-pyridyl)-1,3,5-triazine) was characterized by X-ray single crystal diffraction (Fig.1), having two 4tpt ligands, two methanol molecules and two thiocyanate ions. 1-D zigzag chains were formed by the strong  $\pi$ - $\pi$  stacking of molecules. Two methanol molecules were contained in the space of molecular packing.

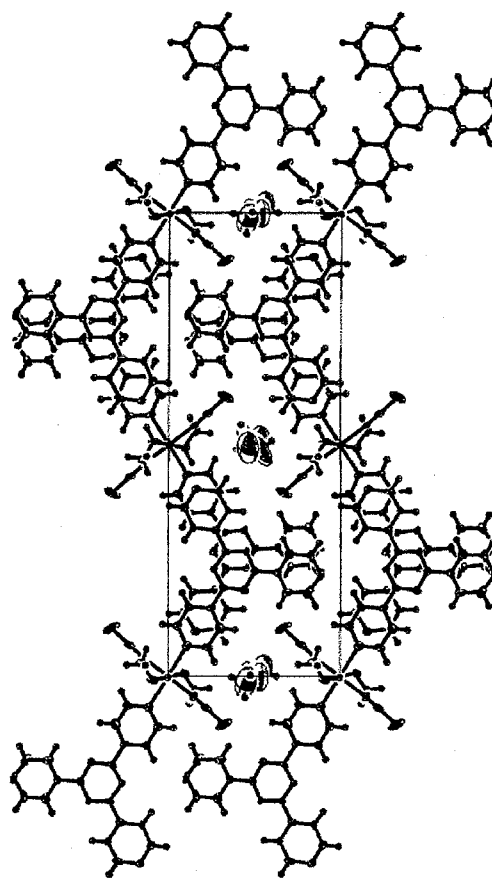


Fig.1 Crystal packing view for  $[\text{Fe}(\text{4tpt})_2(\text{NCS})_2(\text{CH}_3\text{OH})_2] \cdot \text{CH}_3\text{OH}$  (1) at 90K.

## DEVELOPMENT OF THE MEASURING SYSTEM FOR ELECTRONIC X RAYS FOLLOWING ATOMIC CAPTURE OF NEGATIVE PIONS

K. Goto<sup>1</sup>, K. Takamiya<sup>2</sup>, Y. Kasamatsu<sup>1</sup>, Y. Shoji<sup>1</sup>, A. Yokoyama<sup>3</sup>, T. Miura<sup>4</sup>, Y. Hamajima<sup>3</sup>  
and A. Shinohara<sup>1</sup>

<sup>1</sup>Department of Chemistry, Graduate School of Science, Osaka University, Toyonaka, Osaka 560-0043, Japan

<sup>2</sup>Research Reactor Institute, Kyoto University, Kumatori, Osaka 590-0494, Japan

<sup>3</sup>Department of Chemistry, Faculty of Science, Kanazawa University, Kanazawa, Ishikawa 920-1192, Japan

<sup>4</sup>High Energy Accelerator Research Organization (KEK), Tsukuba, Ibaraki 305-0801, Japan

Various experiments have been carried out to investigate the negative-pion capture process. Recently we observed the influence of the valence electrons on the pion capture and pion transfer processes, and proposed a new pion capture model<sup>1-3</sup>. It is necessary for a further understanding of the mechanism that the initial step in the capture process is directly observed and the whole of the capture process is microscopically investigated.

The measurements were performed at the  $\pi\mu$  channel of the 12-GeV proton synchrotron (KEK-PS) in the High Energy Accelerator Research Organization (KEK). We measured the electronic and pionic X rays that were emitted from the target during the pion irradiation. When a pion was captured on an atom with the atomic number  $Z$ , the electronic X rays for  $Z$  and  $(Z-1)$  atoms were observed in the photon spectrum. The experimental results indicated that the intensity patterns for these X rays changed with the chemical state of the target such as Tl and  $Tl_2O_3$ . The correlation measurement of the electronic and pionic X rays is required to investigate the rearrangement of atomic inner-shell electrons following negative pion captures. The test experiments were carried out to measure the electronic and pionic X rays correlated with a pionic X ray. The electronic X rays of  $(Z-1)$  for the  $Z$  atom were observed in the coincidence of the pionic X rays, though the statistics were very low.

To measure the electronic and pionic X rays correlated with the pionic X rays in detail, we are designing a measuring chamber to measure simultaneously the low energy electronic X rays and pionic X rays with high detection efficiency.

1. A. Shinohara *et al.*, *Phys. Rev. A* **53**, 130 (1996).
2. A. Shinohara *et al.*, *Phys. Rev. Lett.*, **76**, 2460 (1996).
3. T. Muroyama *et al.*, *Radiochim. Acta*, **80**, 31 (1998).

MÖSSBAUER SPECTROSCOPIC STUDIES OF  
PEROVSKITE-TYPE OXIDES  $\text{Ln}_{1-x}\text{A}_x\text{BO}_3$  ( $\text{Ln}=\text{La}, \text{Eu}$ ;  $\text{A}=\text{Ca}, \text{Sr}$ ,  
 $\text{Ba}$ ;  $\text{B}=\text{Fe}, \text{Mn}$ ) SYNTHESIZED BY SOL-GEL METHOD

T. YAMAUCHI, M. KATADA

Graduate School of Science, Tokyo Metropolitan University,  
Hachioji, Tokyo 192-0397, Japan

In perovskite type oxides  $\text{Ln}_{1-x}\text{A}_x\text{BO}_3$  ( $\text{Ln}=\text{La}, \text{Eu}$ ;  $\text{A}=\text{Ca}, \text{Sr}, \text{Ba}$ ;  $\text{B}=\text{Fe}, \text{Mn}$ ), electric and magnetic properties depend on B-O-B bond angle, oxygen defect and valence state of B site ion. Their structures can be determined by powder X-ray diffraction measurement. Their electric and magnetic properties can be studied by Mössbauer spectroscopy. Ln and A atoms at A-site were put at same A-site (Fig.1). Therefore, mean of ionic radii is able to be change by changing doping ratio  $x$  and selecting A-site atom. And the valence state of B-site ion can be controlled by doping ratio  $x$ .

Nevertheless, when B-site atom is iron, oxidation state of iron is difficult to change into 4+. Oxygen defect takes place easily. Therefore, sol-gel method was selected. Samples are synthesized at lower temperature by this method than by ceramic method; they have less oxygen defect and large surface ratio to the volume. This is good for catalyst or gas absorption. In previous study, perovskite type oxides  $\text{Eu}_{1-x}\text{A}_x\text{BO}_3$  ( $\text{A}=\text{Ca}, \text{Ba}$ ;  $\text{B}=\text{Fe}, \text{Mn}$ ) were synthesized at  $990^\circ\text{C}$  and  $850^\circ\text{C}$  in air atmosphere. Although  $\text{Eu}_{1-x}\text{Ba}_x\text{MnO}_3$  samples were tried to synthesize, they became mixture in  $x \geq 0.6$ . When perovskite type oxides  $\text{Eu}_{1-x}\text{A}_x\text{FeO}_3$  ( $\text{A}=\text{Ca}, \text{Ba}$ ) have large  $x$ , the large oxygen defect was found. We found that to obtain the precursor without  $\text{BaCO}_3$  impurity by sol-gel method needs much amount of citric acid and ethylene glycol. The precursor without  $\text{BaCO}_3$  impurity for  $\text{BaFeO}_3$  can be made by heating at  $250^\circ\text{C}$  in air atmosphere. In this study, another perovskite type oxides were synthesized by using the precursor made by this method.

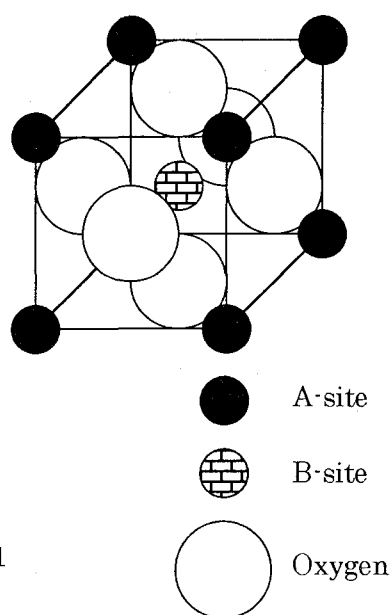


Fig. 1

## <sup>161</sup>Dy Mössbauer Spectra for Bridged Cyano Coordination Compounds

Katsuya Suzuki, Takafumi Kitazawa, Masashi Takahashi, and Masuo Takeda

Department of Chemistry, Faculty of Science, Toho University,  
Miyama 2-2-1, Funabashi, Chiba 274-8510, JAPAN

There is a potentially wide interest in coordination polymer compounds containing Dy(III) ions because of the expected magnetic properties of 4f electrons. Dy[Fe(CN)<sub>6</sub>]4H<sub>2</sub>O is a typical three-dimensional coordination polymer. The structure consists of infinite polymeric arrangement of octahedral Fe(III) bridged through cyanide linkages to Dy(III) ions coordinated by six N atoms of cyanide and two O atoms of water.

The Mössbauer effect has been reported for many Dy isotopes (<sup>160</sup>Dy, <sup>161</sup>Dy, <sup>162</sup>Dy, <sup>163</sup>Dy, <sup>164</sup>Dy). <sup>161</sup>Dy is most frequently used for Mössbauer spectroscopic studies. The 25.7 Kev transition is usually employed due to the narrow linewidth and the large recoil-free fraction. <sup>161</sup>Dy Mössbauer spectroscopy has been applied to investigate the electronic and magnetic structures of Dy intermetallic compounds. However, few <sup>161</sup>Dy Mössbauer spectroscopic study on coordination polymer compounds has been reported. Thus we have applied to the coordination polymer compounds Dy[Fe(CN)<sub>6</sub>]4H<sub>2</sub>O (1), KDy[Fe(CN)<sub>6</sub>]3H<sub>2</sub>O (2), Dy[Co(CN)<sub>6</sub>]4H<sub>2</sub>O (3), KDy[Ru(CN)<sub>6</sub>]3H<sub>2</sub>O (4) to obtain information on the molecular structure and bonds.

A <sup>161</sup>Tb/GdF<sub>3</sub> Mössbauer source (161 MBq) was prepared by a neutron irradiation of <sup>160</sup>GdF<sub>3</sub>, prepared by solid state reaction of <sup>160</sup>Gd<sub>2</sub>O<sub>3</sub> and NH<sub>4</sub>F at 300°C, in a JRR-3M reactor of JAERI. <sup>161</sup>Dy Mössbauer spectra of 1-4 were measured in the temperature region of 78 to 290 K. Each spectrum shows a slightly asymmetric absorption due to quadrupole interactions. The observed isomer shift (δ, relative to the source) at 78 K for 1, 2, 3 and 4 are -0.39, -0.35, -0.74 and -0.05 mm s<sup>-1</sup>, respectively. These values are similar to those for EDTA complexes reported. Fig. 1 shows the spectra of 1 at 78K and 290 K. The linewidth apparently increases on lowering the temperature. The broadening of the linewidth is also observed for 2-4. This suggests the existence of the paramagnetic relaxation at low temperature.

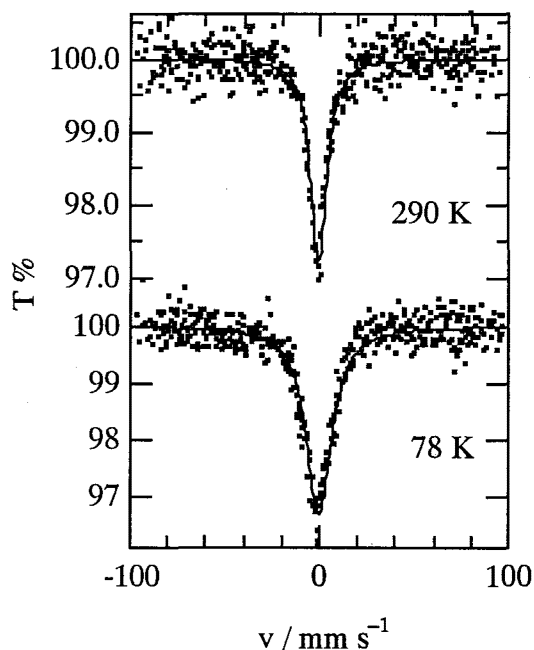


Fig. 1 <sup>161</sup>Dy Mössbauer spectra for  
Dy[Fe(CN)<sub>6</sub>]4H<sub>2</sub>O at 78 K and 290 K

**$^{121}\text{Sb}$  Mössbauer Spectra of Alkali Metal  
Antimonides  $\text{M}_3\text{Sb}$  ( $\text{M}_3 = \text{Na}_3, \text{K}_3, \text{Na}_2\text{K}, \text{Rb}_3$ )**

Kunihiko Kitadai, Masashi Takahashi and Masuo Takeda

Department of Chemistry, Faculty of Science, Toho University  
Miyama, Funabashi 274-8510, JAPAN

Zintl phases, intermetallic compounds consisting of electropositive metals and posttransition elements, show some remarkable structural and bonding characteristics that are closely related to both cluster compounds and classical valence compounds obeying the octet rule. In the alkali metal-pnictide alloy systems, when a pnictide atom accepts some extra electrons from the alkali metal atoms the pnictide ion behaves as the isoelectronic element or ion. For example, tellurium-like spiral chains have been found in  $\text{MSb}$ . Similarly  $\text{Sb}^{3-}$  ion in the  $\text{M}_3\text{Sb}$  is isoelectronic to  $\text{I}^-$  and  $\text{M}_3\text{Sb}$  adopts a salt-like structure. If the interactions between alkali metals and antimony atoms are completely ionic, there would be no differences among the alkali metal atoms, but some interactions have been suggested from the band structure calculations. This work was carried out to obtain the information on the alkali metal-antimony interactions in  $\text{M}_3\text{Sb}$  using the  $^{121}\text{Sb}$  Mössbauer spectroscopy.  $\text{Na}_3\text{Sb}$ <sup>1)</sup>,  $\text{K}_3\text{Sb}$ <sup>1)</sup> and  $\text{Rb}_3\text{Sb}$ <sup>2)</sup> have the  $\text{Na}_3\text{As}$  structure in which Sb is surrounded by 5 alkali metal atoms as trigonal bipyramidal, and  $\text{Na}_2\text{KSb}$  has the  $\text{Cu}_2\text{MnAl}$  structure<sup>3)</sup> in which Sb is surrounded by 6 potassium atoms octahedrally and by 8 sodium atoms square antiprismatically.

Samples were prepared by reacting stoichiometric amounts of alkali metal and antimony in an alumina tube.<sup>1-3)</sup> The products were identified by XRD.  $^{121}\text{Sb}$  Mössbauer spectra were measured at 12K on the absorbers containing 15  $\text{mgSb cm}^{-3}$  sample using a  $\text{Ca}^{121\text{m}}\text{SnO}_3$  source.

The values of isomer shift ( $\delta$ : relative to  $\text{InSb}$  at 12K) for  $\text{Na}_3\text{Sb}$ ,  $\text{K}_3\text{Sb}$  and  $\text{Rb}_3\text{Sb}$  are 0.67, 0.38, 0.21  $\text{mm s}^{-1}$ , respectively and are considerably larger than that for elemental antimony ( $-3.11 \text{ mm s}^{-1}$ ). This indicates that the s electron densities of antimony atoms in  $\text{M}_3\text{Sb}$  are much smaller than that of Sb. This is interpreted by the shielding effect of the p electrons; i.e.  $\delta$  values are increased due to increase in p electron densities. The value of quadrupole coupling constant is experimentally 0  $\text{mm s}^{-1}$ , showing clearly that the electrons are distributed equally in three p orbitals. These facts show that the valence state of Sb in  $\text{M}_3\text{Sb}$  is  $-3$ . There are some differences in  $\delta$  values. The value for  $\text{Na}_2\text{KSb}$  (0.71  $\text{mm s}^{-1}$ ) is the largest, indicating that ionicity in the crystal is the largest among them. Thus assuming the ionic radius for  $\text{Na}^+$  to be 116pm, the ionic radius for  $\text{Sb}^{3-}$  is estimated to be 218pm from the Na-Sb distance in  $\text{Na}_2\text{KSb}$ <sup>3)</sup>. Using this value, the ratio of observed and expected interatomic M-Sb distances are calculated. The values are 0.93, 0.95 and 0.96 for  $\text{Na}_3\text{Sb}$ ,  $\text{K}_3\text{Sb}$  and  $\text{Rb}_3\text{Sb}$ , respectively. This is exactly the order of the isomer shift value. Thus the small differences in  $\delta$  suggest the difference in the ionicity in M-Sb interactions.

1) G. Brauer; E. Zintl, *Z. Physik. Chem.*, **37B**, 323 (1937).

2) G. Gnutzmann; F. W. Dorn; W. Klemm, *Z. anorg. allg. Chem.*, **309**, 210 (1961).

3) W. H. McCarroll, *J. Phys. Chem. Solids*, **16**, 30 (1960).

## STRUCTURE OF A NOVEL NITRIDO TECHNETIUM COMPLEX WITH PEPTIDE CHELATE LIGAND KYCAR

Shinji SATO, Tsutomu TAKAYAMA, Tsutomu SEKINE and Hiroshi KUDO

Department of Chemistry, Graduate School of Science, Tohoku University, Sendai 980-8578, Japan

### Introduction

Technetium-99m complexes with peptides are interested in the utilization for diagnostic radiopharmaceuticals. We have previously studied the structure of oxo technetium ( $^{99}\text{Tc}$ ) complex with KYCAR<sup>1)</sup>. However, nitrido technetium complex with KYCAR have not been investigated. In the present paper, we report the plausible structure of nitrido technetium ( $^{99}\text{Tc}$ ) complex with KYCAR synthesized for the first time.

### Experimental

The nitrido technetium complex with KYCAR was synthesized by the reaction of the KYCAR ligand with  $[n\text{-Bu}_4\text{N}][\text{TcNCl}_4]$  in methanol. Characters of the complex was analyzed by  $^1\text{H}$ -,  $^{13}\text{C}$ -NMR and IR spectroscopies as well as elemental analysis.

### Result and Discussion

$^1\text{H}$ -NMR signals of the  $\alpha$  and  $\beta$  sites of the cysteine show a downfield shift from those of free KYCAR. Although the complex has two KYCAR ligands, only one  $^1\text{H}$ -NMR signal is observed for the  $\alpha$  proton as well as the  $\beta$  protons of the cysteine. The result indicates that the complex have a square pyramid structure in which two KYCARs coordinate to the technetium atom through a nitrogen atom and a deprotonated sulfur atom of the cysteine. The nitrogen and sulfur atoms are in the *trans* position each other (Fig. 2).

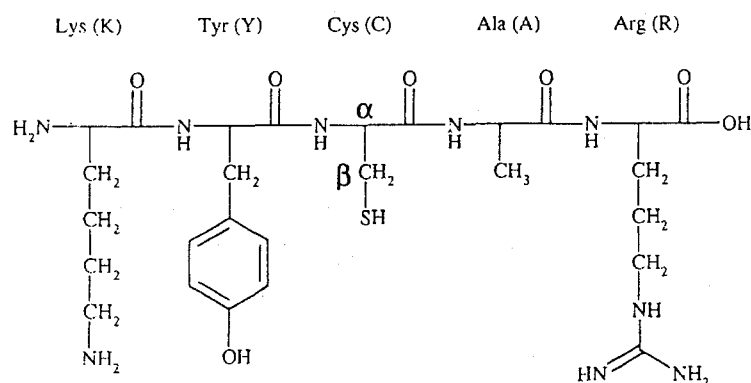


Fig. 1. Structural formula of KYCAR.

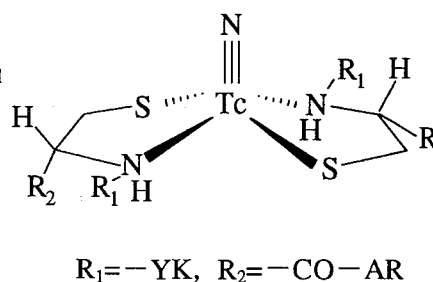


Fig. 2. Structure of the complex with KYCAR ligands.

1) T. Takayama, K. Suzuki, T. Sekine, H. Kudo. *Radiochim. Acta.*, **88**, 247 (2000).

Takao Morimoto<sup>1</sup>, Shigeru Banba<sup>1</sup>, Tetsuo Hashimoto<sup>2</sup>

<sup>1</sup>Japan Chemical Analysis Center, Sanno-cho, Inage, Chiba, 263-0002, Japan

<sup>2</sup>Department of Chemistry, Faculty of Science, Niigata University, Igarashi-cho, Niigata, 950-2181, Japan

### 1. Introduction

During alpha-decay process, the residual or recoiled daughter nuclide might be transferred from its parent position to a new site. Recently much attention has been paid on such direct recoil phenomena to explain significant fractionation of <sup>234</sup>U atoms against parent <sup>238</sup>U in many natural materials.<sup>1</sup> In this study, the authors try to get quantitative information of the alpha-recoil atoms using <sup>232</sup>U or <sup>226</sup>Ra (having descendants). The ejection and injection behavior of recoil atom <sup>224</sup>Ra from its parent <sup>228</sup>Th or <sup>222</sup>Rn from its parent <sup>226</sup>Ra were investigated on both source and collector.

### 2. Experimental

In order to prepare the thinly deposited source, the <sup>232</sup>U(Th-series) or <sup>226</sup>Ra(U-series) solutions were followed to the electrodeposition on a mirror polished stainless steel plate.<sup>2</sup> As a direct contact of the collectors (platinum, stainless steel, glass or organic materials) may cause the physical contamination, a spacer (0.1~0.2mm thickness) having a hole of 5mm diameter was inserted between the source and the collector. The assembly was fixed with an adhesive tape and stored in a vacuum chamber of about 1.3 Pa. At the end of the recoil exposure or collection, the collectors were measured by alpha-spectrometry to determine the activity strength.

### 3. Results and discussion

The distribution of the deposited <sup>232</sup>U or <sup>226</sup>Ra on the stainless steel plate was examined by alpha track on a polycarbonate film after the electrodeposition. In the case of U-decay series, the spectrum showed the alpha-spectrum due to <sup>222</sup>Rn along with their daughters on the collectors. These findings show that <sup>222</sup>Rn is ejected from <sup>226</sup>Ra source and moved to the collector owing to recoil behavior. Generally, the activity ratios of <sup>222</sup>Rn (in the collector)/<sup>226</sup>Ra (in the source) in inorganic material collector gave higher ratios in comparison with in organic materials. In the case of Th-decay series, the radioactive equilibrium state between <sup>224</sup>Ra and <sup>220</sup>Rn on the collectors showed interesting behavior, rendering apparently recoiling loss in almost all of the organic collectors. The activity ratios of <sup>224</sup>Ra on the collector against <sup>228</sup>Th on the source have been gradually grown with exposure time. The ejection ability of recoil atom <sup>224</sup>Ra is dependent on the collector materials.

1. T. Hashimoto, *Radioisotopes*, **43**, 212(1994). 2. W. Parker, *Nucl. Instr. and Meth.* **16**, 355(1962).



## **2P 32 Radiochemistry Research and Education at Clemson University**

J. D. Navratil, Department of Environmental Engineering and Science,  
Clemson University, Clemson, SC 29634

The Department of Environmental Engineering and Science at Clemson University has started an internship program for graduate students in radiochemistry. The program is funded through the Department of Energy (DOE) and the South Carolina University Research and Education Foundation (SCUREF) to contribute to ongoing actinide and radiochemistry research programs at DOE facilities and prepare students for careers in actinide and radiochemistry. SCUREF funds come from the Westinghouse Savannah River Company. This paper reviews the objectives, program description, and details of the program set up for this curriculum. The variety of radiochemistry research projects under way at Clemson will be highlighted.

## Characterization of uranium series nuclides in the geological materials by selective leaching method

Yutaka Kanai<sup>1</sup>

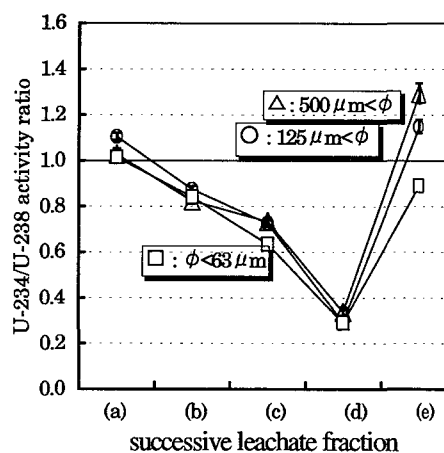
<sup>1</sup>Geological Survey of Japan, National Institute of Advanced Industrial Science and Technology (AIST), Higashi 1-1-1, Tsukuba, Ibaraki 305-8567, Japan

Uranium series nuclides are one of the most important and well-known sources of natural radioactivity. The parent nuclide, U-238, is popular as uranium element, and uranium ores have been explored and surveyed for the use of nuclear reactor fuel. So, uranium geochemistry is of much concern for geochemical exploration, mining, and recently nuclear waste management as natural analog.

Uranium has some characteristics; (1) it has the decay-chain daughters, (2) it has two typical oxidation states, U(IV) and U(VI), (3) it has a constant half-life. Therefore, uranium and its daughter nuclides have become very useful and important nuclides for elucidation of the geological and geochemical events from these viewpoints. Furthermore, the detail behaviors of these nuclides can be elucidated by using the selective leaching method<sup>3</sup> because this technique provides some more information for characterization.

In this study, uranium series nuclides in some geological materials were examined by selective chemical leaching methods. The used technique contains HCl leaching<sup>1</sup>, the successive leaching<sup>3</sup> by (a) ammonium acetate, (b) sodium acetate/acetic acid, (c) hydroxylamine/hydrochloric acid, (d) hydrogen peroxide, (e) HF/HNO<sub>3</sub>/HClO<sub>4</sub> solutions. The studied samples are collected from the weathered bauxite deposit in China, the weathered phosphorite deposit in Niigata, Japan, the conglomerate deposit in Gifu, Japan, and the Lake Shinji sediment in Shimane, Japan. The powdered samples are mixed with the leaching solutions and U and U-234/U-238 activity ratios in the leachates are determined by fluorimetry and alpha spectrometry.

The each leachate was separated as fraction. Uranium was abundant in the iron-rich fraction of the weathered sediment, and also in the carbonate and iron-rich fractions of conglomerate sediment. The U-234/U-238 activity ratios of these fractions were varied (see Figure), suggesting the difference of environmental conditions. Several examples are shown to indicate the importance of characterization of uranium series nuclides in the environmental samples.



1. Y. Kanai, *Geochem. J.*, **26**, 207-218 (1992).

2. Y. Kanai, Y. Sakamaki, *Appl. Geochem.*, **9**, 547-552 (1994).

3. Y. Kanai, Y. Okuyama, T. Seo, Y. Sakamaki, *Geochem. J.*, **32**, 351-366 (1998).

RELEASE OF PO FROM WATER SUPPORTED BY  
MICROORGANISM

Noriyuki MOMOSHIMA,<sup>1</sup> Li-Xiang SONG,<sup>2</sup> Susumu OSAKI<sup>3</sup> and Yonezo MAEDA<sup>2</sup>

<sup>1</sup>Department of Environmental Science, Faculty of Science, Kumamoto University, Kurokami 2-39-1, Kumamoto, 860-8555, Japan.

<sup>2</sup>Department of Chemistry and Physics of Condensed Matter, Graduate School of Science, Kyushu University, Hakozaki, Higashi-ku, Fukuoka, 812-8581 Japan

<sup>3</sup>Radioisotope Center, Kyushu University, Hakozaki, Higashi-ku, Fukuoka, 812-8581 Japan

Behavior of Po in fresh waters was examined at laboratory culture experiments using fresh waters those were collected from a small pool in Kyushu University, Fukuoka, Japan (about 1.5 km from the seacoast), Xi river and Xiqing lake at Guilin, Guangxi Territory, China (at least 400 km far away from nearest seacoast). The fresh water with Po-208 tracer was incubated at 30 °C by bubbling room air that was filtered with a 0.25 µm membrane filter to avoid contamination of microorganism in room air. The bubbled air was, then, passed through a cotton layer (ca. 7 cm length) in a testing tube to remove mist in the air and introduced to three successive 20 ml glass-vials in which liquid scintillator was contained to collect emitted volatile Po. The activity of the glass vials was measured by liquid scintillation counting. All of the fresh water culture experiments showed increases in Po activity in the glass vials. This result suggests a possibility of a new source for atmospheric Po that is biologically supported. At present abiotic sources have been believed to be responsible to atmospheric Po; radioactive decay of <sup>222</sup>Rn that escaped from the earth's surface; release accompanied by volcanic eruption and savanna combustion; migration of sea salt and soil dust.

The emission from original fresh waters is very small for Po but above the detection limit of the liquid scintillation counting system and Po is certainly emitted by microorganism's activity in fresh waters. Addition of tryptone to the fresh water cultures increased the emission of Po considerably along with a growth of microorganism, suggesting concerning of chemoheterotrophs to Po emission. Participation of photoautotrophs was also considered because Po emission was increased when NaHCO<sub>3</sub> was added to the fresh water cultures. The quantity of Po emitted was comparable to our previous culture experiments<sup>1</sup> in which artificial culture medium containing 3% NaCl was used and inoculated sea sediment extract.

The biologically support Po emission would be a general phenomenon in fresh water environment as well as seawater environment<sup>1</sup> and is a new finding on the source for atmospheric Po.

1. N. Momoshima; L.-X.Song; S. Osaki; Y. Maeda, Formation and Emission of Volatile Polonium Compound by Microbial Activity and Polonium Methylation with Methylcobalamin. *Environ. Sci. Technol.*, in printing. (2001).

R.SIVAKUMAR

Department of Physics, Bharathiar University, Coimbatore - 641 046, India.

S.SELVASEKARAPANDIAN

Department of Physics, Bharathiar University, Coimbatore - 641 046, India.

V.KANNAN

Environmental Survey Laboratory, BARC, Kalpakkam - 605 102, India.

Natural Radionuclides  $^{226}\text{Ra}$ ,  $^{210}\text{Pb}$  and  $^{210}\text{Po}$  exist ubiquitously in the environment and significantly contribute to the effective dose equivalent to human being. The concentration of  $^{226}\text{Ra}$ ,  $^{210}\text{Pb}$  and  $^{210}\text{Po}$  in different vegetables cultivated in Gudalur in South India, other food materials and total diet samples have been estimated using radiochemical methods. The daily intakes of these radionuclides by an adult population in this region have also been estimated. The higher concentrations of  $^{210}\text{Po}$  and  $^{210}\text{Pb}$  have been observed in leafy vegetables and the lowest value in tuberous vegetables.  $^{226}\text{Ra}$  is recorded high in ginger (tuberous vegetable) and low in Brinjal (other vegetable category). The  $^{210}\text{Po}/^{210}\text{Pb}$  ratio in different vegetables have also determined and it found to vary from 0.40 to 1.9. The concentrations of  $^{226}\text{Ra}$ ,  $^{210}\text{Pb}$  and  $^{210}\text{Po}$  in the soil under the sampled plants have also estimated using radiochemical method. The transfer coefficients of  $^{226}\text{Ra}$  and  $^{210}\text{Pb}$  have also been estimated for different vegetables cultivated in this region. The equivalent doses received by the population through consumption of food have been estimated. The dose received by the population through the consumption of non-vegetarian diet is more than that through vegetarian diet samples.

## 2P 36 The Study of Uranium Isotope Dilution Method Used to Estimate the Volume Mixing of River Waters

Jeng-Jong Wang<sup>1</sup> and Tieh-Chi Chu<sup>2</sup>

1. Institute of Nuclear Energy Research, Atomic Energy Council, Taiwan, Republic of China

2. Department of Nuclear Science, National Tsing Hua University, Taiwan, Republic of China

### Abstract

Alpha spectrometer was used in this study to analyze the radioactive concentrations of  $^{238}\text{U}$  and  $^{234}\text{U}$  from the river waters of Waishuang stream, the Nanhuang stream and the Huangkang stream within the Tatun volcano group area in Northern Taiwan. The radioactive concentrations of  $^{238}\text{U}$  and  $^{234}\text{U}$  of river waters in this study are 0.80-48 mBqL<sup>-1</sup> and 1.2-51 mBqL<sup>-1</sup>. Furthermore, the radioactive concentrations of  $^{238}\text{U}$  and  $^{234}\text{U}$  from the river waters of upstream, tributary and downstream of the Waishuang stream, the Nanhuang stream and the Huangkang stream are used to estimate the volume mixing ratio  $\frac{V_u}{V_r}$  of the upstream and the tributary river water in the downstream river water using the isotope dilution method. The results of the  $\frac{V_u}{V_r}$  are 6.5, 5.4 and 5.3 for the Waishuang stream, the Nanhuang stream and the Huangkang stream, respectively.

Keywords: Alpha spectrometer, Volume mixing ratio, Isotope dilution method

Tel: 886-3-4711400 ext.7610, Fax: 886-3-4711171, e-mail: jjwang@iner.gov.tw

## 2P 37 Removal of Impurities from Environmental Water Samples for Tritium Measurement by means of LS Counter

Yoichi SAKUMA<sup>1</sup>, Yoshimune OGATA<sup>2</sup>, Naruhito TSUJI<sup>3</sup>, Hirokuni YAMANISHI<sup>1</sup> and Takao IIDA<sup>4</sup>

<sup>1</sup>Safety and Environmental Research Center, National Institute for Fusion Science, Oroshi-cho 322-6, Toki 509-5292, Japan

<sup>2</sup>School of Health Sciences, Nagoya University, Daiko-cho, Higashi-ku, Nagoya 461-8673, Japan

<sup>3</sup>Japan Air-conditioning Service Co. & Ltd. Terugaoka 239-2, Meito-ku, Nagoya 465-0042, Japan

<sup>4</sup>Graduate School of Engineering, Nagoya University, Furou-cho, Chikusa-ku, Nagoya 464-8603, Japan

Liquid scintillation counting is now the most popular method to measure the tritium concentration in the low level water samples such as environmental water samples. However, it takes much time with a lot of doing to distill off the impurities in the sample water before mixing the sample with the liquid scintillation cocktail. In the light of it, we investigated the possibility of an alternative method with membrane filters for purification. As published before, the filtration method was proved to be available to be alternatively used for tritium measurement<sup>1)2)</sup>.

In the present environment water, the tritium concentration has become nearly 0.5-1.0Bq/kg-H<sub>2</sub>O which is within the detective limit by the low background liquid scintillation counter. As for the samples lower than the detective limit they will be treated by electrolysis concentration with liquid scintillation analyzer. Recently an electrolysis tritium enriching method using a solid polymer electrolyte has been developed. According to the method, there is no need to add any electrolyte, neither is the neutralization after concentration. If we could replace the distillation process with the filtration, the procedure would be simplified very much. We investigated the procedure and we were able to prove that the filtration was available.

### References

- 1) Yoichi SAKUMA, Mitsuyasu NODA, Yoshimune OGATA and Naruhito TSUJI, Proc. 10<sup>th</sup> Intern. Congress on Radiation Protection, P-4a-248, (Hiroshima, Japan, May 15-19, 2000).
- 2) Yoichi SAKUMA, Proc. Intern. Conference on Advances in Liquid Scintillation Spectrometry (Karlsruhe, Germany May 7-11, 2001) to be published.

## 2P 38 DETERMINATION OF TRACE RHENIUM CONTENTS IN RIVER WATER SAMPLES BY Q-ICP-MS AND HR-ICP-MS

Shigeo UCHIDA<sup>1</sup>, Keiko TAGAMI<sup>1</sup> and Masahiro SAITO<sup>2</sup>

<sup>1</sup>Environmental and Toxicological Sciences Research Group, National Institute of Radiological Sciences, Anagawa 4-9-1, Inage-ku, Chiba 263-8555, Japan

<sup>2</sup>Nuclear Safety Research Division, Kyoto University Research Reactor Institute, Noda, Kumatori-cho, Sennan-gun, Osaka 590-0494, Japan

Understanding the behavior of Re in fresh water will assist our understanding of Tc behavior in the aquatic environment. However, Re is known as one of the least abundant metals in the earth's surface; there are many data on Re in seawater samples but its concentration in fresh water is not well known. In this study, a simple separation method was applied to determine Re at trace levels in river water by quadrupole ICP-MS (Q-ICP-MS) and high resolution ICP-MS (HR-ICP-MS). In addition, the determined values were compared with values derived directly by HR-ICP-MS analysis.

Six river water samples collected in Japan were filtered through 0.45µm Millipore filters. To each sample was added 0.5 mL concentrated HNO<sub>3</sub> and a small portion of H<sub>2</sub>O<sub>2</sub> per 100 mL. The solutions were heated for 1 h to convert all Re into ReO<sub>4</sub><sup>-</sup>. Using TEVA resin minicolumns (Eichrom Ind. Inc.), Re was concentrated from 420 - 925 mL river water. The resin extraction method can separate Re from most sample matrices and trace elements by using nitric acid of different molalities. Almost 100% recovery was found throughout the method as determined using radioactive multitracers. The Re fraction (ca. 5 mL of 8M HNO<sub>3</sub>) was diluted 10 or 20 times with deionized water prior to analyzing by ICP-MS.

Table 1 shows the measured Re contents in the river water samples. The literature values in terrestrial water samples are also listed. The concentrations ranged from 0.9 to 6.5 pg/mL and the results by these three methods showed good agreement for each sample (data are not shown). For a direct analysis, it is essential to consider generation of isobars (oxides, chlorides and hydrides with rare earth elements or W at masses 185 and 187). Most REEs in Japanese river waters are usually low, thus, the direct analysis by HR-ICP-MS is applicable for Re determination in river water and indeed there were no significant difference between the results, though it is better to use the developed method to secure a more accurate measurement.

Table 1. Rhenium contents in terrestrial water samples.

Location	Re (pg/mL)		Reference
	Average	Range	
Japan*	2.2 ± 2.2	0.9 - 6.5	This study
U.S.A.†	8.2 ± 6.1	0.9 - 35	Hodge et al. <sup>1</sup>
Amazon & Orinoco*	5.4 ± 11.9	0.2 - 47	Colodner et al. <sup>2</sup>
Black sea*	14.1 ± 4.6	7.4 - 20.3	Colodner et al. <sup>3</sup>

\*: River water, †: Groundwater

1. V.F. Hodge; K.H. Johannesson; K.J. Stetzenbach, *Geochim. Cosmochim. Acta* **60**, 3197 (1996).

2. D.C. Colodner; E.A. Boyle; J.M. Edmond, *Anal. Chem.* **65**, 1419 (1993).

3. D.C. Colodner; J.M. Edmond; E.A. Boyle, *Earth Planet. Sci. Lett.* **131**, 1 (1995).

## ATOMOSPHERIC DEPOSITION OF Be-7, K-40, Cs-137 AND Pb-210 DURING 1993-2001 AT TOKAI-MURA, JAPAN

T. UENO, S. NAGAO and H. YAMAZAWA

Department of Environmental Sciences,  
Japan Atomic Energy Research Institute  
Tokai-mura, Naka-gun, Ibaraki-ken, 319-1195, Japan

To evaluate the migration of radionuclides to the ground surface, whole dry and wet deposition was collected during the period from September, 1993 to June, 2001 with a water-filled basin with the surface area of 0.5 m<sup>2</sup> set up at Japan Atomic Energy Research Institute at Tokai-mura, Ibaraki-ken. Monthly basin samples were evaporated to dryness without ebullition to obtain residual samples. These samples were measured by a well type Ge detector (normal measuring time was 200,000s) for natural radionuclides such as Be-7, K-40, Pb-210 and fallout radionuclide, Cs-137.

Monthly depositions of Be-7, K-40, Cs-137 and Pb-210 were 11 to 514, 0.74 to 10.49, N.D. (under detection limit of 0.01Bq) to 0.31, and 1.94 to 29.01 Bq/m<sup>2</sup>, respectively. These monthly depositions showed a clear seasonal variation with peaks in the early spring from February to April, and also in May in some years. The depositions of K-40 and Cs-137 have good correlation with the dry weight of deposited material, the correlation coefficient being 0.96 and 0.94, respectively. On the other hand, the depositions of Be-7 and Pb-210 showed much lower correlation coefficients of 0.47 and 0.25, respectively. This difference in the correlation coefficient between these two groups of radionuclides can be attributed to the difference in the originating processes.

Monthly values of concentration, that is defined as the activity in the unit mass of dried sample, were depicted in Fig. 1 for K-40 and Pb-210. It is clear that, although the concentrations of the both nuclides have sharp peaks, they are not correlated with each other as shown by the low correlation coefficient of 0.12. K-40 concentration has a relatively high base-line concentration of about 0.4 to 0.5 Bq/g with conspicuous peaks in, for instance late 1996 and late 2000. On the other hand, the base-line concentration of Pb-210 is low and the range of variation from minima to maxima is large as compared with that of K-40. These features in the concentration are thought to be caused by the difference in mechanism and location of origination, which would result in difference in the contributing particle size, and hence by the difference in the transport and deposition processes.

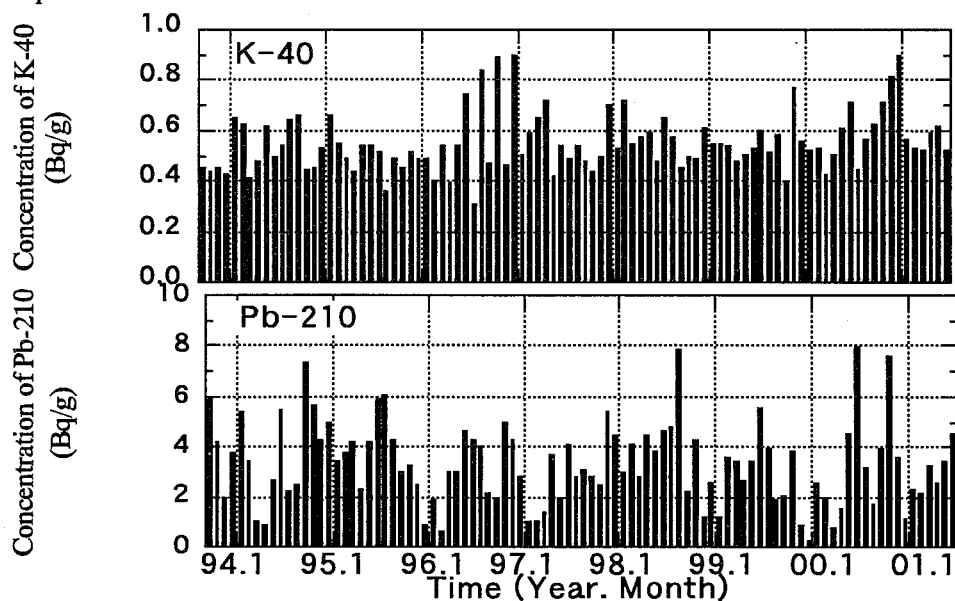


Fig.1 Variation of concentration of K-40 and Pb-210 in monthly basin sample



Yoko SAITO, Yutaka MIYAMOTO, Masaaki MAGARA, Satoshi SAKURAI and Shigekazu USUDA

Department of Environmental Sciences, Japan Atomic Energy Research Institute,  
Shirakata Shirane 2-4, Tokai 319-1195, Japan

### Introduction

For better understanding of impact of nuclear activities on the environment, determination of quantity and distribution of nuclear materials, i.e., environmental monitoring, is necessary. As air particles are direct carriers of radionuclides and air pollutants, they are often used as an indicator for monitoring. Air samplers are usually used to collect the particles, however, there is restriction on sampling timing and place.

The surface of plant leaves is known to adsorb air particles, therefore, we selected pine needles, which is a common plant in Japan and exist around nuclear facilities, to collect adsorbed compound and examined the feasibility of the adsorbed compound for environmental monitoring of uranium.

### Experimental

The needles were collected at a pine grove in Tokai, Ibaraki. Adsorbed compound was recovered by solvent washing of the needles with ultra pure water to wash down the compound from the needle surface (Sample A) and with acetone to remove the remaining compound together with wax layer of the needles (Sample B). After solvent washing, the needles were dried and cut into small pieces for analysis. The air particles were collected with an Andersen-type air sampler at the same location. The composition of the samples was determined by Instrumental Neutron Activation Analysis (INAA). The concentrations and isotopic ratios of uranium in the adsorbed compounds were measured by ICP-MS.

### Results and Discussion

The concentration patterns of elements in the adsorbed compounds were measured by INAA and compared with those of air particles and pine needles (Figure 1). The concentration patterns of Samples A and B had similarity. The concentrations of Sample A were higher than those of Sample B. This was due to the wax involved in Sample B. The patterns in the both the samples corresponded to that of the particles but differed from that of the needles, which meant that air particles were the main component of the adsorbed compounds and that the adsorbed compounds had possibility to be a useful indicator for environmental monitoring.

The concentration and isotopic ratio of uranium in the adsorbed compounds were measured (Table 1). It was found the origin of uranium in both the samples was natural.

In the future, we will accumulate the distribution and isotopic composition data and make use of them to elucidate the source and behavior of uranium in the environment.

Table 1 The concentration and isotopic ratio of uranium  
in the adsorbed compounds

	Sample A	Sample B
U [ppb] ( $3\sigma$ )	419 (2.5%)	25.3 (1.6%)
$^{235}\text{U}/^{238}\text{U}$ ( $3\sigma$ )	0.00736 (3.6%)	0.00725 (1.1%)

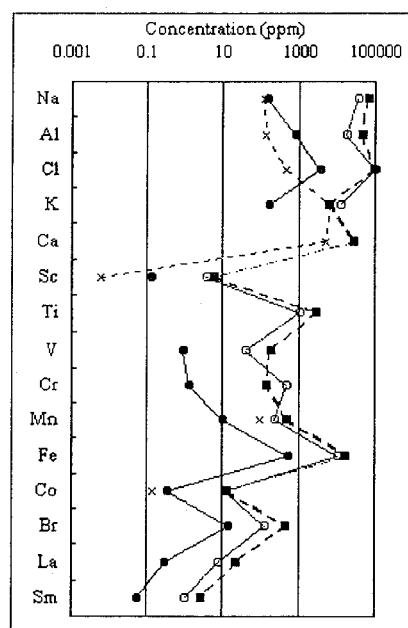


Figure 1 The elemental concentration pattern.

○: Sample A, ●: Sample B,  
×: Pine needles, ■: Air particles.

## Distribution and circulation of radionuclides originating from fallout in a forest

S. Ko<sup>1</sup>, T. Aoki<sup>2</sup>, H. Ohnishi<sup>1</sup>, Y. Katayama<sup>3</sup>

1 Graduate School of Agriculture, Kyoto University, Sakyo, Kyoto 606-8502, Japan

2 Radioisotope Research Center, Kyoto University, Sakyo, Kyoto 606-8501, Japan

3 The University of Human Environments, Motojuku-cho Okazaki, 444-3505, Japan

Many scientists have studied the behavior of radionuclides in the environment, but precise behavior of them in the forest ecosystem has been unknown. About 70% of Japan are covered with forest area, and it is important to know it to predict future's state of radionuclides in Japan. In this study, radiation from environmental samples from forested area was measured to study the distribution and behavior of radionuclides in forest ecosystem.

Sampling points locate in Kiryu experimental site in Shiga Prefecture. Four types of water samples (precipitation, throughfall, stemflow, and stream) and soil samples from various depth of 0-32cm, 5 types of plant samples (stem of hinoki (Japanese cypress), bark of hinoki and pine, and litter of conifer and broadleaf tree) were collected. The radioactivity of <sup>137</sup>Cs and <sup>40</sup>K in the samples were measured by pure Ge semiconductor detector. The concentration of natural Cs and K were measured by INAA.

The concentration of <sup>137</sup>Cs in most of water samples were below detection limit. Only in the case of stemflow, <sup>137</sup>Cs was detected, but it was so small amount to determine precisely. The <sup>137</sup>Cs concentrations of plant samples ranged from 0.06Bq/kg of hinoki wood to 5.6 Bq/kg of broadleaf tree litter. The reason for high content of <sup>137</sup>Cs of broadleaf tree litter had may be attributed to contact with the soil. The concentration of <sup>137</sup>Cs in the soil decreased with depth, while natural Cs and <sup>40</sup>K were almost constant at each sampling depth (Fig.1.) This result supports the report of Agapkina et al.<sup>(1)</sup> that <sup>137</sup>Cs stays in the 3-6 cm of the forest clay soil.

These results show that <sup>137</sup>Cs inflow and outflow occurring in the forest ecosystem are in small magnitude since atmospheric nuclear explosion has not occurred. It is suggested that most of the <sup>137</sup>Cs once entered in the forest ecosystem is trapped in the surface soil and a small part of that circulates in the ecosystem.

1. G.I.Agapkina, A.I.Scheglov, F.A.Tikhomirov, L.N.Merculova, *Chemospher*, 36(4-5), 1125 (1998).

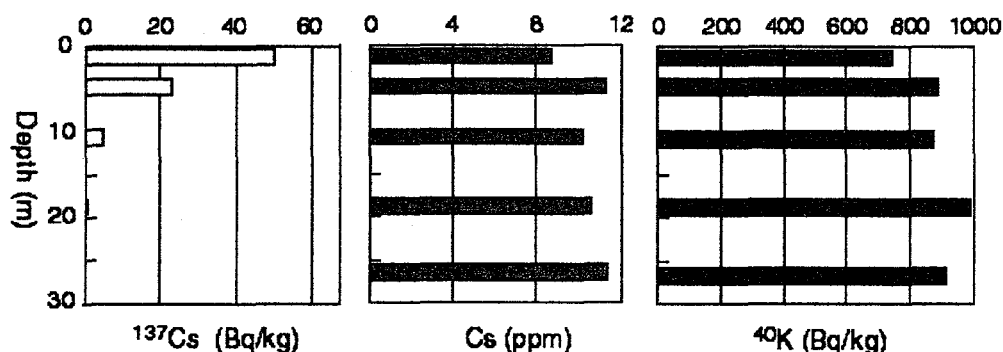


Fig. 1 Distribution of <sup>137</sup>Cs, Cs and <sup>40</sup>K in the soil.

Shin SATO<sup>1</sup>, Yuya KOIKE<sup>2</sup>, Takashi SAITO<sup>2</sup> and Jun SATO<sup>2</sup>

<sup>1</sup>Takushin Junior High School, Onishibetsu, Sarufutsu, Hokkaido 098-6234, Japan

<sup>2</sup>School of Science and Technology, Meiji University, Kawasaki, Kanagawa 214-8571, Japan

Atmospheric  $^{210}\text{Pb}$  (half-life: 22.3 y) is one of the progenies of  $^{222}\text{Rn}$  (half-life: 3.8 d) generated from the earth crust, and exists in the atmosphere attached to aerosol particles. As the source of the atmospheric  $^{210}\text{Pb}$  is essentially the earth surface, the atmospheric concentration of  $^{210}\text{Pb}$  over the continental areas is generally higher than that over the oceanic areas, and can reflect the geological and meteorological background of the observing localities <sup>1)-3)</sup> Atmospheric  $^7\text{Be}$  (half-life: 53.3 d) is the product from the spallation reaction of cosmic rays on the constituents of the atmosphere, and is transported in the atmosphere attached to aerosol particles.

The seasonal variation patterns and the levels of the atmospheric  $^{210}\text{Pb}$  concentrations at the Pacific coast are different from those observed at the Japan Sea coast in Japan. These differences are supposed to be originated from the elimination of aerosol particles containing large amount of  $^{210}\text{Pb}$  from the atmosphere on the mountainous districts running through the central Japan. Sarufutsu ( $45^\circ\text{N}$ ,  $142^\circ\text{E}$ ) is located on the coast of the Sea of Okhotsuk in the northern part of Hokkaido, and is apart from any large facilities which discharge air pollutants with some kinds of the progenies of Rn. It can be possible to measure the development of the atmosphere from the Eurasian Continent, and to determine the atmospheric concentrations of the progenies of Rn on the background level.

Aerosol samples were collected almost for one day once a week on glass fiber filters using a high volume air sampler ( $600\text{ dm}^3/\text{min}$ ) from February to May in 2001. Radioactivity of  $^{210}\text{Pb}$  was determined by the 46.5-keV  $\gamma$ -ray with an LEPS and  $^7\text{Be}$  was determined by the 478-keV  $\gamma$ -ray with an HPGe spectrometer. The atmospheric concentrations of  $^{210}\text{Pb}$  and  $^7\text{Be}$  ranged from 0.2 to 2.5  $\text{mBq}/\text{m}^3$  and from 1.7 to 4.2  $\text{mBq}/\text{m}^3$ , respectively. The lower concentrations of atmospheric  $^{210}\text{Pb}$  can be inferred to be contributed by the maritime atmosphere associated with such meteorological events as sea ice, Yamase (the strong cold wind from the Sea of Okhotsuk) and fog. The atmospheric concentrations of  $^{210}\text{Pb}$  at the higher level can be regarded as a characteristic in winter season. No significant correlation between the atmospheric concentrations of  $^{210}\text{Pb}$  and  $^7\text{Be}$  was obtained at Sarufutsu.

1. T. Doi, J. Sato, *Radioisotopes*, **44**, 701(1995).
2. S. Sato, H. Murai, T. Doi, J. Sato, *Radioisotopes*, **47**, 546(1998).
3. S. Sato, T. Doi, J. Sato, *Radioisotopes*, **49**, 439(2000).

## Influence of OH and metallic impurities on radiation-induced luminescence phenomena from natural quartz

Yuji Yanagawa,<sup>1</sup> Takahiro Yamaguchi,<sup>2</sup> Tetsuo Hashimoto<sup>2</sup>

<sup>1</sup>Graduate School of Science and Technology, Niigata University, Ikarashi-nincho,  
Niigata, 950-2181, Japan

<sup>2</sup> Faculty of Science, Niigata University, Ikarashi-nincho, Niigata, 950-2181, Japan

The blue-thermoluminescent mechanism for natural quartz has been investigated with respect to the OH species, metallic impurities and the color center distribution, by comparing the thermoluminescence color images. Microscopic infrared spectroscopy, ranging of  $3200\text{-}3600\text{cm}^{-1}$ , clarified the behavior of OH species in some slices of natural quartz with and without gamma-ray irradiation.

The mapping due to the Al-OH concentration revealed that the darker color centers corresponded to the weaker Al-OH absorption. On the other hand, the darker color was resulted in the higher intensities of blue thermoluminescence dependent on the thermoluminescence color images. The Al-OH concentrations lead to decrease after irradiation, while the intensity of blue thermoluminescence and the darkness of color center tended to increase<sup>1)</sup>. These results imply that the impurities related to OH in quartz could operate as quenchers or erasers of radiation-induced phenomena and that the hydrogen radicals derived from the irradiation could act as a killer of radiation-induced Al hole centers, associated to blue thermoluminescence and blue radioluminescence.

The spectrophotometric studies of TL properties are currently carried out when the hydrogen radicals and/or electrons are recombined with Al hole centers, owing to temperature rise up to  $400^\circ\text{C}$  from liquid  $\text{N}_2$  temperature. On the basis of this experiment, it was found that natural quartz after irradiation at  $-196^\circ\text{C}$  has 4 TL emission peaks ( $-120$ ,  $-75$ ,  $-20$  and  $12^\circ\text{C}$ ) with the thermal treatment up to room temperature and that the peak wavelength is shorter, nearly close to violet regions, in comparison with the TL from  $80$  to  $400^\circ\text{C}$ . It was confirmed that the lower peak,  $-120^\circ\text{C}$ , could be attributed to phenomenon at recombination of Al hole centers with the hydrogen radicals on the basis of ESR behaviors after irradiation at  $-196^\circ\text{C}$ <sup>2)</sup>.

The roles of some alkali metal contents are also investigated from viewpoints of glowcurves using ICP-MS.

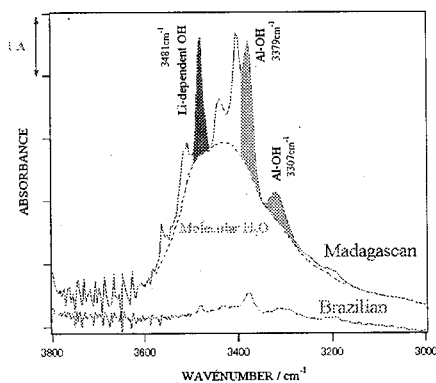


Figure IR absorption spectra from natural quartz.

1) Hashimoto et al., *Radiat. Meas.* **27**, 243-250 (1997)

2) Hashimoto et al., *Radiat. Meas.* **29**, 493-502 (1998)

## 2P 44      Optical stimulated luminescence (OSL) and thermoluminescence (TL) properties of red TL (RTL) quartz using a new automated OSL/TL measuring system

Takahiro NAKAGAWA<sup>1</sup>, Hayato USUDA<sup>2</sup>, Tetsuo HASHIMOTO<sup>2</sup>

<sup>1</sup>Graduate School of Science and Technology, Niigata University, Ikarashi-nincho, Niigata, 950-2181, Japan

<sup>2</sup>Faculty of Science, Niigata University, Ikarashi-nincho, Niigata, 950-2181, Japan

A new automated OSL/TL measuring system, which is measurable for both thermoluminescence (TL) including red-TL (RTL) and optically stimulated luminescence (OSL), has been developed. The OSL technique is well known to be efficient to dating of sediment layers as well as archeological burnt earthenware and kilns. This new system was installed with a small X-ray irradiation instrument; a single-aliquot regenerative-dose (SAR)<sup>1</sup> protocol becomes now applicable by means of repeated irradiations, preheating procedure, and luminescence measurements for a single aliquot.

Accordingly, this system can be used to various experiments of both OSL and TL, since this system is changeable photomultiplier tube, optical filters, and experimental conditions (heating rate, preheat temperatures, measuring temperatures, and so on). In the SAR protocol, the measuring and preheat temperatures were tested to obtain reliable accumulated doses. To perform cross check between OSL and RTL using RTL quartz, relationships of exposure times of blue LED (OSL), OSL intensity and shapes of growth curves (RTL) were tested and the doses evaluated between OSL and RTL measurements on the RTL quartz were compared.

In practice, this system was employed for the evaluation of accumulated doses from OSL and TL on RTL quartz; the RTL-property was revealed by means of thermoluminescence color images (TLCIs). RTL quartz grains extracted from a roof tile of Shin-Yakushiji temple were examined for the evaluation of accumulated doses by means of RTL and OSL measurements combined with SAR protocol. Figure 1 shows response curves. NOSL and NRTL indicate naturally accumulated OSL and RTL in quartz grains, respectively. The naturally accumulated doses (NAD) give excellent concordance in each other.

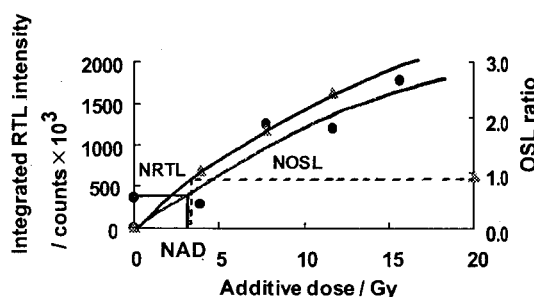


Fig.1. Response curves of OSL and RTL from quartz extracted from a roof tile of Shin -Yakushiji temple. Filled triangles and circles are OSL and RTL, respectively.

1. A.S. Murray, A.G. Wintle; *Rad.Mes.* 32, 57-73(2001).

## 2P 45      DETERMINATION OF DETECTION EFFICIENCY WITH A GE DETECTOR USING MANY ENCAPSULATED SMALL RADIOACTIVE SOURCES

Norio NOGAWA and Yoshihiro MAKIDE

Radioisotope Center, The University of Tokyo,  
Bunkyo-ku, Tokyo 113-0032, Japan

The detection efficiency of samples with a Ge detector is necessary to be determined by experiment and/or calculation for various forms. Standard solution samples or powder/clay samples containing radioactive materials are widely used for the determination. In order to avoid the radioactive contamination in these methods, 1000 encapsulated small radioactive sources of Eu-152 were prepared.

Each capsule of Eu-152 source (35 Bq) used in this work has an outer diameter of 17 mm, a height of 17 mm and a capacity of 0.5 ml (SANPLATEC 2-A). A 300 ml polystyrene vessel (SANOYA 95-1, 95 mm diameter, 58 mm height) was charged with 75 of the Eu-152 sources and the remaining space in the vessel was filled with various powder materials (aluminum oxide, silica gel, manganese dioxide, sodium chloride, potassium chloride, lithium carbonate, sodium carbonate, potassium bromide, ferric oxide and styrene polymer). A Ge detector (counting efficiency: above 18 %) in the shield was used for the measurement of these samples. The detection efficiency of 122 keV  $\gamma$  rays from Eu-152 and the filling density (weight of sample in the vessel divided by volume of the vessel) showed an exponential correlation. When a solution containing Eu-152 or aluminum oxide powder labeled with Eu-152 was put in the same vessel, their detection efficiencies were found on this line. Detection efficiencies of 344 keV and 779 keV  $\gamma$  rays also showed exponential correlations with filling density. Correction of self-absorption of a sample is made possible by the density for  $\gamma$  rays above 122 keV. When the vessel was charged with Eu-152 sources and remaining space was filled with potassium chloride, detection efficiency of Eu-152 and that of K-40 fairly agreed. For correction of detection efficiency for  $\gamma$  rays of below 122 keV, it is necessary to take elemental compositions of the sample into consideration.

When radioisotope solutions are used for the calibration, contamination of the detector or of the vessel may occur. There is no possibility of contamination by using the proposed sources.

Toshiaki KISHIKAWA,<sup>1</sup> Tatsuyoshi ISAGAWA<sup>2</sup>

<sup>1</sup>Faculty of Engr., Kumamoto Univ., Kurokami, Kumamoto 860-8555, Japan

<sup>2</sup>Dept. Sci. Tech., Grad. Sch. Sci. Tech., Kumamoto Univ., Kurokami, Kumamoto 860-8555, Japan

Goal of the present research is to develop ultra-precise measurement method of gamma-ray energy detected by using a gamma-ray spectrometer with high purity Ge detector. The development is made by applying an instrument function, which is proposed by the authors, in the course of photopeak shape analyses. The instrument function is the likelihood estimation function composed of probability functions relevant to induced electronic signal creation events, after the incidence of a photon, of a charge carriers creation and a random escape of the carriers by trapping in holes, together with an event of electronic noise generation. Previously the noise shape function is assumed to be the normal distribution (N.D.) function. However, experimentally obtained shapes of the electronic noise have distorted shape unlike symmetrical one of the N.D. function. The purpose of this paper is to describe of the electronic noise shape as a functional form.

The spectrometer used in the experiments was a Ge-equipped EG&E Ortec 7450 multichannel analyzer at Kurokami Radioisotope Laboratory (KRI).

Figure 1A is an example that noise shape analysis by a Proposed Function (P.F.) and N.D. which were applied to the measured data. Estimation parameters of N.D. function are the centroid of symmetry ( $x_c$ ) and the standard deviation ( $\sigma$ ). The P.F. is the folded function of Poisson distribution function and N.D. function. Parameters of the P.F. are  $x_c$ ,  $\sigma$  and the variance ( $v_t$ ). Figure 1B shows the patterns of converged residue. When two estimation functions are compared, the residue values of the P.F. are smaller than those of the N.D. on the higher side channels. Therefore, the estimation by the P.F. reflects the distortion of the noise shape.

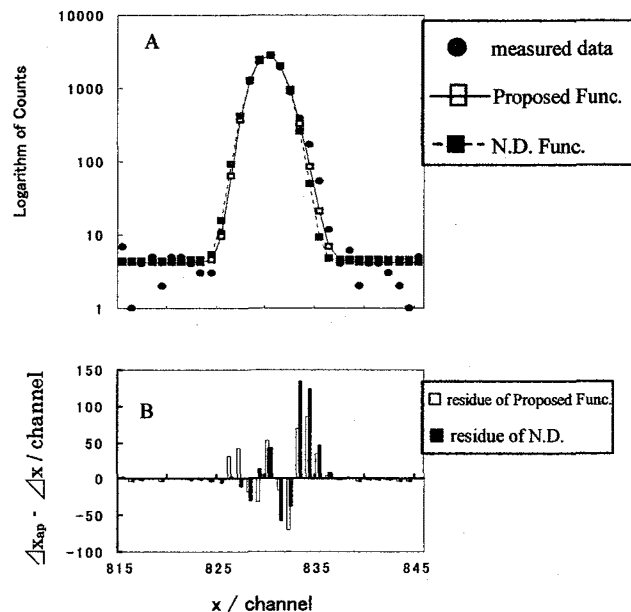


Fig.1 Noise shape (A) and converged residue patterns of proposed func. (□) and N.D. (■) (B)

2P 47      **DETERMINATION OF  $^{54}\text{Mn}$  BY RADIOCHEMICAL  
 $\gamma$ -RAY SPECTROMETRY IN SOILS COLLECTED  
FROM THE JCO CAMPUS**

Yoshimasa MURATA<sup>1</sup>, Toshiharu MUROYAMA<sup>1</sup>, Tetsuji IMANAKA<sup>2</sup>,  
Masayoshi YAMAMOTO<sup>1</sup> and Kazuhisa KOMURA<sup>1</sup>

<sup>1</sup>Low Level Radioactivity Laboratory, Kanazawa University,  
Tatsunokuchi-cho, Nomi-gun, Ishikawa 923-1224, Japan

<sup>2</sup>Research Reactor Institute, Kyoto University,  
Kumatori-cho, Sennan-gun, Osaka 590-0494, Japan

Information on the fast neutron fluence is important to evaluate of the dose to the residents around the JCO site, because the fast neutrons contributes greatly to the exposure doses. However, almost all data reported are thermal neutron fluence by (n,  $\gamma$ ) reaction products. In previous work<sup>1,2)</sup>, we have measured neutron-induced radionuclides in soils collected at the JCO campus by non-destructive  $\gamma$ -ray spectrometry.  $^{54}\text{Mn}$ , which is the only fast neutron products by  $^{54}\text{Fe}(n, p)^{54}\text{Mn}$ , could be detected in only four points within 10 m from precipitation vessel. In order to detect extremely low-level  $^{54}\text{Mn}$  products in the soil from >10 m, radiochemical separation of  $^{54}\text{Mn}$  was inevitable.

About 30-200g soil samples was completely decomposed with  $\text{HNO}_3 + \text{HF}$  mixture. Mn was separated by the forming of  $\text{MnO}_2$  and purified finally by anion exchange method. The Mn fraction thus separated was measured for 7-10 days by ultra low-background  $\gamma$ -ray spectrometer at the Ogoya underground laboratory.

$^{54}\text{Mn}$  could be detected for nine samples collected within 20 m. The concentration of decay collected  $^{54}\text{Mn}$  to October 1 1999, is ranging from 0.02 to 0.55 mBq/g-soil, and its specific activity ( $^{54}\text{Mn}/\text{Fe}$ ) 0.6 to 11 mBq/g-Fe. In NW, W, SW and S direction from precipitation vessel, specific activity of  $^{54}\text{Mn}$  was found to be higher than other direction. Estimation of theoretically calculated value of  $^{54}\text{Mn}$  product by using a three-dimensional neutron transport model is now undertaken.

1. Y. Murata;, T. Muroyama;, Y. Kawabata;, M. Yamamoto;, K. Komura, *J. Radiat. Res.*, 42, (2001)
2. Y. Murata;, T. Muroyama;, H. Kofuji;, M. Yamamoto;, K. Komura, *J. Environ. Radioactivity*, 50, 69-76(2000)



Masato TAKANO,<sup>1</sup> Takashi YAWATA,<sup>2</sup> Tetsuo HASHIMOTO<sup>2</sup>

<sup>1</sup>Graduate School of Science and Technology, Niigata University, Ikarashi-ninocho, Niigata, 950-2181, Japan

<sup>2</sup>Department of chemistry, Faculty of Science, Niigata University, Ikarashi-ninocho, Niigata, 950-2181, Japan

Radiation-induced luminescence such as thermoluminescence (TL) and optically stimulated luminescence (OSL) arises from the recombination between holes and electrons which are released from metastable energy levels within dielectric materials such as natural minerals and artificial ceramics. Measurements of the luminescence signal from quartz or feldspar can offer some information related to their origins and historical conditions, since the accumulation of luminescence signals starts again after the last heating of earthenware or the last sunlight exposure of a sedimentary layer.<sup>1)</sup>

The quartz and feldspar grains were extracted from pieces of ancient earthenwares collected at Okumiomote site, Niigata prefecture. The single-aliquot regenerative-dose (SAR) method<sup>2)</sup> for radiation dosimetry of such minerals was applied to burnt archaeological materials and ceramic samples. The original automated OSL / TL measuring system equipped with X-ray irradiation facility ( c.f. Figure ) was used for all luminescence measurements.

In the case of the extracted quartz, red TL (RTL) and OSL measurements were employed to estimate the naturally accumulated doses (PD). In contrast, infrared stimulated luminescence (IRSL) and blue TL (BTL) measurements were applied to the feldspars. The estimated doses in different luminescence methods were compared to attain reliable dating using the same piece of earthenware.

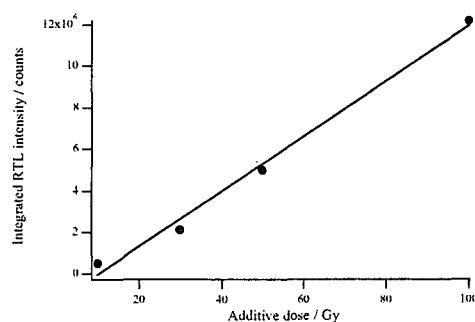


Fig. RTL response relationship against additive dose.

1) Tanaka, K., Hashimoto, T., et al., *Quart. Sci. Rev.*, **16**, 257-264 (1997).

2) Huntley, D.J., Godfrey-Smith, D.I., Thewalt, M.L.W., *Nature*, **313**, 105-107 (1985).

**ANOMALOUSLY HIGH  $^{234}\text{U}/^{238}\text{U}$  RATIOS OF  
TATSUNOKUCHI HOT SPRING WATERS,  
ISHIKAWA PREFECTURE, JAPAN**

Masayoshi YAMAMOTO,<sup>1</sup> Tsutomu SATO,<sup>2</sup> Kei-ichi SASAKI,<sup>3</sup> Kazuhisa KOMURA<sup>1</sup>

<sup>1</sup>Low Level Radioactivity Laboratory, Kanazawa University, Tatsunokuchi,  
Ishikawa 923-1224, Japan

<sup>2</sup>Graduate School of National Science and Technology, Kanazawa University,  
Kakuma, Kanazawa 920-1192, Japan

<sup>3</sup>Department of Cultural Properties and Heritage, Kanazawa Gakuin University,  
Sue, Kanazawa 920-1392, Japan

Since anomalous  $^{234}\text{U}/^{238}\text{U}$  activity ratio was discovered in the water-rock interaction system in 1955 by Cherdynstev et al., this ratio has been widely measured in various samples. The  $^{234}\text{U}/^{238}\text{U}$  radioactive disequilibria have been used as a tool in hydrologic investigations such as water circulation, mixing of water mass and geochronology. In Japan, geochemical studies on uranium isotope ratios have been continued by Sakanoue et al. for river and underground waters, lake and sea waters, and mineral and hot spring waters. During the course of these studies, high  $^{234}\text{U}/^{238}\text{U}$  ratio of about 10 was found in 1977 for the hot spring water of Tatsunokuchi near our laboratory which was made in 1975 by boring to a depth of 600 m. After that, we have continued to collect periodically this hot spring water over a long period of time up to now, and measured its U concentration and  $^{234}\text{U}/^{238}\text{U}$  ratio. The hot spring water of about 48°C has its origin in a conglomerate volcanic tuff layer and contains mainly sodium sulfate with sodium chloride. Uranium isotopes, using 20-30 liters, were separated and purified by conventional anion exchange method and measured by using alpha spectrometer.

Uranium ( $^{238}\text{U}$ ) concentrations varied drastically between 0.045 and 1.02 mBq/l (a factor of about 20), being nearly constant (0.070-0.045 mBq/l) after 1991. On the other hand,  $^{234}\text{U}$  concentrations did not change largely, 2.30-3.07 mBq/l. Resultant  $^{234}\text{U}/^{238}\text{U}$  ratios showed a wide range from 2.7 to as high as 51, with inverse correlation between  $^{234}\text{U}/^{238}\text{U}$  ratios and  $^{238}\text{U}$  contents. The time variations in  $^{234}\text{U}/^{238}\text{U}$  ratios and  $^{238}\text{U}$  contents can be explained by a simple mixing of different two aquifers having a reducing character. Abnormally high  $^{234}\text{U}/^{238}\text{U}$  ratios could be attributed not only to the direct ejection of recoil  $^{234}\text{Th}$  but also to the preferential leaching of  $^{234}\text{U}$  produced by the decay of  $^{234}\text{Th}$ .

## 2P 50 A NEW PERIODIC TABLE FOR RADIOCHEMISTRY

Aratani M

Public Relations and Research Information Office, Institute for Environmental Sciences,  
1-7, Obuchi, Rokkasho-mura, Aomori-ken, 039-3212, Japan

Neutral particles in a nucleus have long remained unknown until Chadwick discovered neutrons in 1932, although J.J. Thomson and Aston suggested (1912) existence of light neon and heavy neon by anode ray analysis, and Rutherford and other scientists independently predicted (1920) that anything neutral should exist in the nucleus. What was the difficulty in history of discovery of neutron ?

A critical accident happened at the Tokai facilities of JCO on Sept. 30, 1999, and was discussed in various contexts at home and, especially, in a severe tone at abroad. A background survey of the environmental neutrons has not been made at any nuclear facilities concerning fission in this country. The neutron monitor which detected and recorded the neutrons from the JCO critical accident was what had been equipped for fusion research, but not for fission application. Radiation education on neutron has not been made in both school and social education. In this country, textbooks of this field have been entirely unchanged these 100 years. "We have three kinds of radiations, alpha, beta and gamma rays". That is all! It is meant that description of neutron was not seen in the textbooks. From this reason, basic scientists also may be responsible for the critical accident through making light of fundamental aspects of radiation education and nuclear technology without revision of the old textbooks.

Just after the JCO accident, some lectures on properties of neutron were made in order to come familiar with neutron and eliminate anxiety from it, and, at the same time, on trial with a clear educational intention for the public in the Peninsula Shimokita (Mutsu and Rokkasho), Chiba and Aomori .

1) Neutron comes to the earth as a cosmic ray. 2) Neutron is derived from spallation in atmosphere due to the cosmic ray, spontaneous and induced fission of transuranium elements, and (x,n) nuclear reactions. 3) Neutron is a beta-emitting nuclide with half-life of 10.6 min to decay into hydrogen. 4) Neutron may be regarded as an element of atomic number of zero. 5) Neutron should be located before hydrogen in the table of isotopes or nuclides. 6) Neutron should be listed up on the periodic table, and location of it should be before, that is, left of hydrogen, and above helium (as eka-helium). The upper part of the left side of this new periodic table /1/ will serve for understanding as "fusion corner". 7) Neutron gives its kinetic energy to hydrogen in the maximum efficiency. Hydrogen-containing materials serve as effective shield of the neutron. 8) Neutron is neutral in charge, and is not affected by both positive and negative charge of atom, so has a great penetrating power against matter. 9) Slow neutron easily gets close to nucleus and is caught by it. The neutron-caught nucleus will act as beta-emitting nucleus. So, neutron will make radioactive matter, that is, activate other matter. 10) Neutron reacts with boron to give alpha particles. This reaction is made use of both detection and protection of neutron.

A series of these explanations are arranged in a historical sequence and logically natural order. A new periodic table has been formed as a result of public acceptance activities after JOO critical accident and through discussions with audience, and has been shown to be a powerful tool for radiation education and basic understanding of dynamical aspects of atoms, in other word, radiochemistry.

1. M. Aratani, *Proceedings of the First Workshop on Environmental Radioactivity*, 65, KEK, Tsukuba, Japan, March 30-31, 2000.

## AMS Radiocarbon Dating Ancient Japanese Documents of Known Age

Hiroataka Oda<sup>1</sup>, Takashi Masuda<sup>2</sup>, Etsuko Niu<sup>1</sup>, and Toshio Nakamura<sup>1</sup>

<sup>1</sup> Center for Chronological Research, Nagoya University, Chikusa, Nagoya 464-8602, Japan

<sup>2</sup> Aichi Bunkyo University, Komaki, Aichi 485-0802, Japan

History is a reconstruction of past human activity, evidence of which is preserved in the form of documents or relics. Ancient documents provide valuable information for historical study and the dates of writing the documents are particularly important. Radiocarbon age is generally converted into calendar age with the calibration curve. However, the calibrated age is still different from the historical age when the document was written. The purpose of this study is to clarify the relation between calibrated radiocarbon age and historical age of ancient Japanese document by AMS radiocarbon dating. We have measured radiocarbon ages of Japanese ancient documents whose written dates are clarified from the paleographic standpoint.

Alpha-cellulose was extracted from 20-40 mg paper sample by the following procedure. The samples were washed in distilled water with a supersonic cleaner. Next, each sample was treated with 1.2N HCl and 1.2N NaOH solutions alternately on a hot plate. The above treatments were repeated several times. The samples were bleached with 0.07M NaClO<sub>2</sub> solution under acidic condition adjusted with HCl (70-80°C). This one-hour bleaching treatment was repeated four times. Alpha-cellulose was separated finally by washing the residue with 17.5% NaOH solution for 30 min at room temperature. The alpha-cellulose was sealed in a glass tube with CuO and converted to CO<sub>2</sub> at 850°C. After purification in a glass line, CO<sub>2</sub> was reduced to graphite to produce a target for AMS radiocarbon dating. Conventional radiocarbon ages were measured with two sets of AMS system at Nagoya University.

The radiocarbon ages of the ancient documents were consistent with those of tree rings which compose the calibration curve. Japanese paper had been made mainly from deciduous trees: *Kozo*, *Ganpi* and *Mitsumata*. Although there is time interval from trimming off branches to writing document on manufactured paper, the result indicates that the interval is negligible and the calibrated radiocarbon ages are hardly different from the corresponding historical ages. Since the fiber of old branch yields paper of poor quality, fresh branches grown within a few years were harvested selectively for paper manufacture. In addition, *Kozo* paper is usually used within one year, because long-preserved paper is not fit to write with Indian ink. The little gap observed between calibrated radiocarbon age and historical age is supported by such characteristics of manufacturing and using Japanese paper traditionally.

**RADIOCARBON CONCENTRATION OF AEROSOLS  
COLLECTED AT FUKUOKA, JAPAN**

Hidehisa KAWAMURA<sup>1</sup>, Nobuaki MATSUOKA<sup>1,2</sup>, Noriyuki MOMOSHIMA<sup>3</sup>,  
Toshio NAKAMURA<sup>4</sup>, Yonezo MAEDA<sup>5</sup>

<sup>1</sup>Kyushu Environmental Evaluation Association, Higashi-ku, Fukuoka 813-0004, Japan

<sup>2</sup>Institute of Environmental Systems, Kyushu University, Higashi-ku, Fukuoka 813-0004, Japan

<sup>3</sup>Faculty of Science, Kumamoto University, Kurokami, Kumamoto 860-8555, Japan

<sup>4</sup>Center for Chronological Research, Nagoya University, Chigusa-ku, Nagoya 464-8602, Japan

<sup>5</sup>Faculty of Science, Kyushu University, Higashi-ku, Fukuoka 813-0004, Japan

Carbonaceous aerosols, especially black soot, are of special concern because of their significant effects on visibility, atmospheric heating, and human health. It is known that carbonaceous aerosols have two primary origins, contemporary and fossil carbon sources. Therefore, it is important to separately evaluate the contribution of the sources to aerosols.

Radiocarbon (<sup>14</sup>C) is a unique indicator of contemporary carbonaceous material. The <sup>14</sup>C concentration of contemporary material is comparable to the atmospheric concentration at the time it was formed, while fossil fuel such as petroleum and coal contains essentially no <sup>14</sup>C, because its age is much greater than the 5730-yr half-life of <sup>14</sup>C. Thus, the ratio of the <sup>14</sup>C concentration in aerosols to that in a contemporary material would be the fraction of contemporary carbon in the aerosols. In this investigation, we measured <sup>14</sup>C concentrations of aerosols collected at Fukuoka, which is located in an urban area, and evaluated the seasonal difference of the fraction.

Aerosols were collected on a silica fiber filter using a high volume air sampler with a flow rate of 1000 L/min. About 7-day sampling was carried out twice in each month from January 1999 to January 2000. Carbonaceous material in aerosols was converted to CO<sub>2</sub> by combustion, followed by preparing graphite target. The <sup>14</sup>C concentrations were determined by AMS at Nagoya University and  $\delta^{13}\text{C}$  values also determined by SI-MS.

The  $\delta^{13}\text{C}$  values ranged from -25.9 ‰ to -24.6 ‰ through the sampling period and were fairly close to those of C3-plants. The fractions of contemporary carbon in the aerosols calculated on the basis of the <sup>14</sup>C concentration showed seasonal variation with low in winter (December, January and February) and high in summer (May, June and July). The results indicate that most of the carbonaceous aerosols are originated from C3-plants and the contributions of contemporary and fossil carbon sources to the aerosols change with season.

